SPY POND STORMWATER CAPTURE FEASIBILITY STUDY

Prepared for

Arlington-Belmont-Cambridge (ABC)
Stormwater Flooding Board

by

Jeffrey D Walker, PhD
Walker Environmental Research LLC
Brunswick, ME

and

Mystic River Watershed Association
Arlington, MA

October 2019

Walker Environmental Research

Mystic River WATERSHED ASSOCIATION

TABLE OF CONTENTS

LIST OF FIGURES

LIST OF TABLES

1 INTRODUCTION

Stormwater management is a topic of great interest within the Alewife Brook watershed. Over the past few decades, flooding has caused major impacts on the neighboring communities of Arlington, Belmont, and Cambridge. These flooding concerns only become greater and more urgent when considering the potential effects of climate change, which is expected to increase the magnitude and frequency of large storm events (City of Cambridge, 2015 and 2017). Continued urban development of the watershed is also expected to increase the risk of flooding. Recently, there have been a number of efforts to better understand the causes and extent of flood events, and to identify and implement stormwater management strategies for reducing flooding along Alewife Brook.

In 2002, a collaboration between the Mystic River Watershed Association (MyRWA), the Massachusetts Department of Environmental Protection and the communities of Arlington, Belmont, and Cambridge was formed to collectively address stormwater flooding issues within the Alewife Brook watershed. This group soon evolved into the Arlington-Belmont-Cambridge Stormwater Flooding Board (also known as the Tri-Community Working Group), which was formally authorized by state legislation passed in 2005. Since then, this group has worked together to identify cost-effective solutions for reducing stormwater flooding along Alewife Brook. One idea that has been considered by the group is to use the largest pond in the Alewife Brook watershed, Spy Pond, as a stormwater capture basin (Tri-Community Working Group, 2005). By drawing down Spy Pond prior to large storm events, increased storage capacity could be made available to capture stormwater runoff and thus reduce pond outflows during the course of each storm.

Spy Pond is a 100-acre kettle pond located in Arlington, MA. Outflows from Spy Pond discharge to Little Pond through a 36-inch concrete pipe, and from there flows continue down the Little River, which becomes Alewife Brook at the Alewife T station (Figure 1-1). Alewife Brook is a major tributary to the Mystic River, which ultimately discharges to Boston Harbor. The watershed draining to Spy Pond is about 730 acres in area and comprises a major portion (16%) of the total 4,500 acre watershed draining to Alewife Brook. Therefore, by fully capturing stormwater runoff and thus eliminating outflows from Spy Pond during large storm events, downstream peak flows and associated flooding could be reduced.

The problems associated with urban stormwater runoff are not unique to the Alewife Brook watershed. Across the country, municipalities are exploring a variety of innovative solutions to address this issue such as low-impact development and other green infrastructure approaches. Another new approach that has recently emerged is the use of so-called “smart stormwater management” systems (Lefkowitz et al., 2016). These data-driven systems use computer algorithms to automate and optimize the operation of existing stormwater infrastructure based on precipitation forecasts and other real-time data sources. These solutions can provide significant benefits in terms of reducing the impacts of urban runoff by improving the effectiveness of existing infrastructure and thus reducing the need to construct new infrastructure. An example of this type of system is a stormwater capture basin, which can be operated by automatically releasing water in advance of an upcoming storm, and thus increase the storage capacity available to fully capture runoff from that storm. Although these systems are generally applied to smaller wet detention basins that capture water from parking lots or other small impervious areas, the same type of approach could be applied to larger systems such as Spy Pond.

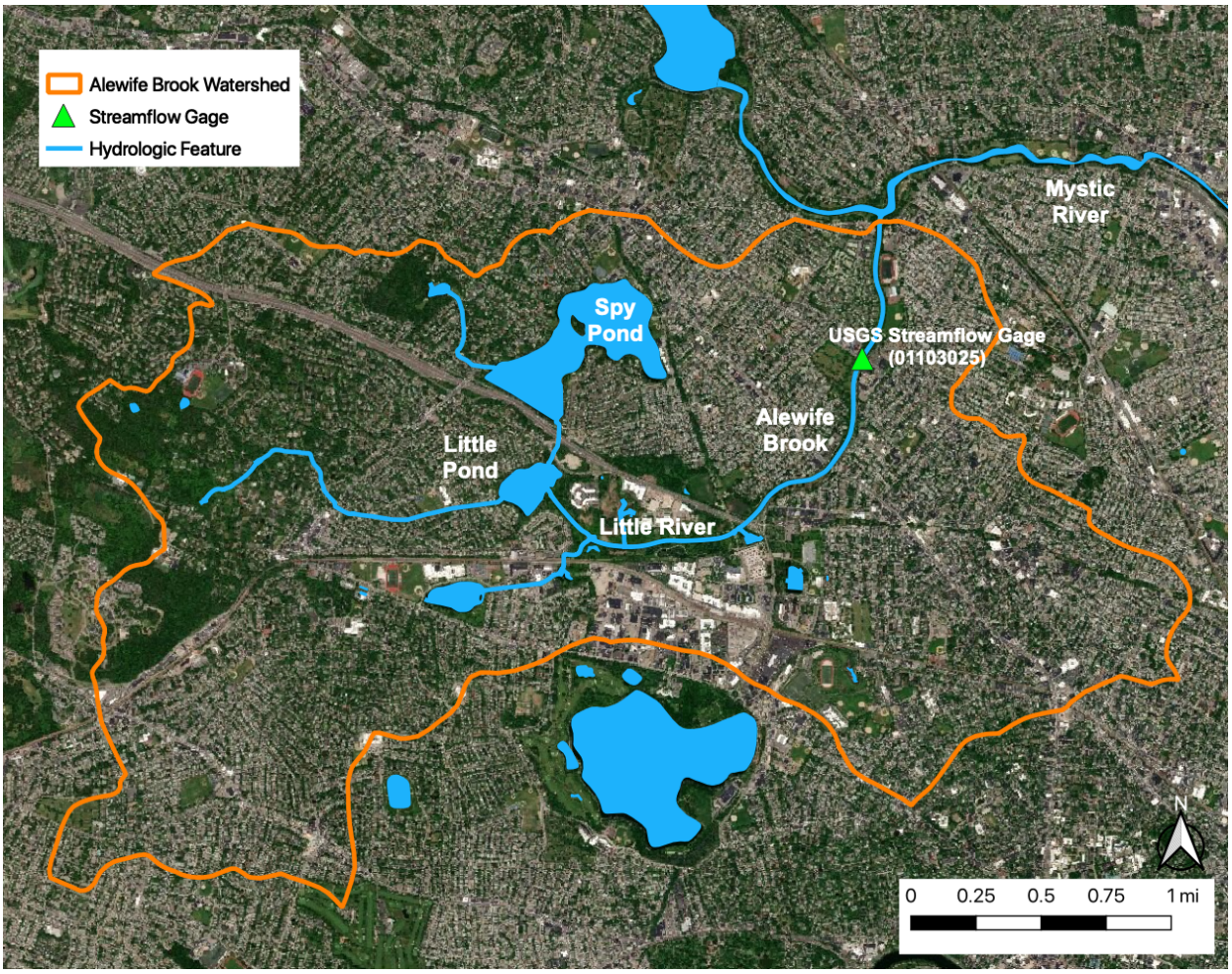

Figure 1-1: Map of the Alewife Brook watershed.

Note: The Alewife Brook watershed shown in this figure excludes the area drainage to Fresh Pond, which is part of the water supply system for the City of Cambridge.

The overall goal of this feasibility study is to estimate the potential benefits of operating Spy Pond as a stormwater capture basin in order to reduce downstream peak flows that can cause flooding in neighboring communities along Alewife Brook. A secondary goal was to evaluate whether these operations could also provide benefits in terms of reducing shoreline flooding by preventing the pond water level from rising above flood stages that would cause inundation of private properties surrounding the pond. This study was performed by developing a series of models to simulate the water budget of the pond with and without stormwater capture operations. Although these models were developed using limited available data and based on numerous simplifying assumptions, the results provide a basis for evaluating whether the potential benefits of these operations are sufficient to warrant further investigation through more comprehensive and detailed analyses.

2 Model Development

A series of datasets and models were developed to evaluate the potential benefits of utilizing Spy Pond as a stormwater capture system (Figure 2-1). The primary model used in this study was a water budget model, which simulates the change in volume (and thus water level) over time based on a simple accounting of the inflow, outflow, precipitation, and evaporation fluxes to and from the pond. Inflow rates were estimated by a separate watershed

runoff model that used historical weather data (precipitation, air temperature) and drainage basin characteristics (area and impervious cover) to generate a continuous timeseries of simulated flows representing the total inflows to the pond due to rainfall and snowmelt. Outflows from the pond were calculated using an empirical relationship of the outflow rate as a function of the pond surface elevation. This relationship was developed using continuous water level measurements to estimate historical volume fluctuations, from which historical outflow rates could be calculated and compared to the observed water levels. The pond bathymetry was used to generate elevation-area-volume curves with which the surface elevation and area could be calculated at each model timestep based on the simulated pond volume. Lastly, the water budget model incorporated historical precipitation measurements and estimated monthly evaporation rates to calculate direct precipitation and evaporation fluxes at the pond surface. The results of the water budget model provided hourly timeseries of the pond surface elevation and outflow rates, which were used to evaluate 1) the potential for flooding along the shoreline of Spy Pond, and 2) the contribution of pond outflows to downstream flows in Alewife Brook, and in particular to the peak flows during major storm events that pose a flooding risk to neighboring communities.

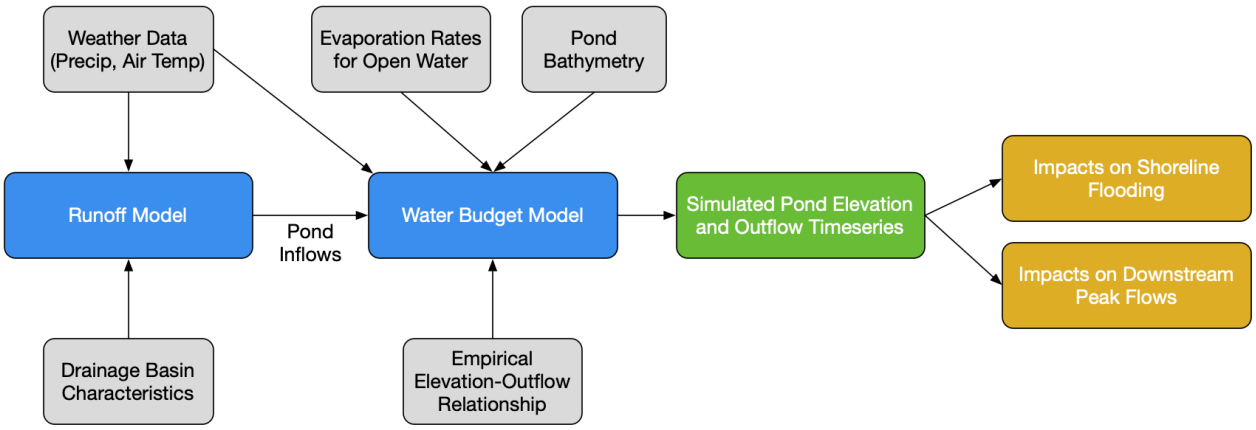

Figure 2-1: Schematic of modeling methodology.

The model simulation spanned a period of 13 water years (WY[1]) from Oct 1, 2005 to Sep 30, 2018 (WY 2006 to WY 2018). The start of this period coincides with the earliest available data collected at the USGS streamflow gage in Alewife Brook and ends with the most recent full water year at the time of this study. Data processing, analysis, and model simulations were performed using version 3.6 of the R programming language (R Core Team, 2019). Geospatial data were processed using version 3.8 of QGIS (QGIS Development Team, 2019). All source code, input and output datasets used in this study are available upon request[2].

2.1 Runoff Model

A watershed runoff model was developed to generate a continuous timeseries of estimated inflows to Spy Pond. This inflow timeseries was then used as an input to the water budget model. The runoff model was developed using algorithms from the P8 Urban Catchment Model (Walker, 1990), which were translated to the R programming language for use in this study. P8 is designed to simulate flows and pollutant loads in urban environments with a focus on supporting stormwater treatment system design and performance evaluation (e.g., detention ponds,

[1] A Water Year (WY) is defined as the period from Oct 1 of the previous calendar year to Sep 30 of the current year. For example, WY 2006 is from Oct 1, 2005 to Sep 30, 2006.

[2] To request the source code or datasets used in this study, please contact Jeff Walker at jeff@walkerenvres.com

bioswales, etc.). P8 was originally developed by William W Walker, Jr., PhD. for the U.S. Environmental Protection Agency (USEPA) and Rhode Island Department of Environmental Management (RIDEM) Narragansett Bay Project in 1990. The model underwent subsequent updates and revisions through the 1990s and 2000s, primarily with support from the Wisconsin Department of Natural Resources and Minnesota Pollution Control Agency. Although P8 includes a number of algorithms for simulating flow and pollutant load transport through the urban environment, only the watershed runoff algorithms were used for this study.

The P8 watershed runoff algorithms are based on a modified version of the SCS curve number method (USDA SCS, 1964) as implemented in the Generalized Watershed Loading Functions (GWLF) model (Haith et al., 1992). Runoff is generated by either rainfall or snowmelt (or a combination of the two). Snowpack is simulated using a simple model based on degree-days for calculating the rates of snow melt. Runoff is calculated based on the amount of impervious area in the drainage basin and using a modified curve number approach that accounts for antecedent moisture conditions. This algorithm is able to better predict runoff responses than a simpler runoff coefficient-based model by accounting for soil saturation at the start of any given event. For example, runoff rates would be higher for a given event if the soils are already saturated at the start of the event than if the event follows a long dry period during which soils would dry out[3].

P8 was chosen for this study due to its minimal input data requirements, incorporation of snowmelt processes, and because it includes default parameters that can be used to generate reasonable runoff estimates in temperate climates like the Northeast U.S. Because no direct measurements of runoff or pond inflows were available for this study, the runoff model could not be calibrated to any observed flow data. Therefore, default values were used for all model parameters aside from the sub-basin characteristics (e.g., area, impervious cover), which were determined from GIS datasets as described below. The complete set of parameter values used for the runoff model are listed in Appendix A.

2.1.1 Input Datasets

2.1.1.1 Weather Data

The runoff model required input timeseries of hourly precipitation and air temperature, which were obtained from the Integrated Surface Dataset (ISD) for WMO Station 725090 (WBAN 14739) located at Logan Airport in Boston, MA over the simulation period from WY 2006 through WY 2018 (NOAA NCEI, 2001). This weather station is located approximately 7.5 miles east-southeast of Spy Pond. Five missing precipitation observations were set to zero, and 14 missing air temperature observations were estimated using linear interpolation between the nearest non-missing observations. The longest continuous gaps of missing data were only 1 hour for precipitation and 2 hours for air temperature. The precipitation data were used to drive the runoff processes in the model. The air temperature data were used to determine whether precipitation fell as rain or snow at any given time step, and to calculate the number of degree days, which determined the rate of snow melt. Air temperatures were also used for estimating the rate of evapotranspiration across the watershed. The total daily precipitation and mean daily air temperature over the simulation period are shown in Figure 2-2.

[3] For more details about the P8 snow and watershed runoff algorithms, see the user documentation: http://wwwalker.net/p8/v35/webhelp/Simulation_Methods.htm

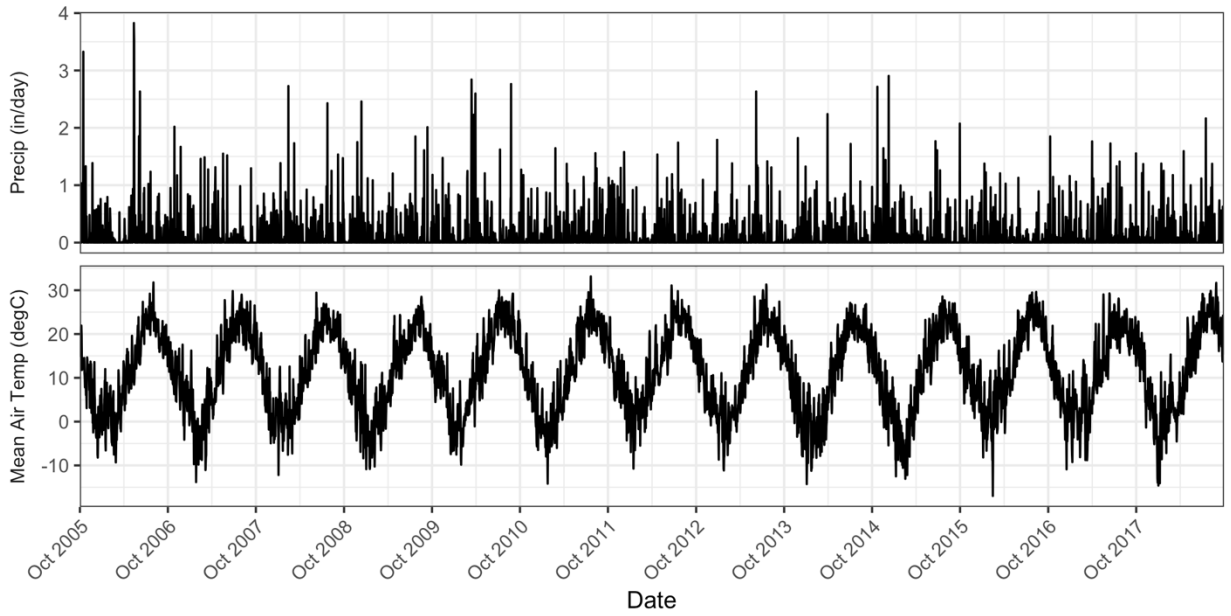

Figure 2-2: Daily total precipitation and mean air temperature over WY2006 – WY2018.

2.1.1.2 WATERSHED DELINEATION

An existing watershed delineation was used to determine the area and land cover characteristics (i.e. impervious cover) of each sub-basin draining to Spy Pond. This delineation was extracted from Figure 6-1 of EDP (1982), which included nine distinct sub-basins (Figure 2-3). The original figure was georeferenced and digitized in QGIS (Figure 2-4), from which the area and land cover composition of each sub-basin could be calculated.

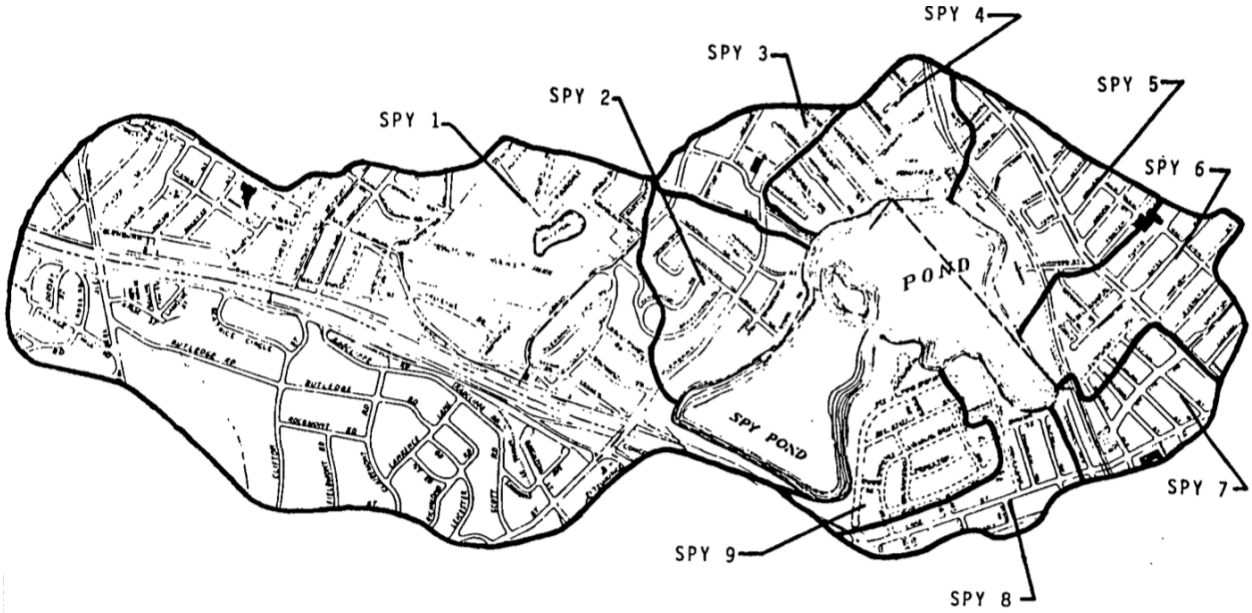

Figure 2-3: Original sub-basin delineation of the Spy Pond watershed.
Extracted from Figure 6-1 of EDPEDP (1982).

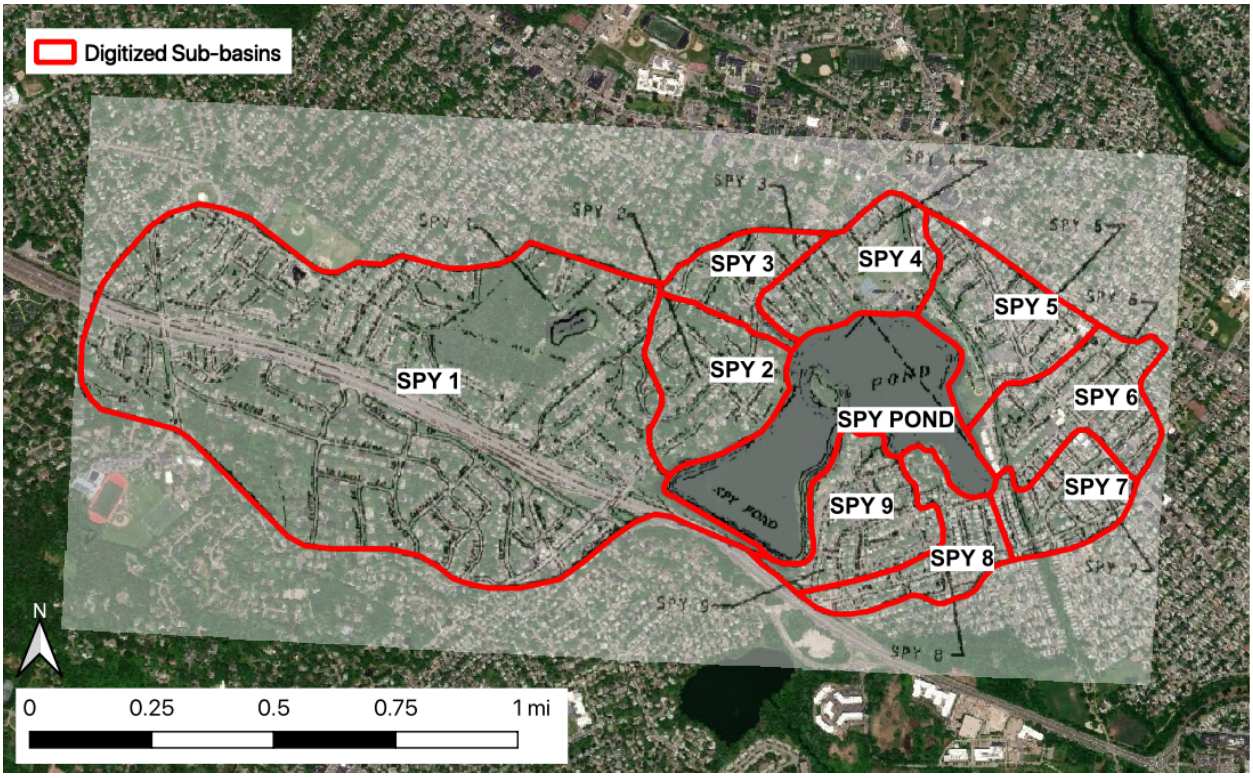

Figure 2-4: Digitized sub-basin delineation of the Spy Pond watershed.

2.1.1.3 IMPERVIOUS COVER

The percentages of directly and indirectly connected impervious cover for each sub-basin were required input parameters for the runoff model. These values were estimated from an impervious cover layer at 1-meter resolution obtained from MassGIS (2013) (Figure 2-5).

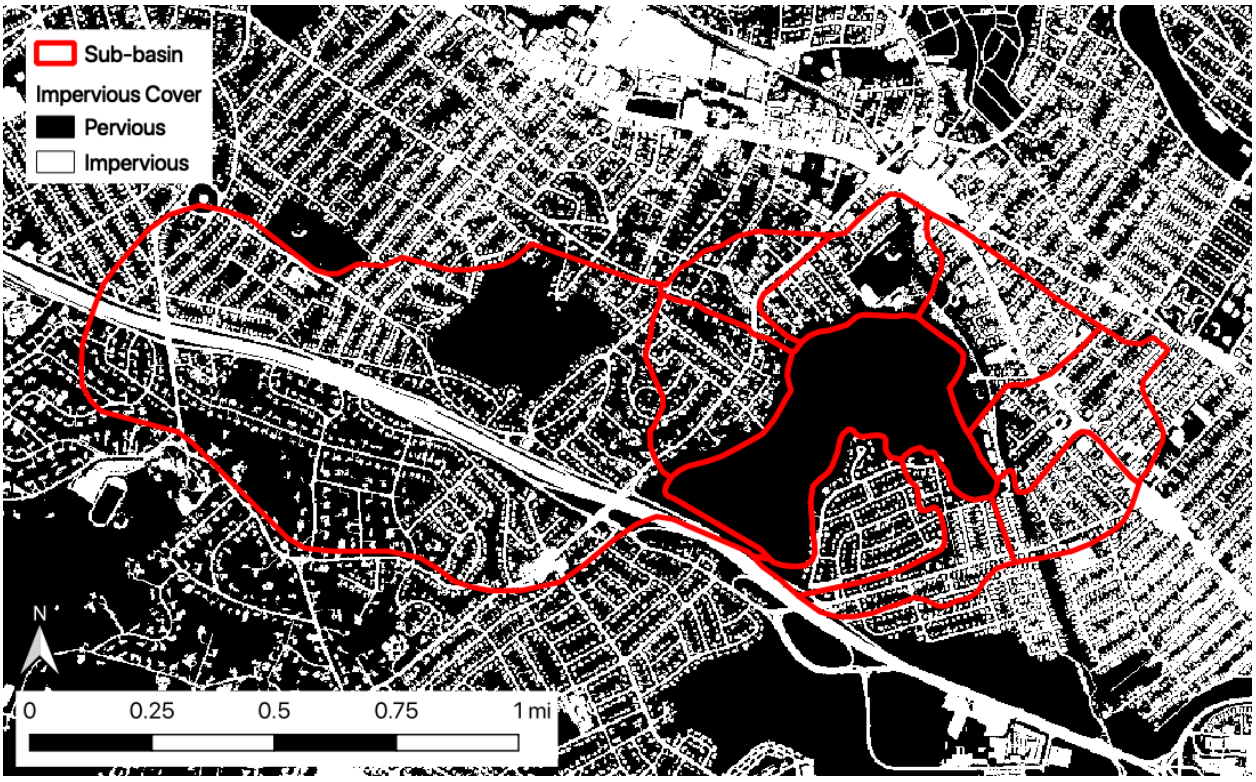

Figure 2-5: Impervious cover of Spy Pond drainage area.

For each sub-basin, the percent of total imperious cover was calculated in QGIS using the zonal statistics tool. The total impervious cover was then sub-divided into the percentages of directly- and indirectly-connected impervious cover using the empirical relationship from Sutherland (2000):

$$DCIA = 0.1(TIA)^{1.5} \quad (1)$$

$$ICIA = TIA - DCIA \quad (2)$$

where $DCIA$ is the percent of directly-connected impervious area (0-100), $ICIA$ is the percent of indirectly-connected impervious area (0-100), and TIA is the percent of total impervious area (0-100) as calculated from the GIS layer. Table 2-1 lists the area and percentages of the directly-connected, indirectly-connected, and total impervious areas of each sub-basin. The total combined drainage basin for Spy Pond has an area of 729.4 acres with an estimated 25.5% and 14.7% directly- and indirectly- connected impervious area, respectively (40.2% total impervious area).

Table 2-1: Drainage areas and impervious cover of each sub-basins and for the total Spy Pond watershed.

Sub-Basin	Drainage Area (acre)	% Impervious Cover		
		Directly Connected	*Indirectly Connected*	*Total*
SPY 1	416.3	22.2	14.5	36.7
SPY 2	47.5	17.9	13.9	31.8
SPY 3	24.2	26.2	14.7	40.9
SPY 4	41.0	24.4	14.6	39.0
SPY 5	48.2	40.0	14.3	54.3
SPY 6	48.0	41.3	14.2	55.5
SPY 7	30.5	44.9	13.7	58.6
SPY 8	32.4	30.4	14.8	45.2
SPY 9	41.4	19.9	14.2	34.1
TOTAL	**729.4**	**25.5**	**14.7**	**40.2**

2.1.2 RESULTS

The runoff model was used to simulate rainfall- and snowmelt-driven runoff at hourly time steps from Oct 1, 2005 to Sep 30, 2018 (WY 2006 – WY 2018). The total watershed runoff to Spy Pond was calculated as the sum of the runoff rates from the individual sub-basins at each hourly timestep. Hourly output timeseries of rainfall, snowfall, snowpack, snowmelt, and total runoff are shown in Figure 2-6. On a water year basis, total annual precipitation ranged from 29.0 to 52.7 inches/year (mean 41.2 inches/year) resulting in total runoff per unit area from 7.8 to 18.0 inches/year (mean 11.7 inches/year) (Figure 2-7). The annual mean runoff flow rate ranged from 0.66 to 1.51 cfs (mean 0.98 cfs) and the annual maximum runoff rate ranged from 118 to 355 cfs (mean 209 cfs).

The timeseries were also aggregated by storm event based on a minimum interevent dry period of 10 hours (Figure 2-8). The largest event began on May 12, 2006 and continued for 155 hours with a total rainfall of 8.4 inches, which yielded a total runoff per unit area of 5.3 inches with a peak runoff rate of 240 cfs. The total runoff per unit area was also plotted against the total rainfall + snowmelt depth of each event to determine the effective runoff coefficient based on the model output (Figure 2-9). A runoff coefficient is the ratio between the runoff per unit area and the total rainfall + snowmelt of the event. In other words, the runoff coefficient indicates how many inches of runoff are generated by one inch of rainfall + snowmelt. Because the P8 watershed runoff algorithm incorporates antecedent soil moisture conditions, the model output reflects a range of runoff coefficients that vary depending on whether the soils were saturated or not at the start of each storm. As shown in Figure 2-9, many of the events fall on a straight line with a slope of 0.255, which represents the minimum runoff coefficient that occurs when soils are completely dry at the start of the event. For some events, the ratio of runoff to rainfall + snowmelt was higher than 0.255 (i.e., the points above the blue line in Figure 2-9) due to the soil being semi- or fully-saturated at the start of the event, in which case there were greater amounts of runoff generated per inch of rainfall + snowmelt. A typical range of runoff coefficient values for residential (suburban) land use is 0.25 – 0.40 (Pilgrim and Cordery, 1993). The minimum runoff coefficient of 0.255 generated by the Spy Pond runoff model thus closely agrees with the lower end of this range.

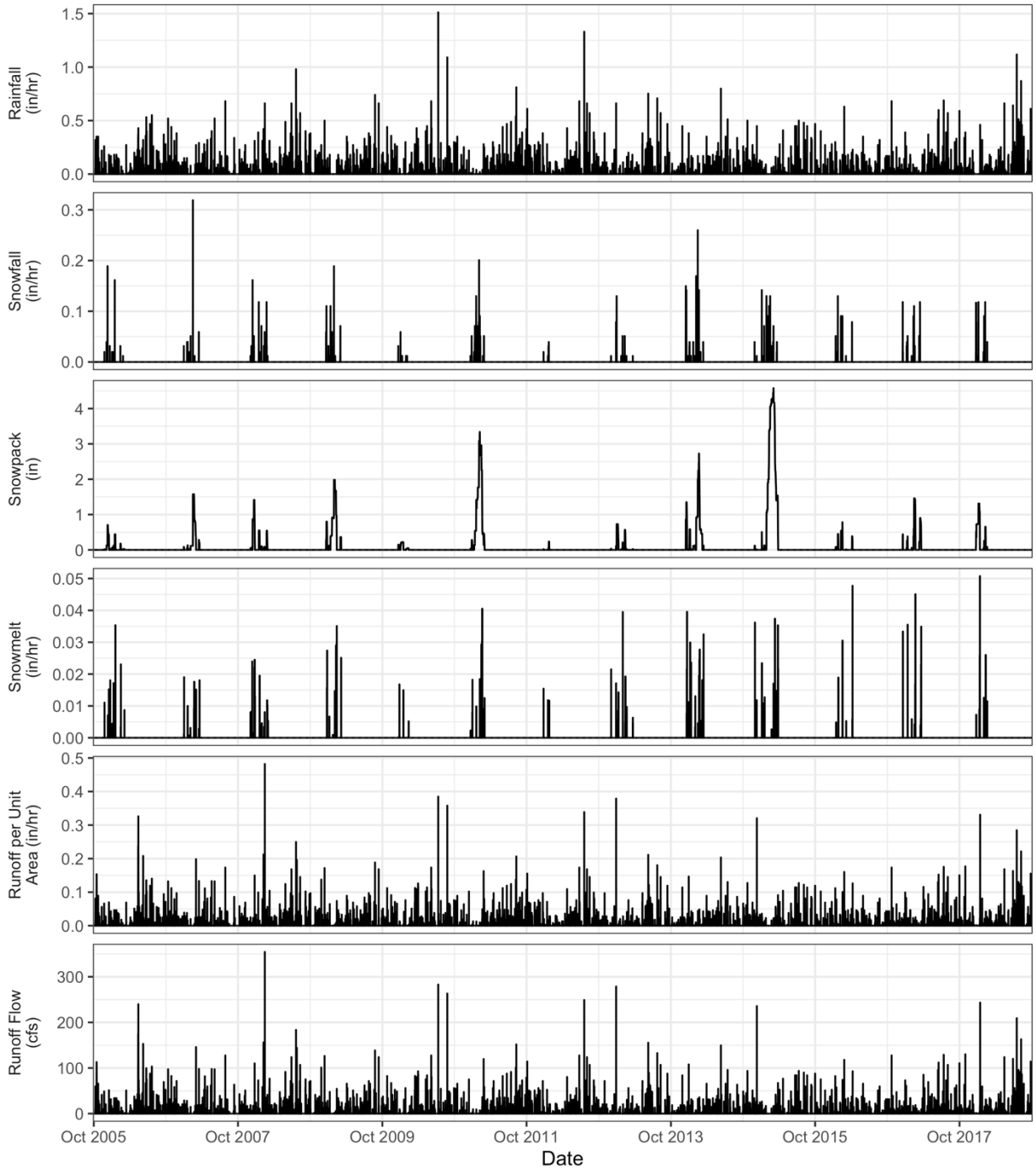

Figure 2-6: Hourly timeseries output from runoff model.

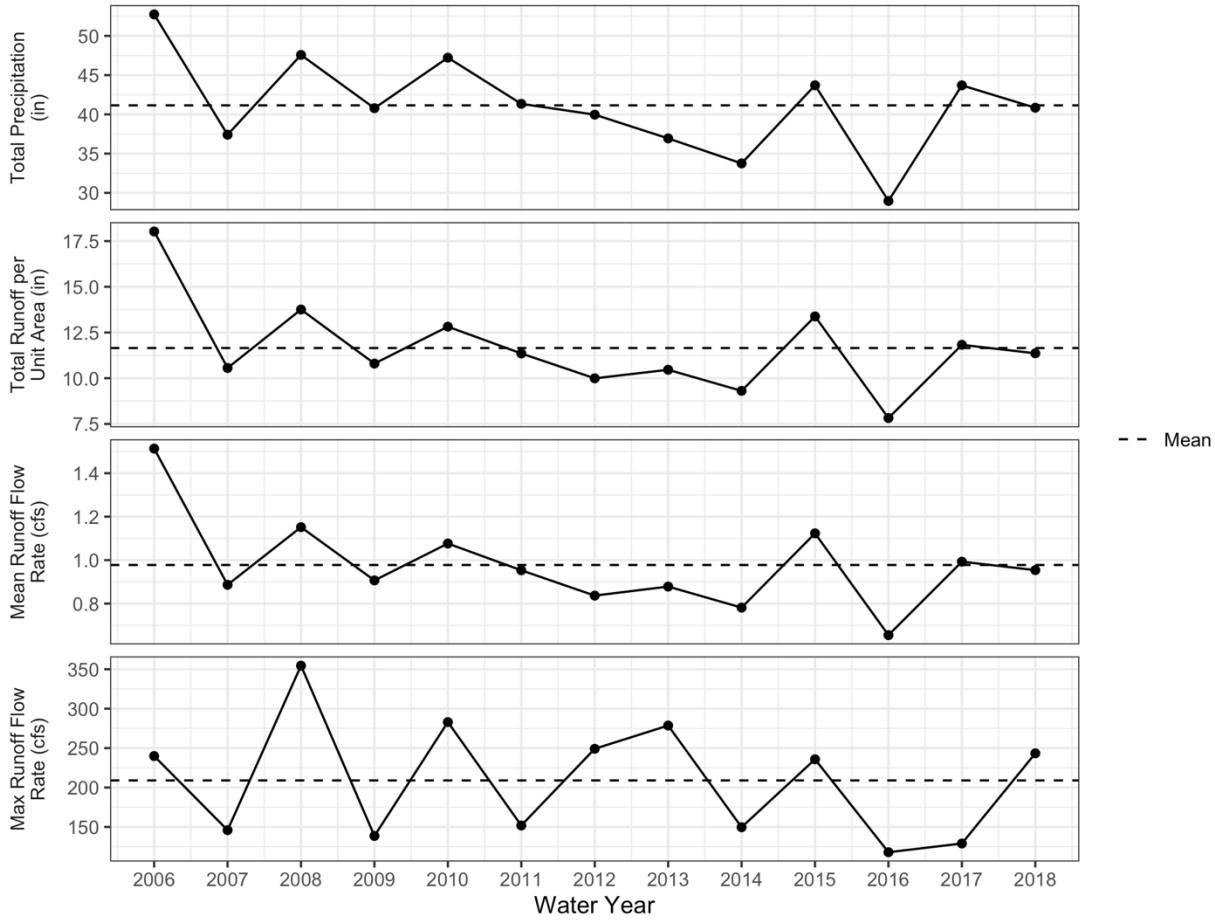

Figure 2-7: Total precipitation, runoff per unit area, and mean and maximum runoff flow rates by water year.

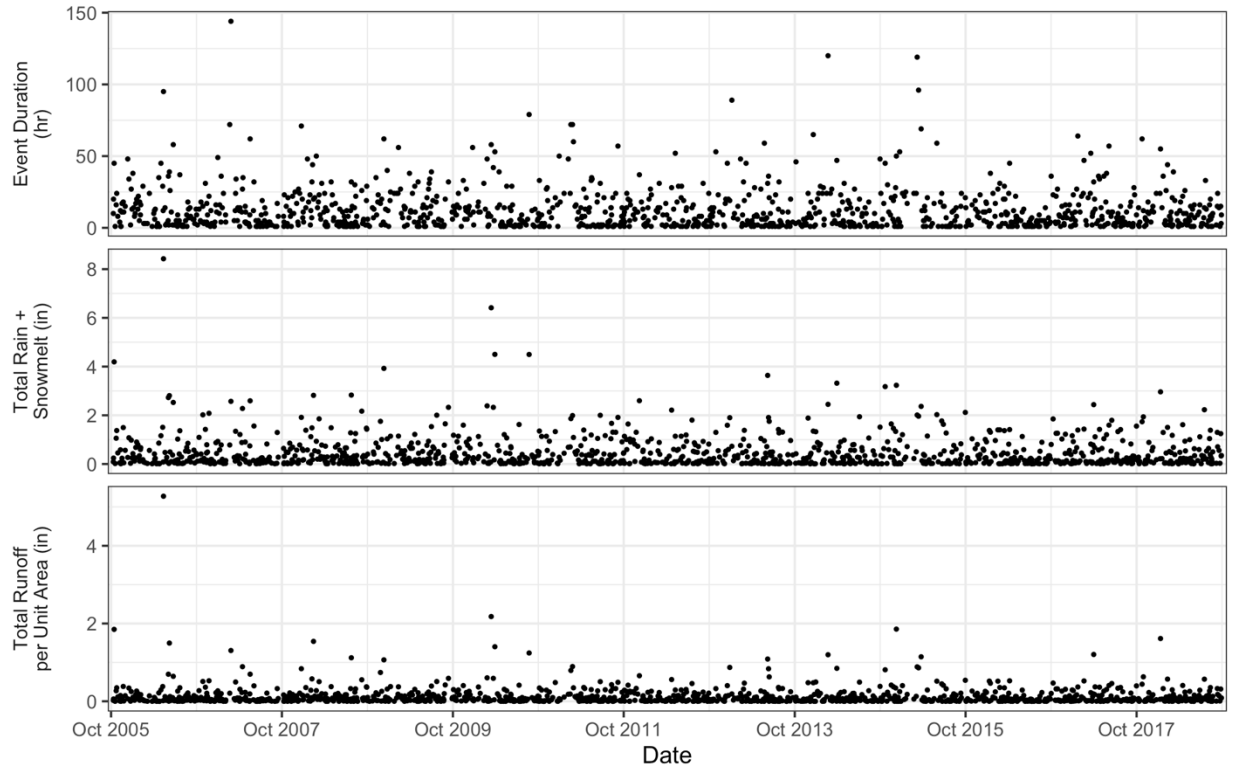

Figure 2-8: Total duration, rainfall + snowmelt, and runoff per unit area of each storm event.

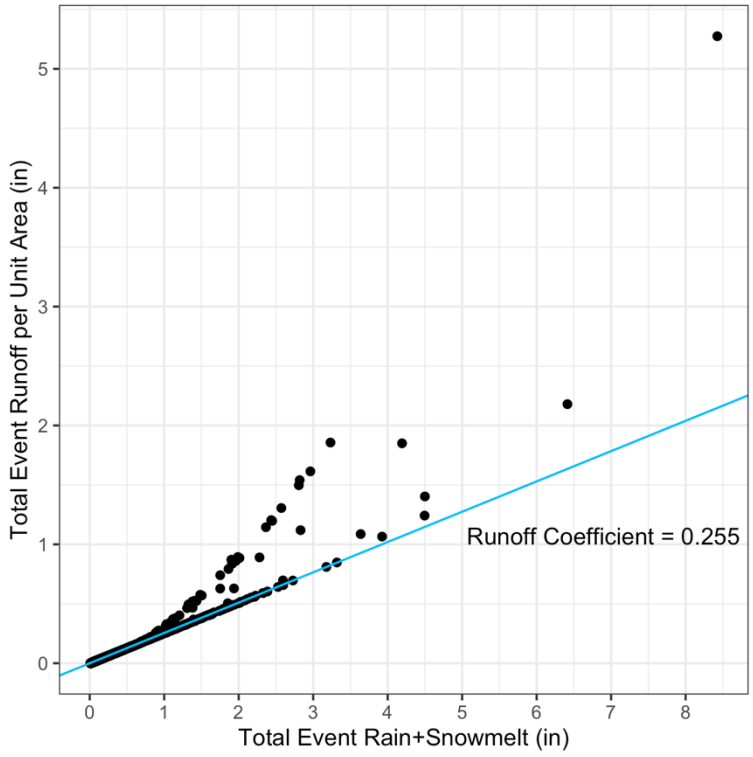

Figure 2-9: Relationship between total runoff per unit area and total rainfall + snowmelt of storm event.

Blue line indicates a constant runoff coefficient of 0.255.

2.2 POND WATER BALANCE MODEL

A water budget model of Spy Pond was developed to simulate the change in pond volume over time (dV/dt) due to both horizontal fluxes (inflows and outflows) and vertical fluxes (direct precipitation and evaporation):

$$\frac{dV}{dt} = Q_{in} - Q_{out}(Z) + A \cdot (P - E) \quad (3)$$

where V is the pond volume (acft), Q_{in} is the inflow rate (acft/hr), Q_{out} is the outflow rate (acft/hr) calculated as a function of the pond surface elevation (Z, ft NGVD29) (see Section 2.2.2 below), A is the surface area of the pond (acres), P is the precipitation rate (ft/hr), and E is the potential evaporation rate for open water bodies (ft/hr). The net groundwater flow between the pond and underlying aquifer was assumed to be zero.

The model was solved as a difference equation using hourly time steps (Δt = 1 hour):

$$V_t = V_{t-\Delta t} + \left(Q_{in} - Q_{out}(Z_{t-\Delta t}) + A \cdot (P - E)\right) \cdot \Delta t \quad (4)$$

At each timestep, the inflow (Q_{in}), precipitation (P), and evaporation (E) rates were extracted from the input time series. The pond surface area (A) and elevation (Z) were calculated from elevation-area-volume curves based on the simulated volume ($V_{t-\Delta t}$) of the previous timestep, and the outflow (Q_{out}) was determined from an empirical relationship between elevation and outflow (see Section 2.2.2).

2.2.1 INPUT DATASETS

2.2.1.1 DIRECT PRECIPITATION

The precipitation dataset used in the runoff model (Section 2.1.1.1) was also used to calculate the direct precipitation onto the pond surface in the water budget model.

2.2.1.2 OPEN WATER EVAPORATION RATES

Monthly average potential evaporation rates for open-water bodies were obtained from MassGIS (2011). This dataset was generated from an empirical model developed by Fennessey and Vogel (1996) that uses monthly mean air temperature, longitude, and elevation to estimate potential evaporation rates across a gridded surface of the Northeast U.S. The dataset was comprised of a series of twelve continuous grids (1 km resolution) with each grid providing the potential evaporation rates for one month of the year. The potential evaporation rates were extracted from these grids using the values for the grid cell containing Spy Pond. The monthly average evaporation rates ranged from 0.04 in/day in Dec and Jan to 0.24 in/day in July with an annual average daily rate of 0.13 in/day (Figure 2-10). The total annual evaporation depth was therefore 47.5 in/yr, which is 6.3 in/yr higher than the annual average precipitation of 41.2 in/yr (Section 2.1.2).

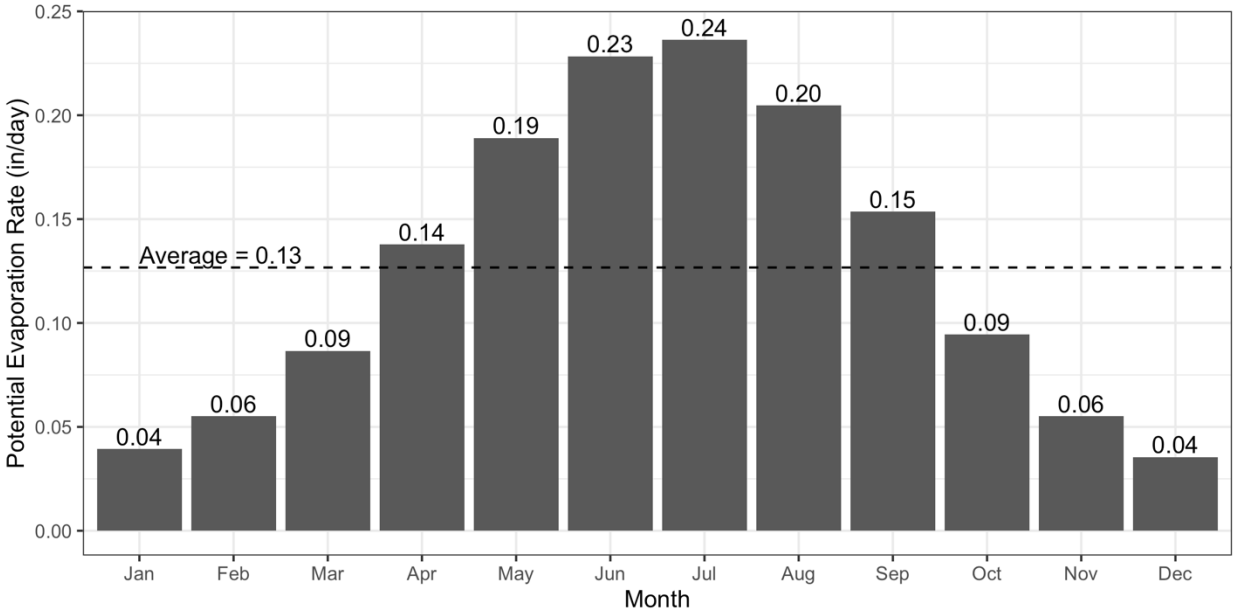

Figure 2-10: Monthly and annual average potential evaporation rates for open water bodies.
Extracted from MassGIS (2011).

2.2.1.3 POND BATHYMETRY

The bathymetry of Spy Pond was used to construct elevation-area-volume curves, which in turn were used to determine the surface elevation and area corresponding to the pond volume at each time step during the model simulation. The surface elevation was then used to calculate the outflow rate (see Section 2.2.2). The pond surface area (acres) was multiplied by the depth-based precipitation and evaporation rates (ft/hr) to calculate the volumetric fluxes (acft/hr) for these terms at each timestep.

The pond bathymetry was extracted from Figure 1 of Shanahan et al. (1997), which contained a 1-meter contour depth map of the pond that was originally presented in Chesebrough and Duerring (1982) (Figure 2-11). This map was georeferenced and digitized in QGIS by drawing a polygon for each contour line. The area of each polygon was then calculated and used to construct cumulative area and volume curves over depth. The volume of each vertical stratum (i.e., contour slice) was calculated using the equation for a truncated cone (Wetzel, 2001):

$$V_i = \frac{h}{3}\left(A_1 + A_2 + \sqrt{A_1 A_2}\right) \quad (5)$$

where V_i is the volume of stratum i (ft^3), h is the vertical depth (ft), and A_1 and A_2 are the top and bottom areas of the stratum (ft^2).

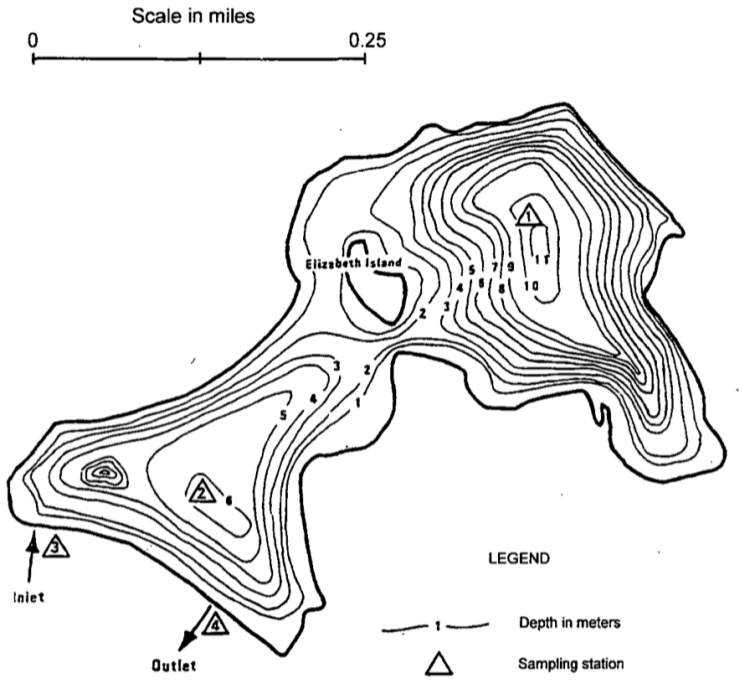

Figure 2-11: Bathymetric map of Spy Pond.
Extracted from Figure 1 of Shanahan et al. (1997), originally from Chesebrough and Duerring (1982).

The depths were converted to elevations relative to the NGVD29 vertical datum assuming that the bathymetry shown in Figure 2-11 reflected the typical water level of the early 1980s[4]. The MADOT outfall structure diagram (Figure 2-13) indicates that the typical water level prior to 1985 was approximately 3.5 – 4 ft NGVD29. Therefore, the surface elevation corresponding to the zero-meter contour in Figure 2-11 was assumed to be 3.75 ft NGVD29, which is the average of that range. Each depth interval was thus converted to an NGVD29 elevation by adding 3.75 ft. This process ultimately yielded a series of curves relating all four morphological variables: elevation, depth, area, and volume (Figure 2-12). Because the model was expected to predict water levels that exceeded the highest elevation (3.75 ft NGVD29) on the bathymetric map during large storm events, these curves were extrapolated to a maximum elevation of 10 ft NGVD29 assuming a power relationship between elevation and area.

[4] The original report containing this bathymetry was published in 1982 (Chesebrough and Duerring, 1982).

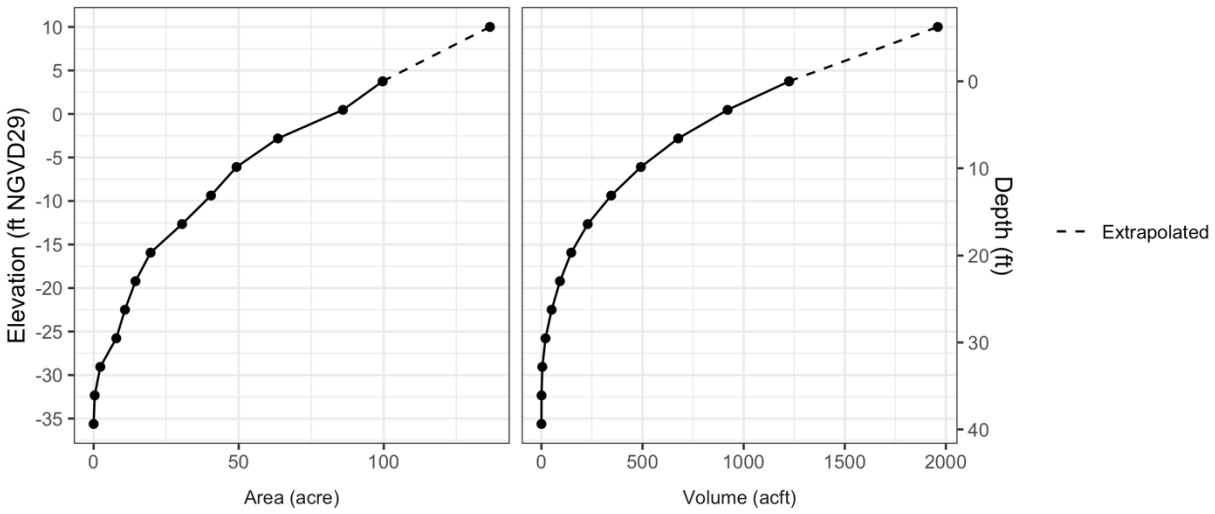

Figure 2-12: Bathymetric relationships between elevation (NGVD29), depth, area, and volume.

2.2.1.4 POND WATER LEVEL MEASUREMENTS

Continuous water level measurements of Spy Pond were collected by MyRWA from July 13, 2017 to July 23, 2018. These measurements were used to 1) develop an empirical relationship between outflow and pond surface, and 2) validate the simulated historical water levels as predicted by the water budget model.

The water level measurements were collected using an Onset HOBO pressure logger that was deployed near the pond's outflow structure at a depth of approximately 1 ft and recorded pressure measurements at 5-minute intervals. The data logger was periodically retrieved by MyRWA staff to recharge the battery and download the recorded data. There was one long gap of missing data from Oct 19 to Nov 16, 2017 and a second shorter gap from Mar 29 to April 6, 2018 during which no data was saved due to the data logger having reached its memory capacity.

The measurements recorded by the data logger were corrected for atmospheric pressure variations using hourly barometric pressure records from the ISD database for WMO Station 725090 (WBAN 14739) located at Logan Airport in Boston, MA (NOAA NCEI, 2001). The corrected pressure readings were then converted to water levels relative to a staff gage that is affixed to the outflow structure based on the depth at which the logger was deployed. The water levels relative to the staff gage were then converted to elevations relative to the NGVD29 vertical datum by adding to each observation a value of 2.29 ft, which is the elevation in NGVD29 of the zero mark on the staff gage[5]. Lastly, the data were aggregated from the original 5-minute intervals to hourly intervals by calculating the mean over each hour (Figure 2-14). During this period, the pond surface elevation ranged over 3.3 – 4.4 ft NGVD29 with a median of 3.9 ft NGVD29.

[5] The distance between the zero mark on the staff gage and the top of the outfall structure, which as an elevation of 7.32 ft NGVD29 (Figure 2-13), was measured as 5.03 ft. The difference of these two elevations (2.29 ft = 7.32 ft – 5.03 ft) is therefore the elevation in NGVD29 of the zero mark of the staff gage (Figure 2-14).

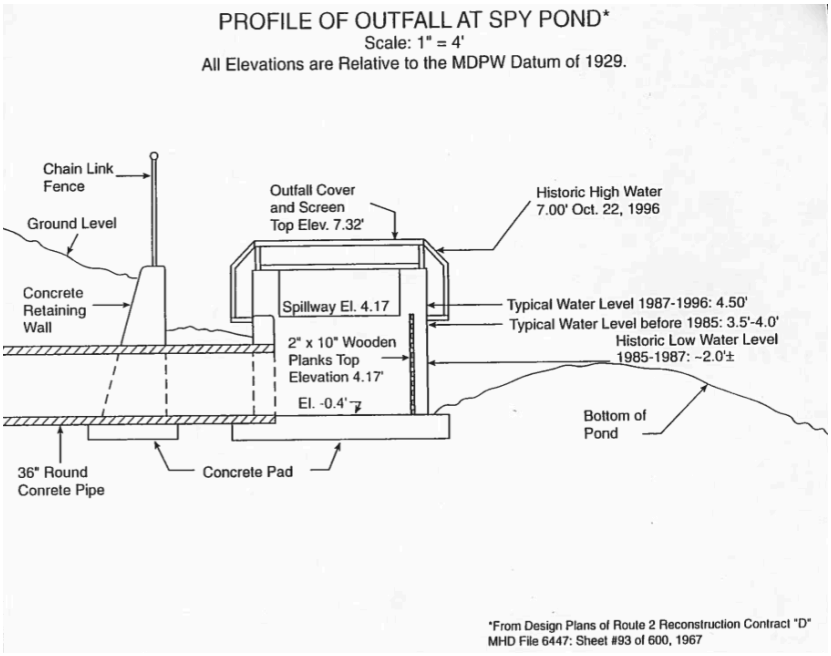

Figure 2-13: Profile diagram of Spy Pond outfall structure.
Note: elevations are relative to the NGVD29 vertical datum.

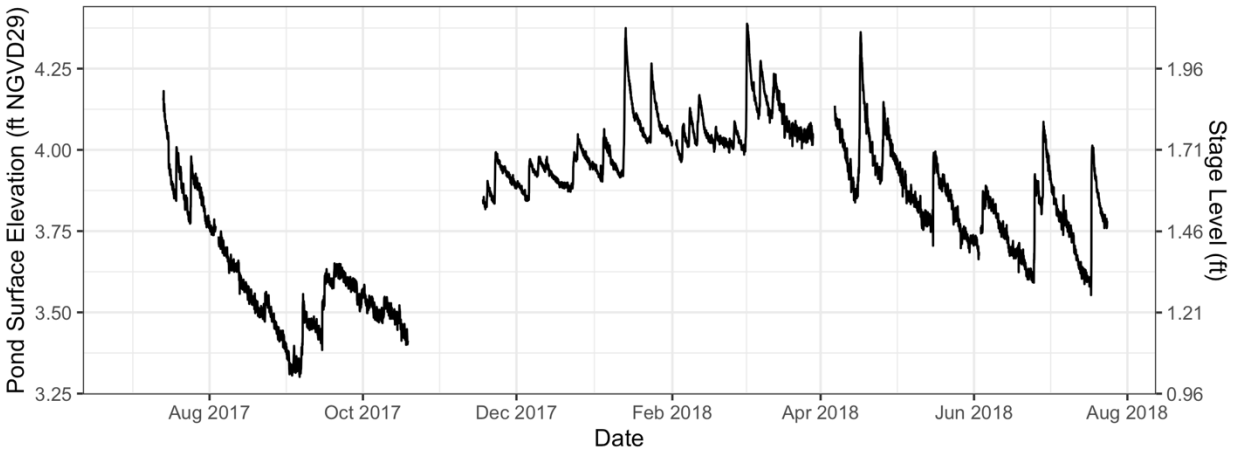

Figure 2-14: Observed hourly mean pond surface elevations measured from July 2017 to July 2018.
Note: secondary y-axis shows values relative to the staff gage affixed to the outfall structure.

2.2.1.5 Land Elevation Dataset

A land elevation data layer was used to quantify the extent of shoreline flooding based on simulated pond surface elevations. A series of tiled raster layers containing a LIDAR digital elevation model (DEM) at 1-meter resolution were obtained from MassGIS (2017). The tiles were merged into a single raster layer and the vertical datum changed first from meters to feet NAVD88, and then from feet NAVD88 to feet NGVD29 by adding 0.81 ft, which is the datum offset as determined using NOAA's VERTCON utility (NOAA, 2019). The resulting elevation layer reveals a steep increase in elevation to the north and west of the pond, and lower lying areas located along the southern and north-eastern shores (Figure 2-15).

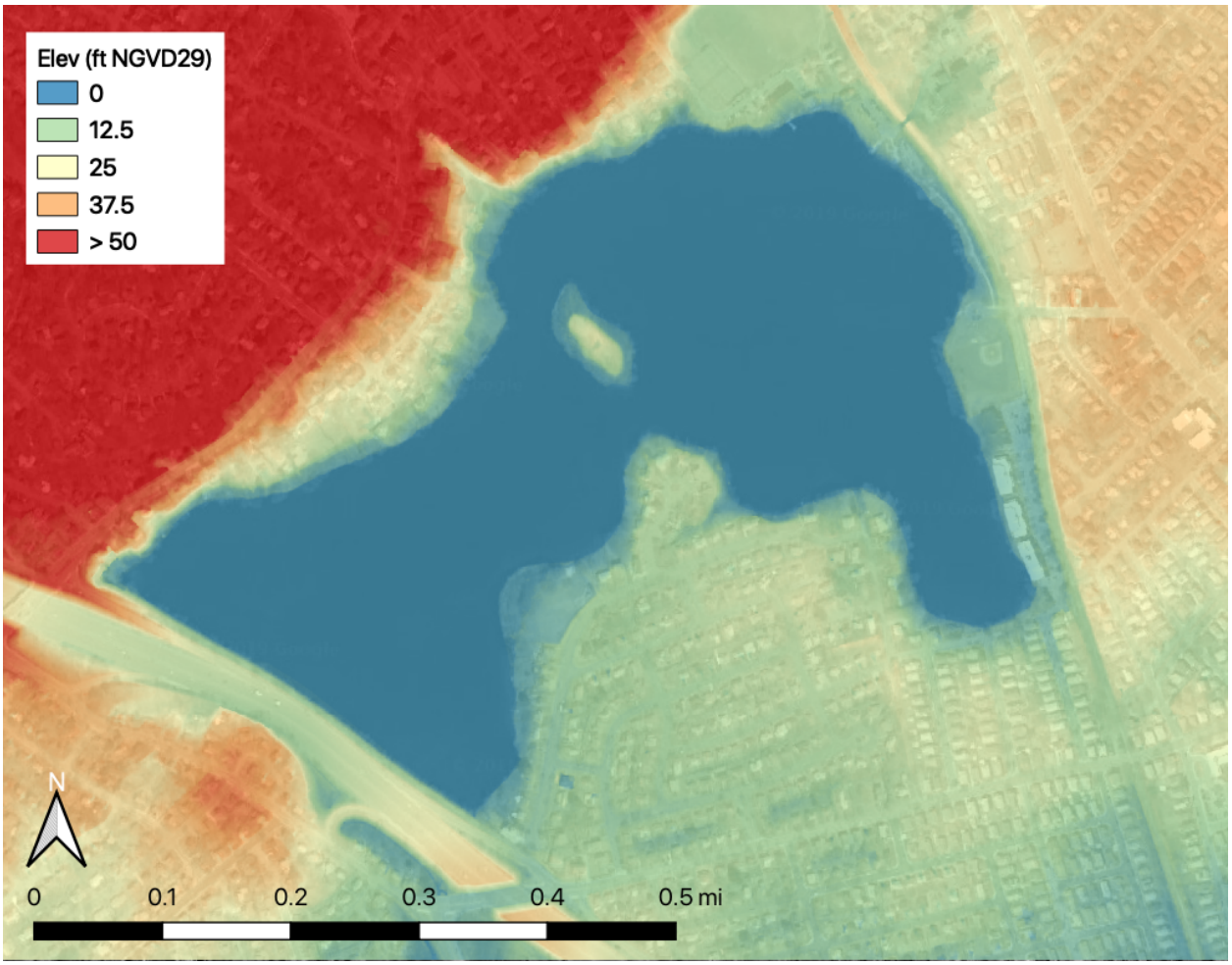

Figure 2-15: LIDAR digital elevation model around Spy Pond.
Underlying basemap shows satellite imagery (ESRI World Imagery).

2.2.1.6 ALEWIFE BROOK STREAMFLOW

Historical streamflow records of Alewife Brook were used to evaluate the potential impacts of Spy Pond outflows on downstream flows, in particular on the peak flows that are associated with the highest flooding risk. Instantaneous streamflow data were retrieved from the U.S. Geological Survey National Water Information System (USGS, 2019) for station 01103025 (Alewife Brook Near Arlington, MA) for the period Oct 6, 2005 to Sep 30, 2018 (Figure 1-1). The instantaneous streamflow data were aggregated from 15-minute intervals to hourly intervals by calculating the mean streamflow over each hour (Figure 2-16). There was one long gap of missing data from Oct 1, 2006 to Sep 30, 2007, which encompasses all of WY 2007. There were also numerous shorter gaps of a few days or less, which were not filled since a continuous timeseries was not required for this dataset.

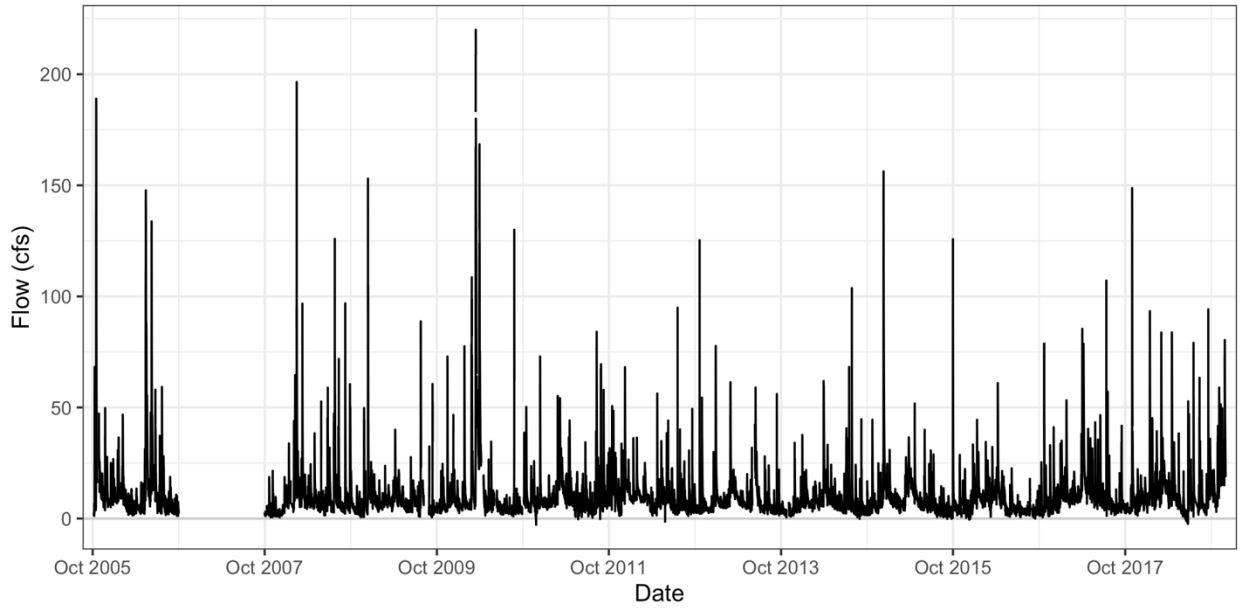

Figure 2-16: Hourly streamflow at the USGS station on Alewife Brook.

2.2.2 Empirical Elevation-Outflow Model

An empirical model was developed to estimate the outflow rate at any given time based on the water surface elevation of the pond. Because direct measurements of pond outflows were not available, historical outflow rates were estimated using the measured water levels (Section 2.2.1.4) to calculate fluctuations in pond volume. By rearranging the water budget equation (Eqn 3, Section 2.2), the outflow rate was estimated based on the calculated change in volume (dV/dt) along with the other fluxes for which historical or estimated values were available.

$$Q_{out} = Q_{in} + A \cdot (P - E) - \frac{dV}{dt} \quad (6)$$

Preliminary results of this analysis revealed that the short-term variability (i.e., noise) in the hourly timeseries of measured water surface elevations caused the estimated outflows to have very high variability, which in turn led to a poor relationship between elevation and outflow. To reduce this noise, the running 12-hour mean of the measured elevations were calculated resulting in a smoother curve for which incremental changes in volume (i.e., the derivative of the time series) were more stable and continuous. As an example, Figure 2-17 shows the elevation, volume, and calculated change in volume (dV/dt) during January 2018 using the raw hourly measurements (gray) and the smoothed timeseries based on the 12-hour rolling average (black). Although the noise associated with the measured data appears small in the elevation and volume timeseries, the change in volume exhibits much higher variability, which in turn caused high variability in the estimated outflows. The calculated change in volume using the smoothed data (black line) resulted in a more continuous and stable timeseries from which estimated outflows could be estimated more reliably.

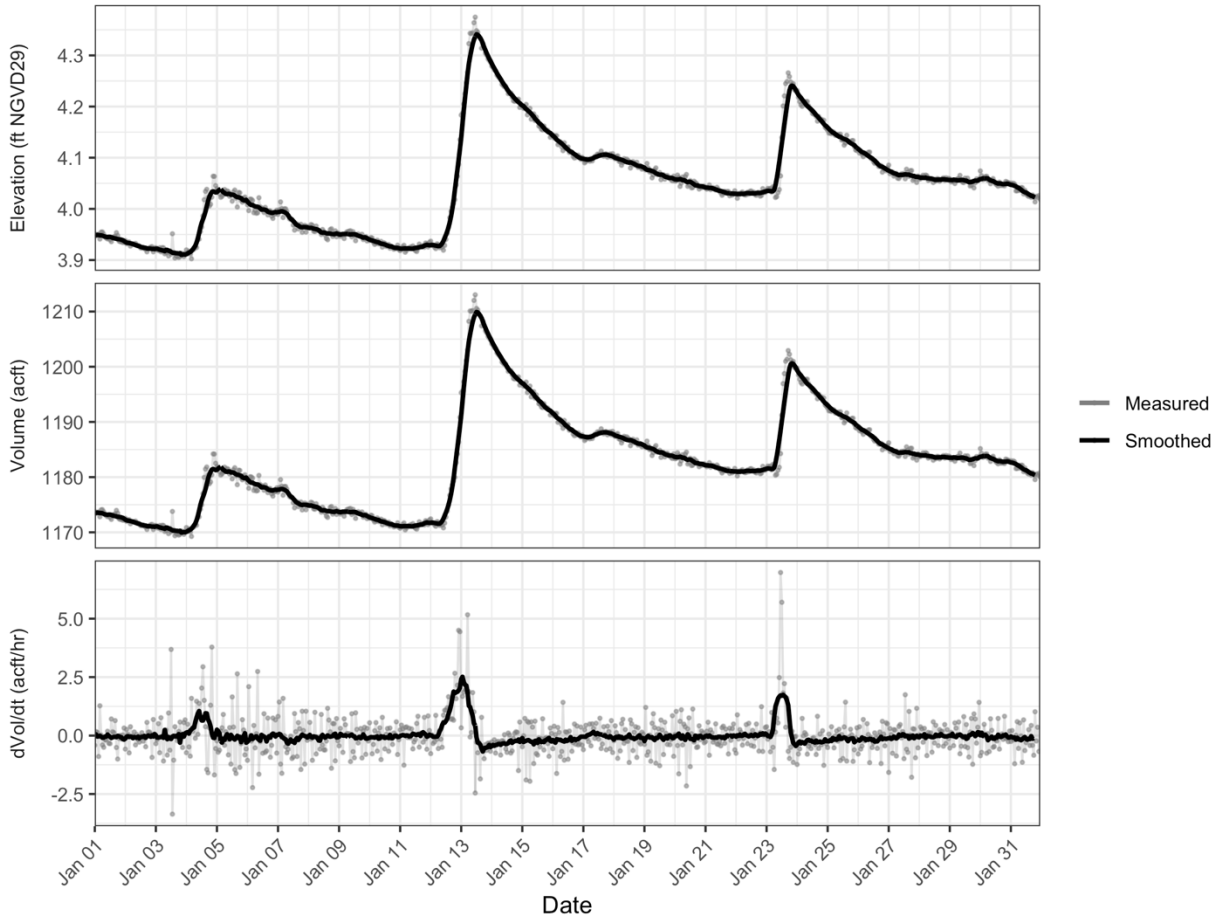

Figure 2-17: Water surface elevation, volume, and calculated change in volume using measured and smoothed timeseries during Jan 2018.

During the preliminary analyses, it also became clear that the estimated outflow rates were very sensitive to the hourly inflow rates, which could be orders of magnitude higher than the other terms during wet weather events. Because inflows were not measured and instead estimated using the runoff model, the calculated outflows would thus incorporate any errors associated with the inflows. Therefore, the empirical outflow model was fitted using only the timesteps during dry weather conditions so that the change in volume would be due solely to evaporation and outflow. Each timestep was considered to represent dry weather conditions if the rolling 24-hour sum of inflows and precipitation was zero. During dry weather, Eqn 6 could thus be simplified to

$$Q_{out} = -\left(A \cdot E + \frac{dV}{dt}\right);\ when\ Q_{in} = P = 0 \quad (7)$$

For each timestep, the surface area (A) was calculated from the measured surface elevation using the elevation-area curve (Section 2.2.1.3), and the evaporation rate (E) based on the monthly values used in the water budget model itself (Section 2.2.1.2). The hourly net change in pond volume (dV/dt) was calculated by first converting the measured water surface elevations to a timeseries of hourly pond volumes using the elevation-volume curve (Section 2.2.1.3), and then calculating the difference between the volume at each timestep and the volume from the previous timestep. The estimated hourly outflow rate was then calculated using Eqn 7.

Figure 2-18 shows an example of these calculations for January 2018. Each timestep is color coded depending on whether it represents wet (red) or dry (gray) conditions. This figure emphasizes how the dry weather timesteps (gray points) represent conditions when the pond was draining following each wet weather event. Only these dry weather

timesteps were therefore used to develop the empirical relationship between pond elevation and outflow (see below). For the wet weather timesteps (red points), the 24-hour inflow + precipitation exceeds zero and the elevation generally increases depending on the amount of inflow. The estimated outflow rates shown in this figure also demonstrate how outflows were highest shortly after the pond had reached its peak elevation following the two largest storms (Jan 13-15 and Jan 24-25, 2018). As the water level receded after these storms, the outflow rate steadily decreased suggesting a positive relationship between the outflow rate and water level.

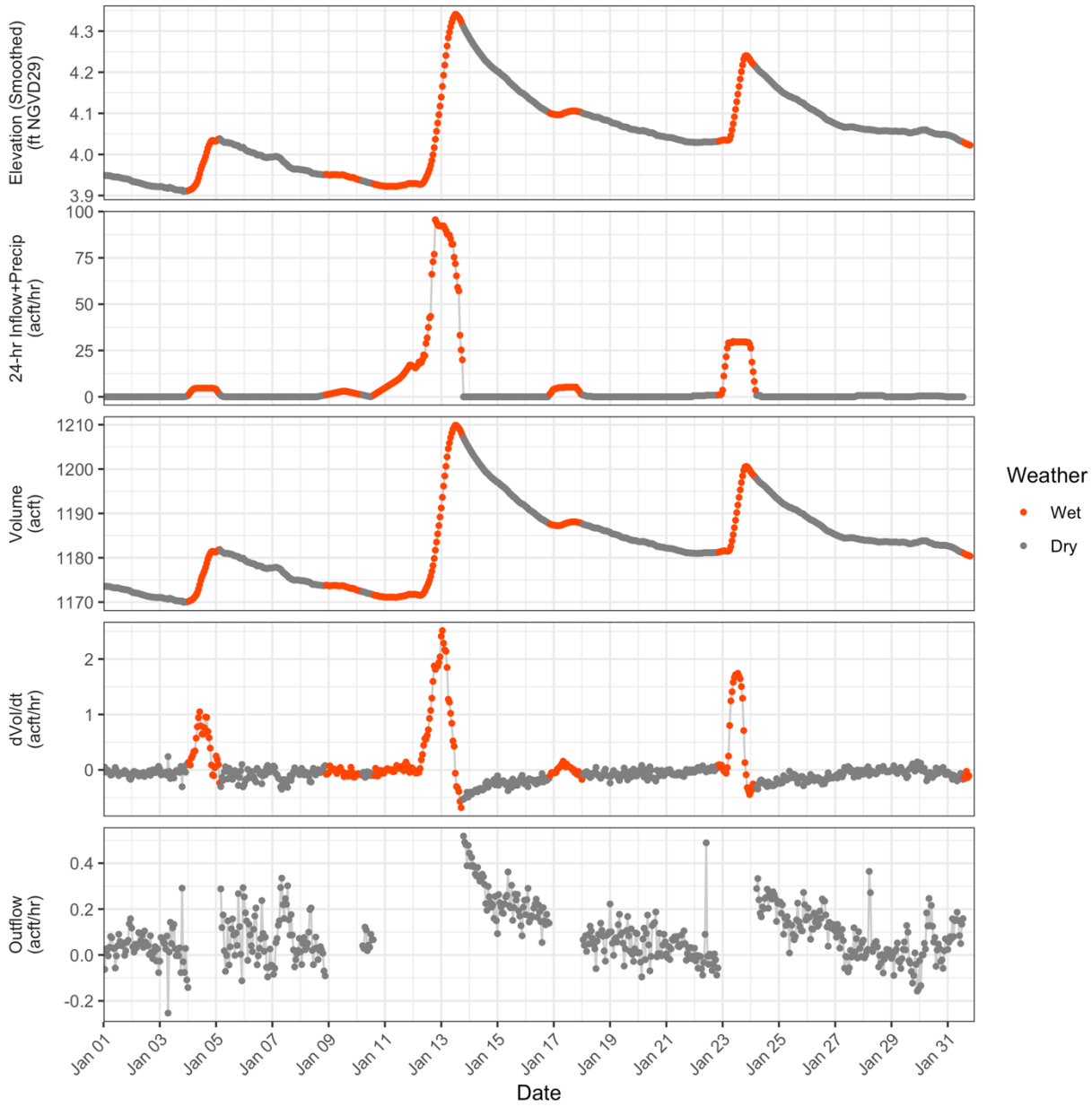

Figure 2-18: Calculations for estimating hourly outflow rates during dry weather in Jan 2018.

Using the results of these calculations for the dry weather periods over the entire monitoring period (July 2017 – July 2018), an empirical relationship between the hourly flow rate and corresponding pond surface elevation was

developed using a piece-wise linear model (Figure 2-19). The dataset was split into two subsets based on whether the elevation was above or below 4.17 ft NGVD29, which corresponds the elevation of the spillway in the pond outfall structure (Figure 2-13). This threshold for splitting the data was selected based on the assumption that the hydraulic relationship between the pond elevation and the outflow rate would differ depending on whether the water surface is above or below the spillway. For each of the two subsets, a linear regression model was fitted to the data using the estimated outflow rate as the dependent variable and the surface elevation as the independent variable. Both fitted models yielded positive slopes that were statistically significant, with the model for the higher elevation subset having a much greater slope as expected due to the ability of water to flow over the spillway (Table 2-2). To create a single continuous relationship between outflow and elevation, the two linear regression models were combined at their intersection point, which occurred at an elevation of 4.14 ft NGVD29 where the estimated outflow was 0.071 acft/hr (0.86 cfs). Because this intersection point is relatively close to the spillway elevation (a difference of only 0.03 ft, or 0.4 inches), this result confirms that splitting the dataset at the spillway elevation accurately reflects a change in the hydraulic relationship. Lastly, because the lower elevation model yields negative estimated outflows rates at elevations below 3.62 ft NGVD29, the relationship was truncated at a value of zero for any elevations below 3.62 ft NGVD29. The combined model, which is shown as the solid black line in Figure 2-19, is therefore represented by the following multi-part equation:

$$Q_{out} = \begin{cases} 0 & if\ Z < 3.62 \\ -0.493 + 0.136 \cdot Z & if\ 3.62 \le Z < 4.14 \\ -11.187 + 2.719 \cdot Z & if\ Z \ge 4.14 \end{cases} \quad (8)$$

where Q_{out} is the estimated outflow rate (acft/hr) and Z is the water surface elevation (ft NGVD29).

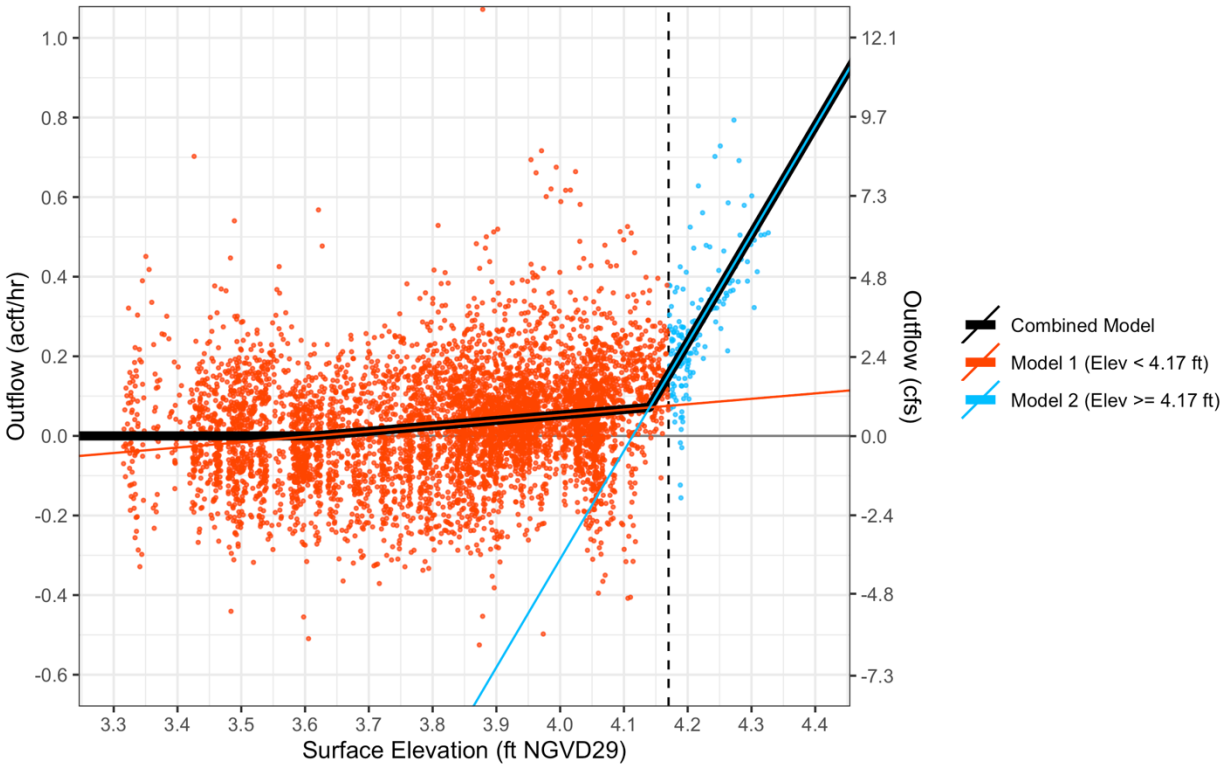

Figure 2-19: Empirical relationship between pond outflow and surface elevation using a piecewise linear model.

Note: Vertical dashed line denotes the spillway elevation of 4.17 ft NGVD, which was used to split the dataset for fitting two separate models

Table 2-2: Coefficient estimates for linear regression models of elevation vs outflow.
Note: Each model predicts the outflow rate (Qout, acft/hr) as a function of pond surface elevation (Z, ft NGVD29)

Model	Term	Estimate	Std. Error	t Value	p Value
Model 1 (Elev < 4.17 ft)	Intercept	-0.493	0.0317	-15.55	< 0.0001
	Slope	0.136	0.00829	16.45	< 0.0001
Model 2 (Elev >= 4.17 ft)	Intercept	-11.187	0.978	-11.44	< 0.0001
	Slope	2.719	0.232	11.72	< 0.0001

2.2.3 Historical Simulation Results

Using the empirical elevation-outflow relationship along with the other input timeseries for inflows, precipitation and evaporation, the water balance model was run at hourly timesteps for the full simulation period from Oct 1, 2005 to Sep 30, 2018 (WY 2006 – WY 2018). The initial water level was set to 3.8 ft NGVD29, which is approximately average for that time of year (Oct 1). Timeseries plots show the simulated hourly elevations along with the hourly fluxes for each of the four water budget terms (Figure 2-20). The cumulative frequency plots show the distributions of the simulated hourly elevations and outflow rates (Figure 2-21).

The simulated pond surface elevation ranged from a minimum of 2.74 ft NGVD on Sep 19, 2016 to a maximum of 5.90 ft NGVD29 on May 14, 2006 (Figure 2-21). The median elevation was 3.96 ft NGVD29, which is below the spillway elevation of 4.17 ft NGVD (Figure 2-13). Elevations were between 3.5 and 4.5 ft NGVD29 for most (93%) of the time. Two extended dry periods in the late summer and early fall of 2007 and 2016 resulted in elevations reaching 3 ft NGVD29 or lower. Elevations exceeded 5 ft NGVD during four events over the simulation period.

The simulated outflow rates were effectively zero (< 0.01 cfs) for 10.8% of the time and reached a maximum of 58.8 cfs on May 14, 2006 when the simulated elevation had also reached its maximum value (Figure 2-21). The median outflow rate was 0.56 cfs. Outflows were greater than 1 cfs for 11.7% of the time, and greater than 10 cfs for only 0.9% of the time. The cumulative frequency distribution for outflows shows a discontinuity at 0.86 cfs, which corresponds to the intersection point of the two linear regression models used for the empirical relationship between elevation and outflows (see Figure 2-19).

It is important to note that the simulation required extrapolation of the elevation-outflow model beyond the range of observed elevations. During the July 2017 – July 2018 monitoring period, the observed pond elevations ranged from 3.3 to 4.3 ft NGVD29 during the dry weather timesteps used to develop the empirical relationship (Figure 2-19). When the simulated elevation was below the minimum observed elevation (3.3 ft NGVD29), the outflow rate was assumed to be zero. When the simulated elevation was greater than the maximum observed elevation (4.3 ft NGVD29), the elevation-outflow relationship was linearly extrapolated using the high-elevation linear regression model (Model 2, Table 2-2). This extrapolation for simulated elevations between 4.3 and the maximum simulated elevation of 5.9 ft NGVD is a major source of uncertainty in this study as will be discussed in Section 4. Additional monitoring data are needed to calculate the observed outflow rates that actually occur in this range of higher elevations. Additionally, a hydraulic analysis could also provide an improved estimate of flow rates at these higher elevations by determining the maximum capacity of the flow structure and the concrete pipe that transports outflows downstream into Little Pond.

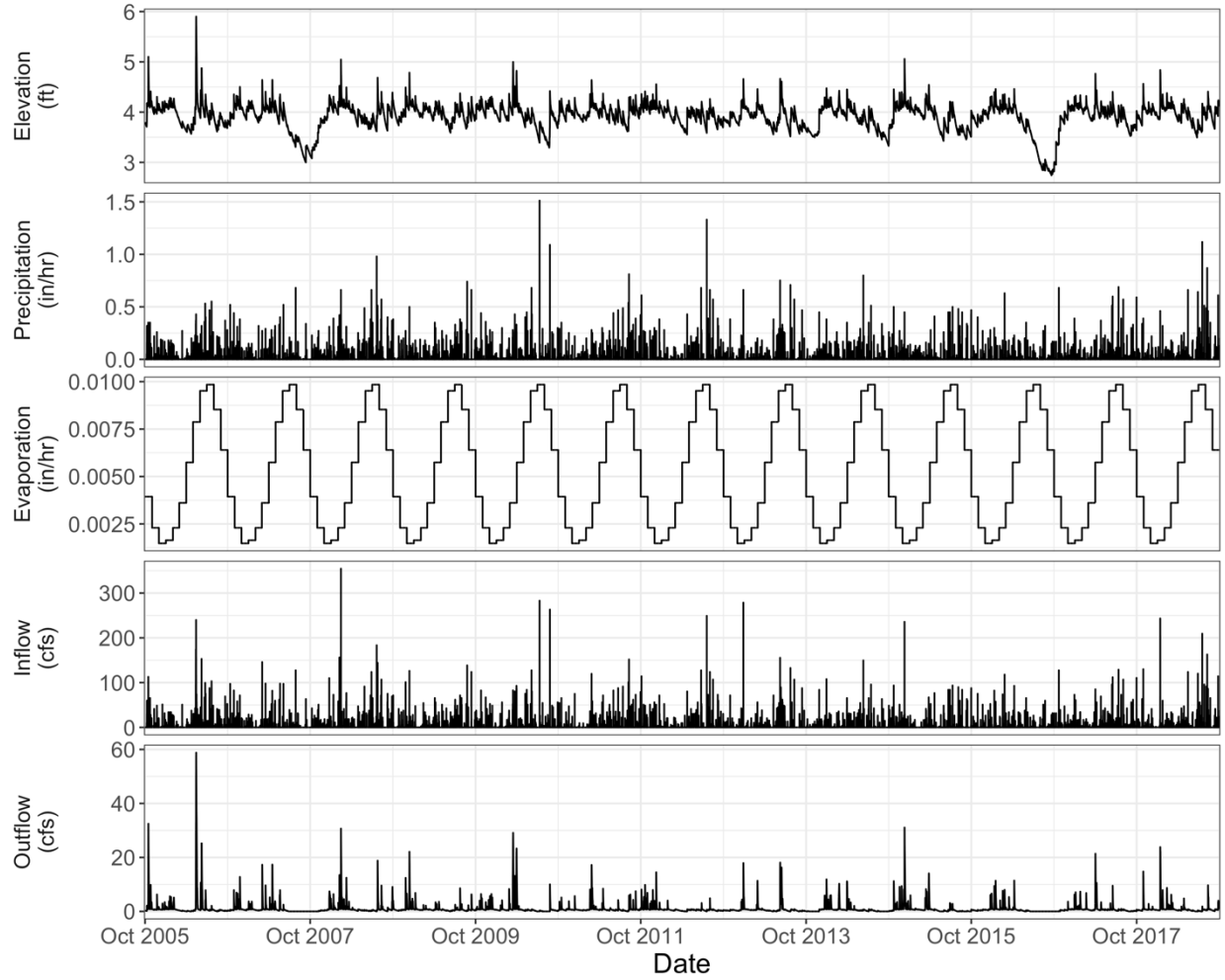

Figure 2-20: Simulated elevation and water budget fluxes for historical conditions, WY 2006 - WY 2018.

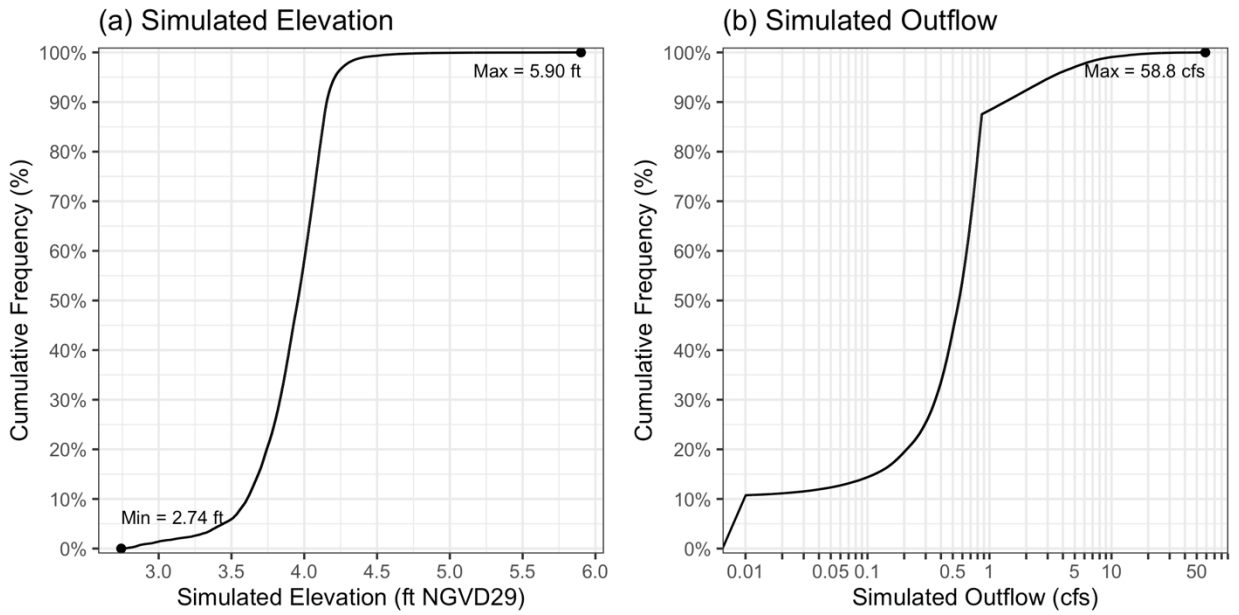

Figure 2-21: Cumulative frequency distributions of simulated elevation and outflow.
Note: the simulated outflow distribution is truncated at a minimum value of 0.01 cfs due to the logarithmic scale.

2.2.3.1 VALIDATION TO OBSERVED WATER LEVELS

A model validation was performed by comparing the simulated and observed water levels during the monitoring period from July 2017 to July 2018. Typically, models like this are first calibrated to one observation dataset, and then validated against another observation dataset that is independent of that used for calibration. During model calibration, the input data and/or parameter values would be adjusted in order to maximize the goodness-of-fit of the model relative to the observed data. However, in this study, neither the runoff model nor the water budget model was explicitly calibrated and all model parameters were either based on default values (e.g., the runoff model) or calculated directly from observed data (e.g., elevation-outflow relationship). Therefore, the following comparison of simulated and observed water levels was considered a model validation, the purpose of which was to ensure that the model results were reasonably accurate in terms of representing the water budget dynamics of the pond.

In general, the comparison of observed and simulated pond elevations showed a reasonably close agreement especially given that the models were not explicitly calibrated (Figure 2-22). The observed and simulated timeseries reflect similar seasonal patterns with lower elevations in the fall and summer and higher elevations in the late winter and spring. As with any timeseries model, errors in any one timestep can propagate over an extended period of time since the simulated value of each timestep depends on the value of the previous timestep. For example, the simulated elevations begin deviating from the observed elevations during a storm event on July 24, 2017 near the start of the simulation due to differences in the initial rise of the water level. During this storm, the observed water levels increased by 0.2 ft from 3.78 to 3.98 ft NGVD29 while the simulated water levels increased by 0.33 ft from 3.81 to 4.14 ft NGVD29. Due to the difference in this initial rise, the two timeseries continue to differ by approximately 0.1 ft as the pond level receded following the storm. This difference was likely caused by errors associated with the inflow rates, which may have been over-estimated by the runoff model due to inaccuracies in the rainfall timeseries (e.g., the rainfall measured at Logan Airport was higher than what actually fell in the Spy Pond watershed). The simulated timeseries also shows that there were two significant storms causing rapid increases in water level, which were not reflected in the observed timeseries (August 1, 2017 and Oct 1, 2017). Again, these differences could be caused by inaccuracies of the rainfall dataset, which may have included observed rainfall at Logan Airport that did not actually occur within the Spy Pond watershed. Lastly, the highest simulated elevation

during this period was 4.84 ft NGVD29 on January 13, 2018, which was 0.47 ft higher than the highest observed elevation of 4.37 ft NGVD on that same day. For this storm, inaccuracies in the amount of snowpack and subsequent snowmelt could have also contributed to the error since it occurred during winter, in addition to potential inaccuracies in the rainfall dataset.

Despite these differences, the rates at which the pond drained following each storm event over the entire period were generally similar in both timeseries (i.e., the two lines are generally parallel even if they are offset by some amount). Therefore, given the expected uncertainty in inflow rates due to inaccuracies in estimated rainfall and snowmelt rates, the model was deemed sufficiently accurate in terms of representing the general dynamics involving storm-driven increases in water levels followed by subsequent draining of the pond. Furthermore, the simulated water levels did not exhibit any consistent bias over the entire monitoring period.

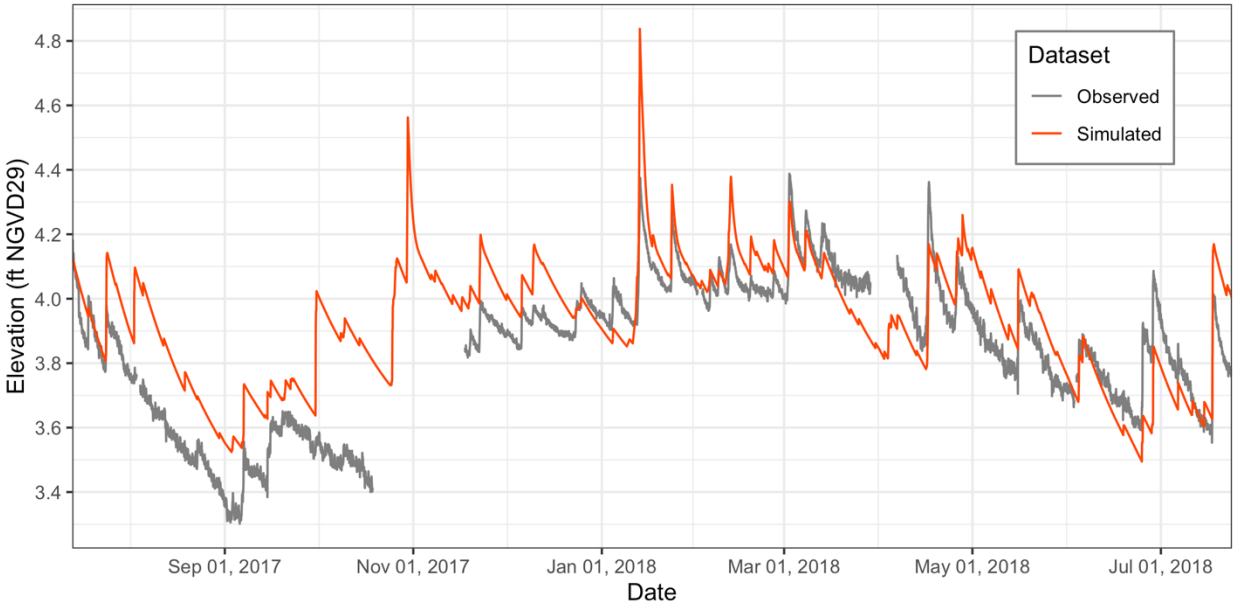

Figure 2-22: Hourly timeseries of observed and simulated pond surface elevation.

A series of goodness-of-fit metrics were calculated based on the difference between the simulated and observed water levels at each hourly timestep (Table 2-3). The maximum absolute error was 0.45 ft (5.9 inches), which occurred on Jan 13, 2018. The median absolute error and root mean squared error were 1.3 and 1.9 inches, respectively, indicating that, on average, the simulated elevations were within 2 inches of the observed elevations.

Table 2-3: Goodness-of-fit metrics of simulated and observed surface elevations from July 2017 to July 2018.

Goodness-of-Fit Metric	Value
# Observations	8,007
Max Absolute Error	0.49 ft (5.9 in)
Median Absolute Error	0.11 ft (1.3 in)
Root Mean Squared Error	0.16 ft (1.9 in)
R^2	0.61

Lastly, the frequency distributions of the simulated and observed elevations provide further confirmation that the model accurately represented the general range and variability of water levels over this period (Figure 2-23). Frequency distribution plots can be beneficial for comparing timeseries as they are not as susceptible to the

propagation of errors over time as timeseries plots. Aside from the tails of the distribution (the lowest and highest elevations), the two distributions are within 2 inches of one another at any given probability level, which is consistent with the average error reflected by the median absolute error and the RMSE.

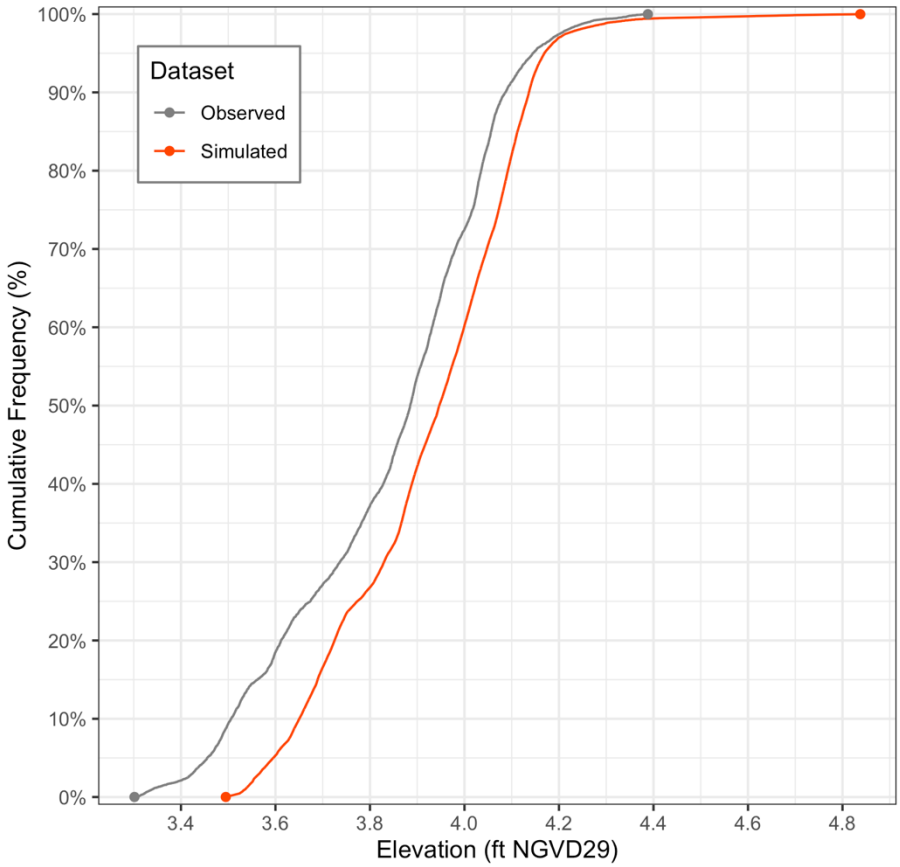

Figure 2-23: Cumulative frequency distribution of observed and simulated surface elevations for July 2017 – July 2018.

Overall, this validation confirmed that the water budget model generated reasonably accurate predictions of the pond water level over the monitoring period from July 2017 to July 2018. However, it is important to note that water surface elevations did not rise above 4.4 ft NGVD29 during this period and, therefore, the performance of the model could not be evaluated at higher elevations where higher outflow rates would presumably occur. Nonetheless, given these data limitations, the model was considered suitable for performing the stormwater capture scenario analysis presented below in Section 3.

2.2.3.2 Historical Shoreline Flooding

The long-term simulated water levels (WY 2006–WY 2018) were used to estimate the historical flooding impacts on shoreline properties due to storm-driven increases in the pond water level. Based on a visual comparison of the land elevation dataset (Section 2.2.1.5) with satellite imagery, the minimum pond elevation at which shoreline flooding would occur was determined to be approximately 5 ft NGVD29[6]. Although the maximum simulated pond elevation was 5.9 ft NGVD29 (Figure 2-21), the flood zone was extended to a maximum of 7 ft NGVD29 to show the full extent

[6] Flooding along the shore of Elizabeth Island, which is located near the center of the pond, and in the wetland area along the southern shore were not considered in order to focus only on flooding of private properties along the main shoreline.

of flooding for events more extreme than those during the simulation period. A map was generated showing the extent of flooding for pond surface elevations ranging from 5 to 7 ft NGVD29 based on the land elevation dataset (Figure 2-24). This map indicates that the greatest flooding risk is for properties along the western end of the southern shore (Figure 2-25). The cumulative inundated area along the main shoreline (excluding Elizabeth Island in the center of the pond) was then calculated over the range of elevations within the flood zone (Figure 2-26). Using this curve, an hourly timeseries was generated from the simulated surface elevations showing the total inundated area over the full period (Figure 2-27).

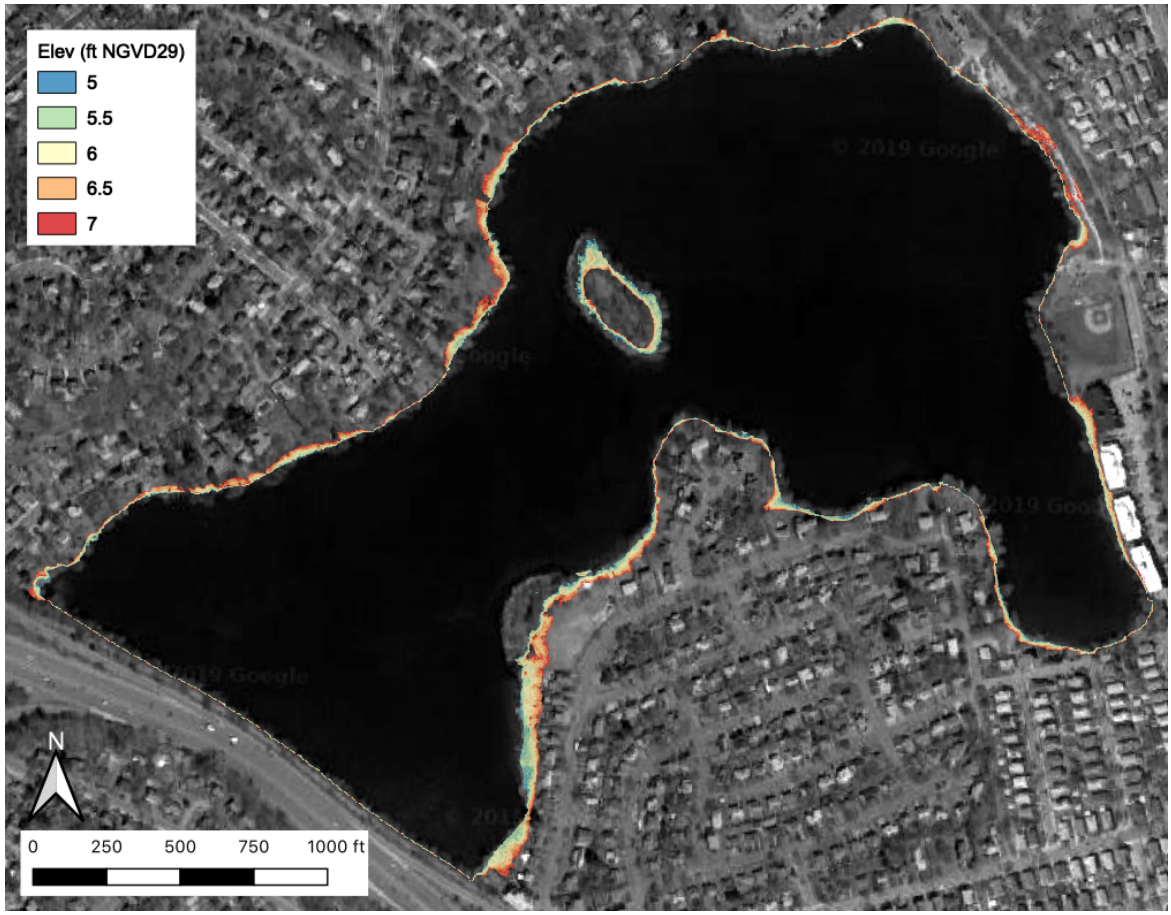

Figure 2-24: Land elevation in shoreline flooding zone from 5 to 7 ft NGVD29.

Figure 2-25: Land elevation in shoreline flooding zone from 5 to 7 ft NGVD29 along southern shore.

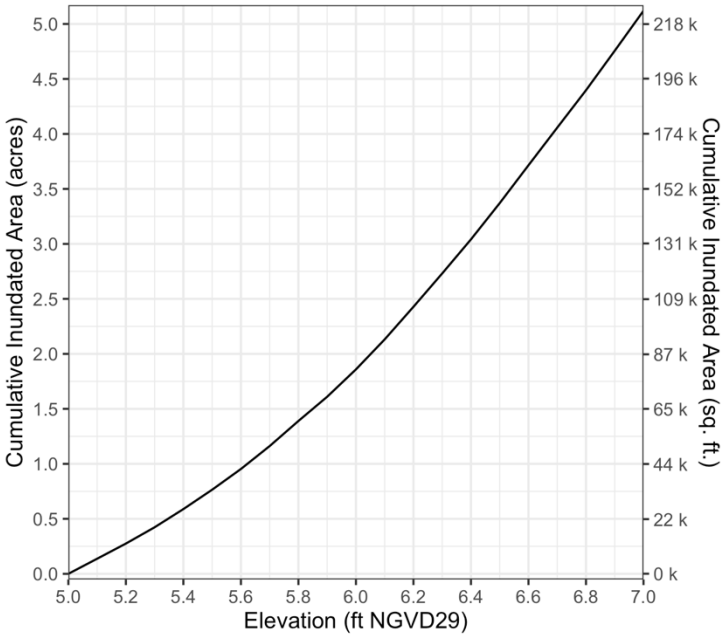

Figure 2-26: Cumulative inundated area in shoreline flood zone from 5 to 7 ft NGVD29.

Note: Excludes area around Elizabeth Island in the center of the pond.

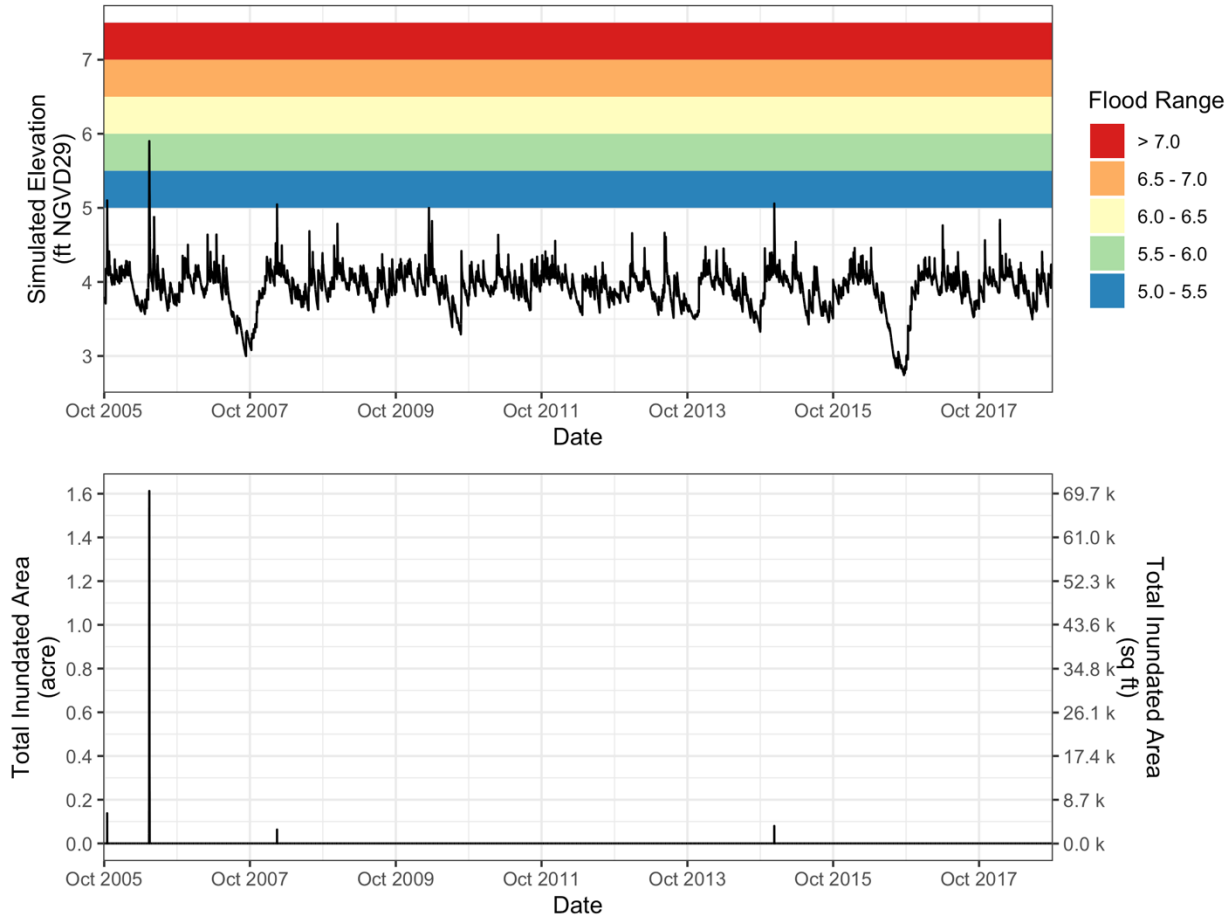

Figure 2-27: Simulated elevations with flood zone ranges and total inundated area for WY 2006–WY 2018.

The total inundated area estimated from the simulated elevations (Figure 2-27) indicates that shoreline flooding may have occurred during four events over the simulation period. Three of these events (Oct 15, 2005, Feb 13, 2008, and Dec 9-10, 2014) had limited flooding with elevations barely exceeding the minimum flood level of 5 ft NGVD29 and resulting in less than 0.15 acres of inundated area. The only major flooding event occurred during May 13-16, 2006 in which the pond elevation reached its overall maximum of 5.9 ft NGVD29 and resulted in 1.6 acres of inundation. Therefore, based on these model results, it did not appear that shoreline flooding is a common occurrence in Spy Pond, and thus stormwater capture may not provide significant benefits in terms of reducing this flooding. But it is important to note that given the model limitations, this does not mean that flooding did not occur over this period or in other periods prior to this. Additional data such as local observations of historical flood events are needed to confirm these results.

2.2.3.3 Historical Impacts on Downstream Flows

The historical impact of outflows from Spy Pond on downstream flows were evaluated using streamflow records for the USGS streamflow gage on Alewife Brook, which is located approximately 2 miles downstream of the pond outfall (Section 2.2.1.6; Figure 1-1). The following analysis is based on the assumptions that 1) outflows from Spy Pond are not attenuated between the pond outfall and the Alewife Brook streamflow gage, and 2) the travel time of peak flows between the pond and the Alewife Brook gage is less than one hour (the simulation timestep). These results therefore reflect the *maximum* potential flow contributions from Spy Pond to Alewife Brook. If the pond outflow is

in fact attenuated as it passes through the intervening reaches (e.g., Little Pond and Little River), then the contribution of any given outflow rate would be lower at the Alewife Brook gage than without any attenuation.

Instead of comparing pond outflows to Alewife Brook streamflow at all hourly timesteps, this analysis focused on comparing outflow rates at the timesteps when Alewife Brook reached its peak flow during each wet weather event. The delineation of the events (i.e., when one event ended and the next began) was generated by the runoff model algorithm based on an interevent time of 10 hours; meaning that at least 10 hours of dry weather must occur between each sequential wet weather event. The timesteps corresponding to the event peak flows were then used to evaluate the impacts of Spy Pond outflows on Alewife Brook. By using the peak flows instead of all hourly flows, the following comparisons give each event equal weight. If all hourly timesteps were used, then events that have a longer duration would contribute a greater number of data points to the comparison, and thus have a greater influence than events with shorter durations.

The individual events were categorized based on whether the peak flow in Alewife Brook was greater than 25, 50, 75, or 100 cfs during the event. These categories are sequentially inclusive meaning that events with peak flows > 25 cfs include all of the events with peak flows > 50 cfs, which in turn includes all events with peak flows > 75 cfs, etc. The contribution from Spy Pond outflows could then be compared between these four sets of events to determine whether outflows contribute more or less flow during only the largest events (> 100 cfs) vs. the full set of events > 25 cfs, or between any of the intermediary categories. Events with peak flows less than 25 cfs were excluded in order to focus on the only those storm events that generated a significant flow response. The hourly timeseries of Alewife Brook flows and Spy Pond outflows highlight the timesteps at which each event peak flow occurred (black, blue, purple, and red points; Figure 2-28). For some events, the timestep at which Alewife Brook reached its peak flow did not correspond to the same timestep at which the pond outflow reached its maximum discharge rate. However, in most of these cases, the outflow at the time of the peak flow was still significant. Since the goal of the stormwater capture scenario analysis was to minimize downstream peak flows (as opposed to peak outflows), the following comparisons focused on the timesteps when peak flows occurred in Alewife Brook rather than the timesteps corresponding to the maximum outflow rates.

As an example, a detailed comparison of these two timeseries focuses on a two-month period from May 1 to June 30, 2006, which shows the change in flows over the course of a few storm events (Figure 2-29). Included in this period is one of the largest events of the simulation when the outflow reached an overall maximum value of 58 cfs (May 14, 2006). However, in this case, the outflow reached its peak a few hours after the peak flow in Alewife Brook occurred. As mentioned above, only the outflows at the time of peak flows in Alewife Brook were used, and therefore the outflow rate corresponding to the peak Alewife Brook flow during this event was 44 cfs instead of the overall maximum of 58 cfs.

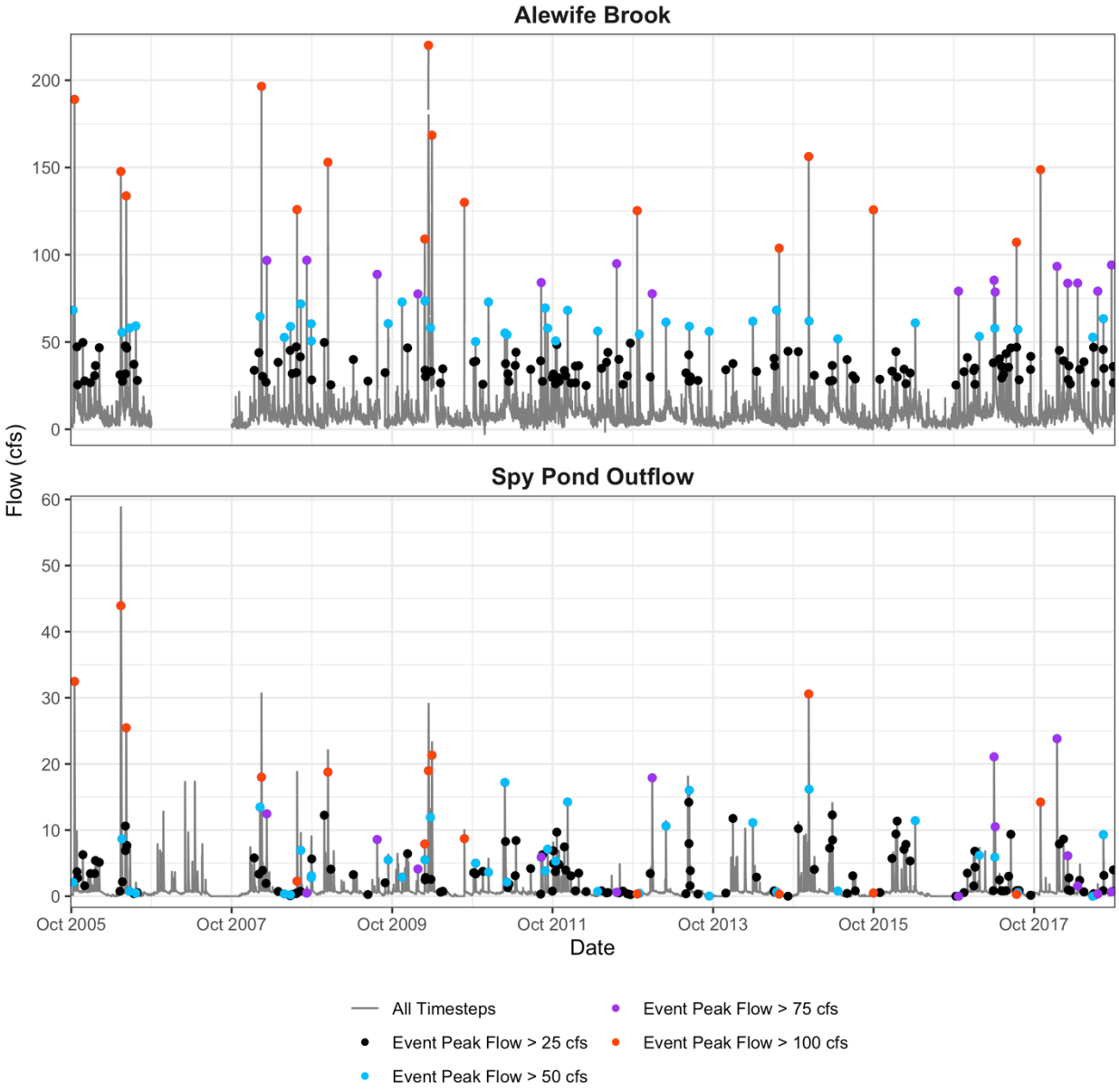

Figure 2-28: Hourly timeseries of Spy Pond outflow and Alewife Brook streamflow, WY2006–WY2018.

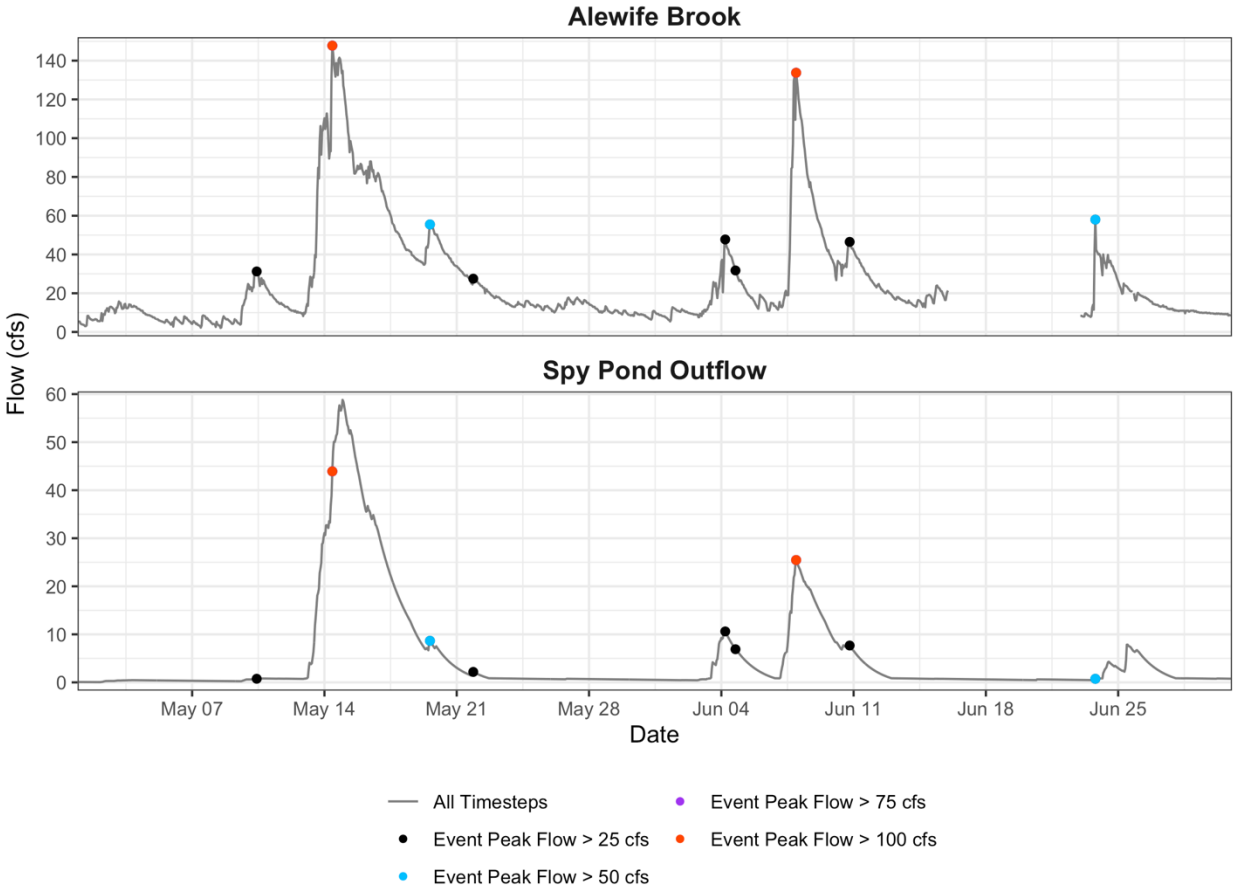

Figure 2-29: Hourly timeseries of Spy Pond outflow and Alewife Brook streamflow, May 1 - June 30, 2006.

A scatterplot comparison of the event peak flows in Alewife Brook and the corresponding Spy Pond outflows shows a generally positive relationship, although there is a wide range of variability at any given peak flow rate (Figure 2-30). For some of the larger events (peak flows > 100 cfs), the Spy Pond outflow rate was very small (< 1 cfs) either due to inaccuracies in the rainfall dataset which may have missed a real event, or because the water level in Spy Pond was already low at the start of the event and therefore did not reach high enough elevations during the event to generate appreciable outflow. But among the largest events with peak flows > 140 cfs, the Spy Pond outflows were all relatively high (14 – 44 cfs).

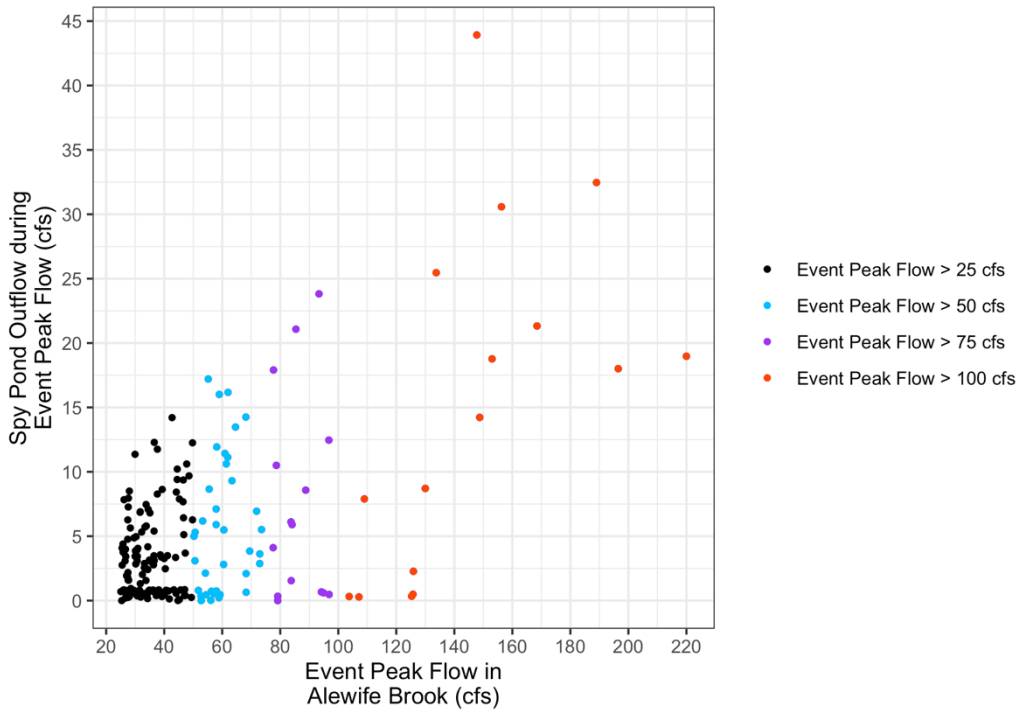

Figure 2-30: Comparison of event peak flows in Alewife Brook and corresponding Spy Pond outflow.

The cumulative frequency distribution of the Spy Pond outflows during each event peak flow was generated for each event category (e.g., peak flow > 25 cfs, > 50 cfs, > 75 cfs, and > 100 cfs) (Figure 2-31). These distributions can be used to compare the different quantiles between these events of varying sizes. For example, the median (50th percentile) outflow during all events with peak flows > 25 cfs was 3 cfs, while the median among only the largest storms (> 100 cfs) was 16 cfs. These values mean that for half of the storms with peak flows > 25 cfs, the pond outflow was 3 cfs or less; while for half of the storms with peak flows > 100 cfs, the pond outflow was 16 cfs or less. Conversely, half of the events with peak flows > 25 cfs had outflow rates greater than 3 cfs, and half of the events > 100 cfs had outflow rates greater than 16 cfs. As one would expect, the average (median) outflow was higher when only using the largest events > 100 cfs (red line) than when all events > 25 cfs were used (black line). Similarly, the higher quartiles also indicate significantly higher outflows among the largest events relative to all events > 25 cfs. For example, the 90th percentile for events > 100 cfs was about 32 cfs meaning that 9 out of 10 of these events had outflows of 32 cfs or less, and the remaining 1 event out of 10 had an outflow greater than 32 cfs.

These cumulative frequency distributions provide a basis for understanding how much Spy Pond outflows contribute to peak flows in Alewife Brook over a wide range of event sizes. Furthermore, they provide not only the average outflow for each set of events (i.e., the median), but the full distribution so that the lower and higher quantiles can also be compared. These outflow distributions thus provide a basis for understanding the potential upper limits with respect to just how much downstream peak flows can be reduced by operating Spy Pond as a stormwater capture system. If these operations can completely eliminate outflows during times of peak flow, then the peak flow reductions that could be achieved during the largest events with flows > 100 cfs would be 16 cfs on average (the median outflow), and as high as 44 cfs (the maximum) in any one storm.

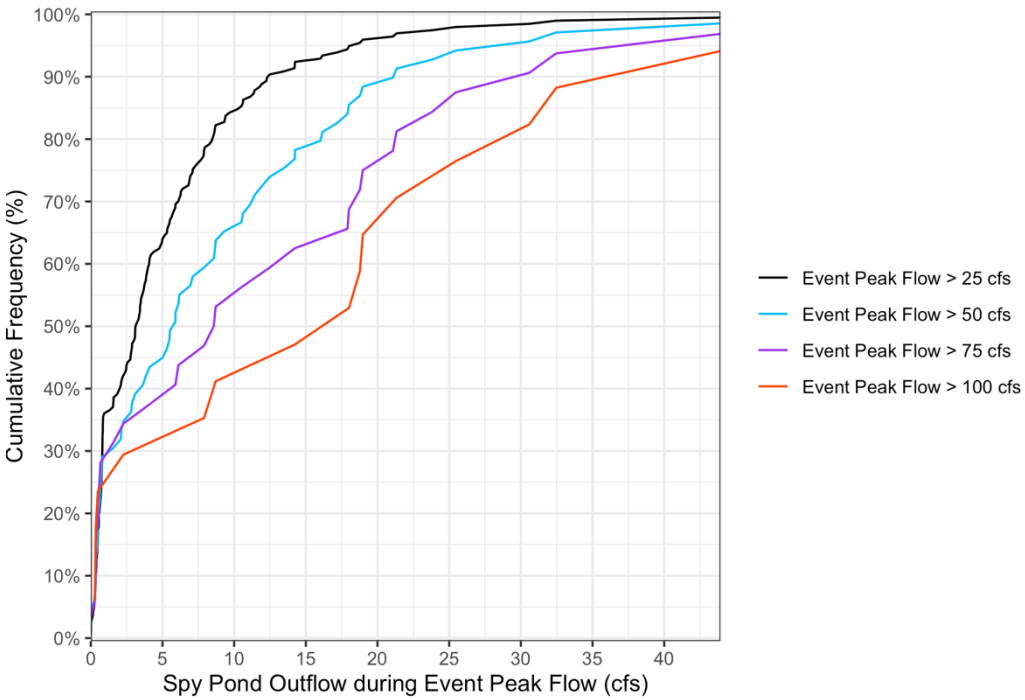

Figure 2-31: Cumulative frequency distribution of Spy Pond outflows during event peak flows.

The contributions of Spy Pond outflows to peak flows in Alewife Brook were also evaluated by calculating the ratio of the two flows (Spy Pond outflow / Alewife Brook streamflow) as a metric that reflects the relative amount of Alewife Brook peak flows originating from Spy Pond (Figure 2-32). For some timesteps, the ratio exceeded 100% meaning outflows were greater than flows in Alewife Brook; however, this only occurred during low flow periods when both the outflow and Alewife Brook flows were very small and can therefore be ignored. The flow ratios occurring at the time of peak flow in each event were highlighted using the same set of event categories as the previous comparison (black, blue, purple, red points in Figure 2-32). The relative contributions of Spy Pond outflows to Alewife Brook were then evaluated by comparing cumulative frequency distributions of the flow ratios using only the peak flow timesteps of events with varying magnitudes (Figure 2-33). The distribution based on all timesteps (not just during the peak flow of each event) is also shown for reference (gray line).

Unlike the distributions of outflows (in cfs) shown above (Figure 2-31), the distributions of the flow ratios among the four event size categories were very similar indicating that relative outflow contributions do not vary widely based on the size of the event. If the distributions for the event categories with larger peak flows (> 75 or > 100 cfs) were different from the category with all events > 25 cfs, then this would suggest that the outflows have a smaller or larger relative contribution during larger events. However, this does not appear to be the case. The median values (50th percentile) for all three event categories were all within 7-9% meaning that for half of the events Spy Pond outflows were 7-9% or less of the total peak flow at Alewife Brook, and for the other half of the events outflows were more than 7-9%. Similarly, the 90th percentiles of the event peak flow distributions ranged from 19-23% meaning for 9 out of 10 events outflows were 19-23% or less of the total Alewife Brook flow. These distributions of relative peak flow contributions thus provide an alternative means to evaluate the impacts of reducing Spy Pond outflows based on values that are normalized relative to the peak flow (in cfs) of each event.

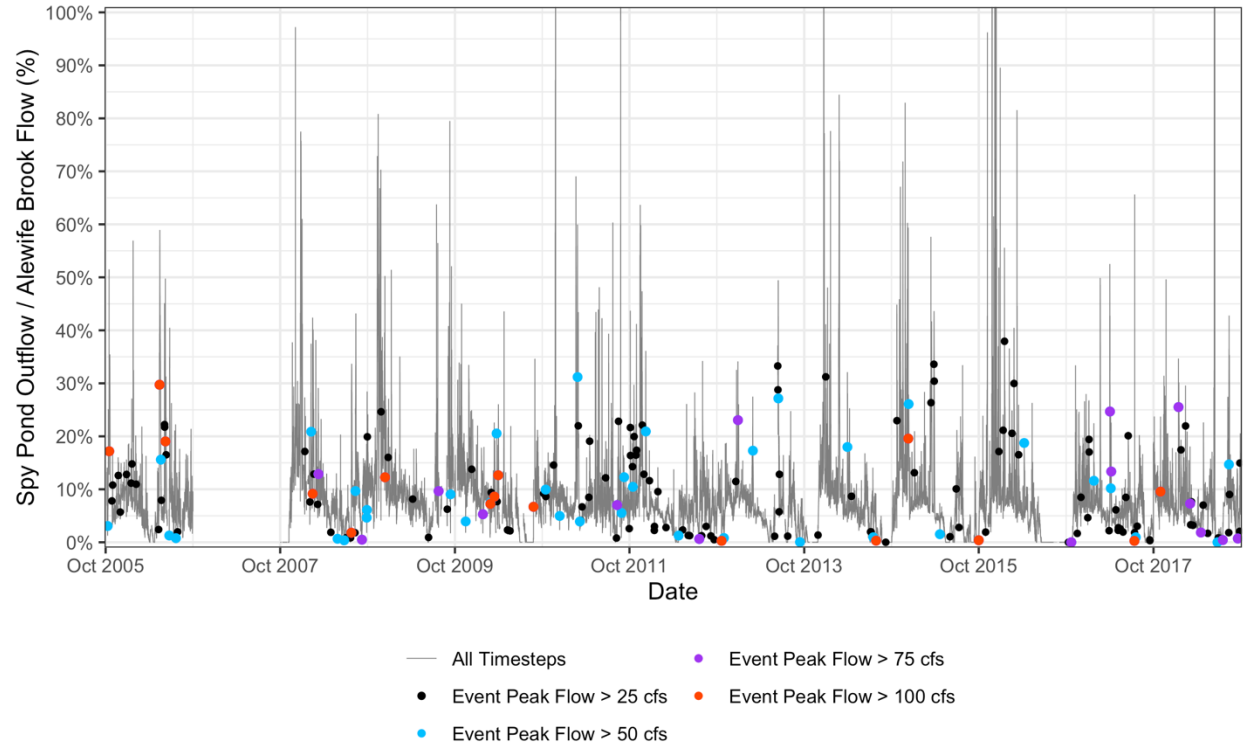

Figure 2-32: Timeseries of ratio between Spy Pond outflow and Alewife Brook streamflow for all hourly time steps and event peak flows, WY2006–WY2018.

Note: Ratios (y-axis) are truncated to a maximum value of 100%. Event peak flows based on max Alewife Brook flows during each storm event.

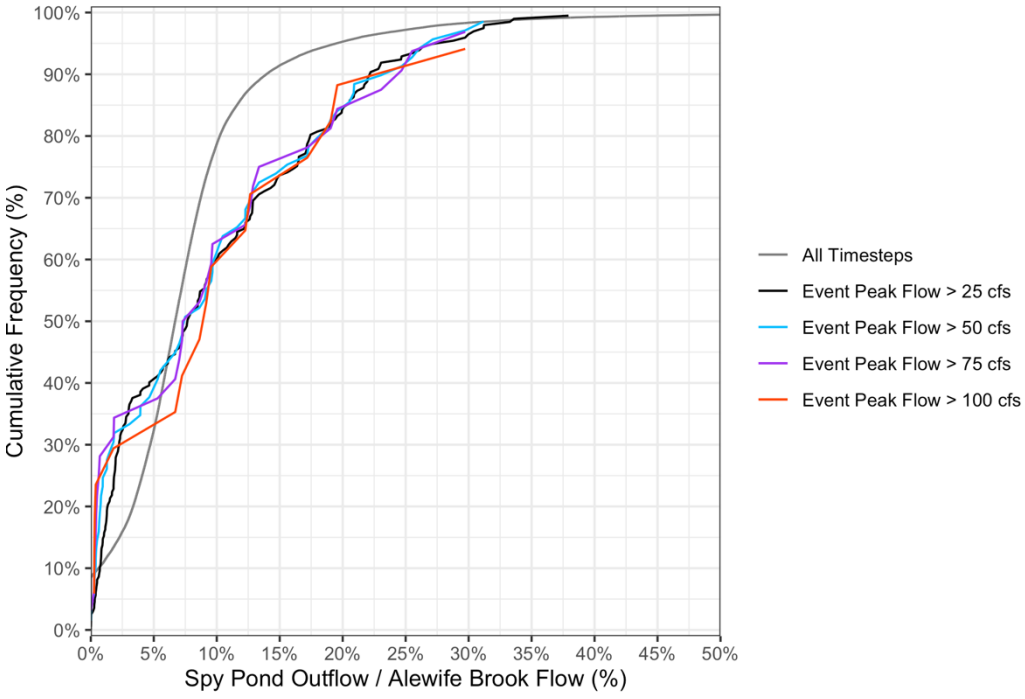

Figure 2-33: Cumulative frequency distribution of the ratio of Spy Pond outflows to Alewife Brook streamflow.

Note: Ratios (x-axis) are truncated to a maximum value of 50%. Event peak flows based on max Alewife Brook flows during each storm event.

3 STORMWATER CAPTURE SCENARIO ANALYSIS

The long-term historical simulation of the water budget model indicated that there is significant potential to reduce peak flows in Alewife Brook by reducing or eliminating outflows from Spy Pond. Among the historical events with peak flows > 100 cfs in Alewife Brook, Spy Pond outflows contributed 16 cfs (or 9% of the peak flow) on average, and reached values as high as 44 cfs (30% of peak flow) in a single storm (Figure 2-31; Figure 2-33; Section 2.2.3.3). Therefore, if Spy Pond can be operated in such a way as to fully capture stormwater runoff by releasing water prior to each storm and thus eliminate outflows during the times of peak flow, then downstream peak flows can be potentially reduced by up to 16 cfs (9%) on average, or 44 cfs (30%) in a single event. The goal of these scenarios was thus to determine whether these maximum potential reductions can be achieved, and if so, to estimate the flow capacity required for releasing water in advance of each storm.

For the scenario analysis, the water budget model was used to simulate operation of Spy Pond as a stormwater capture basin with the goal of reducing outflows during downstream peak flow events and thus to reduce the risk of flooding in downstream communities along Alewife Brook. Initially, a secondary goal of this analysis was to reduce or eliminate shoreline flooding around Spy Pond by preventing the pond level to reach flood levels during extreme events; however, the results of the historical simulation suggest that shoreline flooding was already infrequent with only one significant flooding event occurring over the entire 13-year simulation period (Section 2.2.3.2). Therefore, the impact on shoreline flooding was not explicitly included in this scenario analysis.

As a feasibility study, this scenario analysis was based on a simple set of operational rules and assumptions in order to identify the maximum potential benefits without being limited by various real-world constraints and complexities (e.g., hydraulic capacities, forecast uncertainty, cost, etc.). Should the results of this study show that operating Spy Pond as a stormwater capture basin could potentially provide real and tangible benefits, then these additional limitations will require further research and study using more detailed analyses as will discussed in Section 4. This analysis also focused on determining how much additional discharge capacity would be required to effectively release water from the pond prior to large storm events so that runoff can be captured and outflows reduced or eliminated. In short, the goal of this study is simply to determine the maximum potential benefits based on data that is currently available, and to then estimate how much additional discharge capacity would be needed to achieve those benefits.

To operate Spy Pond as a stormwater capture basin, it was assumed that additional outflow capacity would be required to supplement the existing outfall structure in order to drawdown the pond prior to each storm event. Although some additional capacity might be achieved by removing the boards (stoplogs) from the existing outfall structure, there was insufficient data available to estimate how much additional capacity this could provide. Furthermore, basing this analysis on any kind of gravity-driven outflow structure (whether it be the existing structure or an additional one) would introduce significant complexity since the flow rate would presumably depend on both the upstream and downstream water surface elevations, and determining those relationships would require a series of additional assumptions. Therefore, these scenarios are based on the simplifying assumption that some additional outflow mechanism with a fixed capacity (e.g., a fixed capacity pump) would be used. By running a series of simulations over a wide range of discharge capacities, the relative benefits could be compared and used to determine the point of diminishing returns whereby further increasing the discharge capacity provides less and less benefit in terms of reducing downstream peak flows.

To incorporate these additional outflows, a release term ($Q_{release}$) was added to the original equation for the water budget model:

$$\frac{dV}{dt} = Q_{in} - Q_{out}(Z) - Q_{release} + A \cdot (P - E) \quad (9)$$

The model was simulated over the same period as the historical simulation (WY 2006 – WY 2018) and using the same difference method as the original model (Eqn 4, Section 2.2), but with the additional release term included. Note that the original outflow term was not removed or modified. Therefore, in these scenario simulations, the existing outfall structure was assumed to remain and generate the same outflow rates for any given pond elevation, which would be in addition to the supplemental releases. For evaluating the impacts on downstream flows, the sum of the outflow and release terms (i.e., the total outflow) were compared to downstream flows since the supplemental release was assumed to discharge to the same location as the current outflow structure (i.e., to Little Pond).

3.1 Operational Rules

A simple set of rules were defined to simulate operation of Spy Pond as a stormwater capture basin (Figure 3-1). These rules were designed to release water from Spy Pond prior to each storm event in order to increase the storage capacity that is available to capture runoff during the course of the event. By capturing this runoff, outflows from the pond could be reduced or eliminated that would otherwise contribute to peak flows downstream in Alewife Brook.

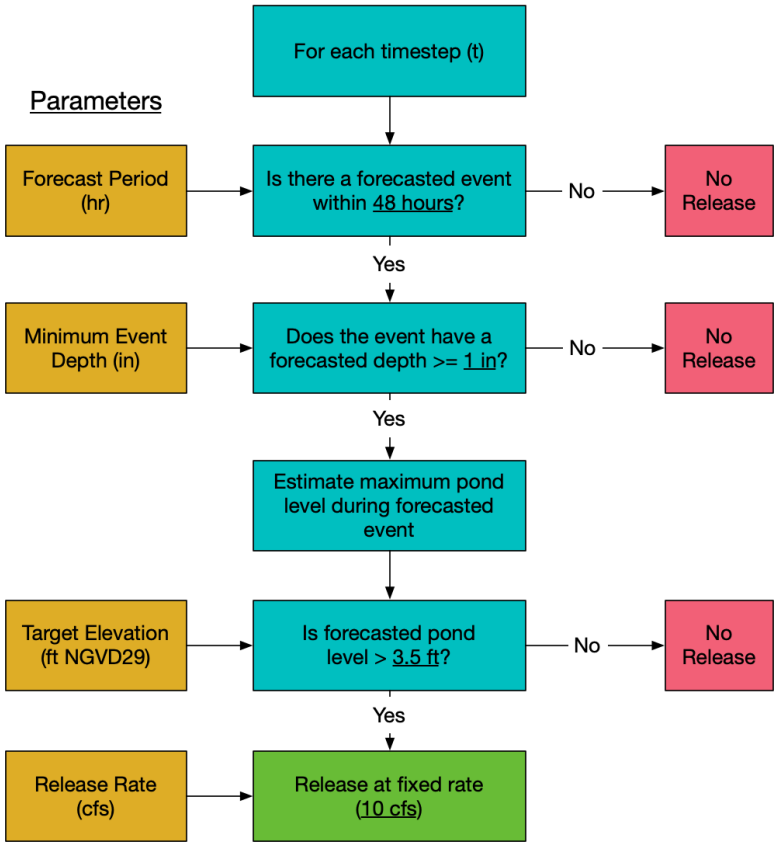

Figure 3-1: Operational rules for stormwater capture.

At each timestep, these rules are used to determine whether a release is needed to increase the available storage capacity for an upcoming event. Releases only occur if 1) there is an upcoming event within the specified forecast period, 2) that event has a depth exceeding the minimum event depth, and 3) that event would cause an increase in the pond level above the target level based on the water level at the current timestep. The rules thus depend on four parameters:

- **Forecast period (hr)**: the amount of time before the start of the next storm event for which a reasonable estimate of the event magnitude (precipitation depth) can be forecasted. This parameter effectively determines how long before an event the pond can start being drawn down in order to increase its available storage capacity.
- **Minimum event depth (in)**: the smallest event magnitude (depth of precipitation) for which the pond would be drawn down. Events having total precipitation less than this minimum depth would not trigger releases in order to avoid operations for small events which would provide no real benefit in terms of reducing large downstream peak flows.
- **Target pond elevation (ft NGVD29)**: the target elevation of the pond determines how much water needs to be released based on the current water level and an estimate of the runoff volume that will be generated for the upcoming storm.
- **Release rate (cfs)**: the rate of supplemental outflow (i.e., pump capacity) determines how quickly the pond can be drawn down prior to an event.

The historical timeseries of hourly precipitation was used to forecast the total depth of the next event at any given time step. Use of the historical timeseries for forecasting events implies perfect knowledge of when the next event will begin and what its total depth will be. In reality, precipitation forecasts are highly uncertain, and that uncertainty increases the earlier the forecast is made. However, incorporating such uncertainty would introduce greater complexity and was thus deemed beyond the scope of the current study. Therefore, the results of this analysis should be interpreted as an estimate of the maximum potential benefits since forecast uncertainty would presumably lead to less-than-optimal operations.

To estimate how much the pond level would increase during an upcoming event, the historical simulation was used to develop a relationship between the total inflow volume of an event based on the total precipitation depth of that event (Figure 3-2). This relationship was fitted using a quadratic equation to capture the non-linear increase in inflow at greater event depths. Using this relationship, a forecast of the maximum pond volume during the upcoming event could be calculated at each timestep by:

$$V_{max} = V(t) + Q_{in}(D) \tag{9}$$

where V_{max} is the forecasted maximum pond volume (acft) that will occur in the upcoming event, $V(t)$ is the current pond volume (in) at timestep t, and $Q_{in}(D)$ is the forecasted inflow volume (acft), which is estimated using the total precipitation depth of the event (D, in) from the relationship in Figure 3-2. The forecasted maximum pond level is then calculated from the forecasted maximum volume using the elevation-volume curve (Section 2.2.1.3; Figure 2-12). The forecasted maximum pond level is then compared to the target elevation to determine whether a release is needed. If the forecasted level is below the target, then there is already sufficient capacity available to capture the upcoming storm without exceeding the target elevation and no release is needed. Otherwise, water is released to increase the available capacity.

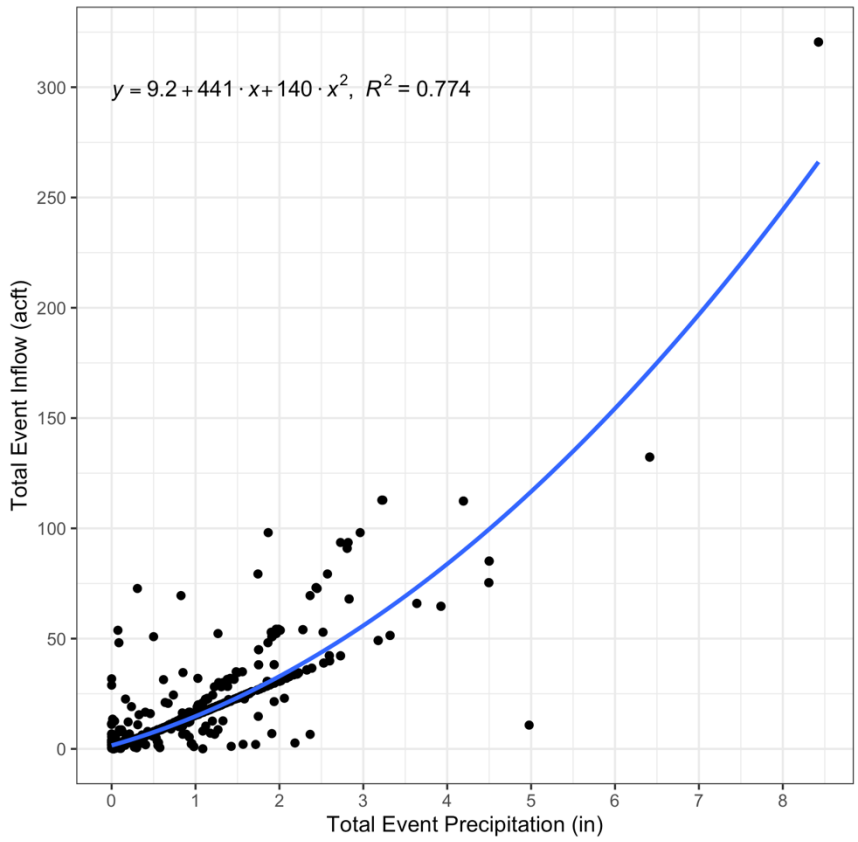

Figure 3-2: Relationship between total event inflow and total event depth based on historical simulations.

To determine a suitable range of release rates for these scenarios, a set of curves were developed that show the total release duration (in hours) required to capture an event of any given total depth at varying fixed release rates (Figure 3-3). These curves were estimated from the following equation:

$$T = \frac{Q_{in}(D)}{Q_{release}} \cdot \frac{43560\ ft^2}{acre} \cdot \frac{hr}{3600\ sec} \quad (10)$$

where T is the total drawdown duration (hr) required to fully capture the inflow volume (Q_{in}, acft) generated by an event of depth D (in) at a constant release rate, $Q_{release}$ (cfs). The resulting curves are non-linear due to the non-linear relationship between the total event depth and resulting inflow volume (Figure 3-2). These curves show, for example, that a release rate of 15 cfs would require 45 hours of continuous release to fully capture a 3-inch storm. A release rate of 30 cfs would require about half that amount of time, or 23 hours. Assuming a maximum potential forecast period of 72 hours, the largest storms (>= 4 inches) would require release rates of 15 cfs or more to fully capture the runoff. Lastly, the maximum release rate of 50 cfs could capture the largest storm (8.4 inches) in less than 72 hours. Therefore, a range of release rates from 1 to 50 cfs was considered suitable for the scenario analysis as it includes both low release rates which would be least costly, as well as the highest necessary release rates to adequately capture the largest event.

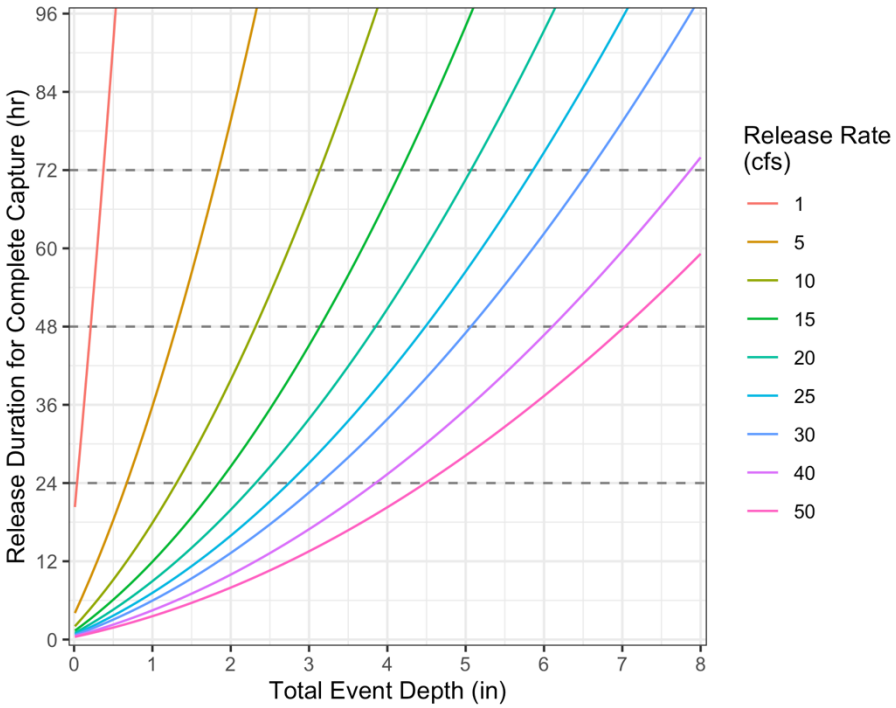

Figure 3-3: Estimated total release durations to fully capture runoff from events with varying depths.

A primary set of scenarios were run using default values for the forecast period, minimum event depth, and target pond elevation (Table 3-1). For these primary scenarios, only the release rate was varied from 1 to 50 cfs in order to focus on the relative benefits of different release rates (Section 3.3). Additional scenarios were later run to test the sensitivity of the results to alternative values for those first three parameters using the ranges listed in Table 3-1 (Section 3.4).

Table 3-1: Ranges and default values for the operational parameters.

Parameter	Range	Default Value
Forecast Period	24 – 72 hours	48 hours
Minimum Event Depth	1 – 3 inches	1 inch
Target Pond Elevation	3.5 – 4.0 ft NGVD29	3.5 ft NGVD29
Release Rate	1 – 50 cfs	N/A

3.2 Example Event

To illustrate the impacts of these operations on reductions of peak flow in Alewife Brook at varying release rates, an example simulation was performed for a single event from March 27 to April 4, 2010, which had a total precipitation depth of 4.5 inches (Figure 3-4). A series of nine scenarios were run with release rates varying from 0 to 50 cfs and using the default values for the other three operational parameters (Table 3-1). The scenario with a 0 cfs release rate reflects the historical results (no stormwater capture operations) from which the other scenarios could be compared.

The results for this event show that release rates of 20 cfs or less were unable to fully draw down the pond prior to the start of the storm event (Figure 3-4). This is reflected in both the timeseries of hourly release rates, which show those scenarios having releases for the full 48 hours prior to the start of the event (i.e., the full forecast period), as well as in the pond elevation timeseries which shows those scenarios ultimately exceeding the target elevation of

3.5 ft NGVD29. The scenarios with release rates of 30 cfs or more required successively shorter durations in which to draw down the pond: the 30 cfs scenario released for 40 hours while the 50 cfs scenario released only required 24 hours. All three of those high release scenarios ultimately resulted in the same maximum elevation during the event, which was slightly higher than the target elevation due to uncertainty in the inflow volume forecast. Therefore, given a forecast period of 48 hours, a release rate of 30 cfs or more was needed to draw down the pond a sufficient amount (about 1.1 ft) in order to fully capture the runoff volume without causing the pond level to exceed the target elevation of 3.5 ft NGVD29 during the course of the storm.

The outflow timeseries (fourth row of Figure 3-4), which reflects the outflow rate only from the existing outfall structure and does not include the supplemental release, shows significant outflow rates (> 1 cfs) for release rates of 5 cfs or less at the time of the peak flow in Alewife Brook (vertical dashed line; Figure 3-4). With 10 cfs or more, the releases were able to draw down the pond enough to prevent outflows at the time of peak flow. Note that the 10 cfs release scenario resulted in significant outflows (> 1 cfs), but only after the time of peak flow. Therefore, although release rates between 10-20 cfs did not fully draw down the pond, they were able to draw it down enough to prevent significant outflows during the time of peak flow.

The bottom two rows of Figure 3-4 show the resulting changes in hourly flows at Alewife Brook accounting for both the pre-storm release during which Alewife Brook flows increased, and for reductions in the outflows during and after the storm that caused Alewife Brook flows to decrease. Prior to the start of the event, the releases cause increases in the Alewife Brook flows, which are equal in magnitude to the release rates themselves as expected. During the event, Alewife Brook flows decrease due to reductions in the pond outflows, which vary depending on the release rate of each scenario. Scenarios with larger release rates caused greater reductions in outflow, and thus greater reductions in downstream flows in Alewife Brook. However, these results also show that there is a point at which increasing the release rate does not provide any additional benefit in terms of reducing Alewife Brook flows. At the time of peak flow (vertical dashed line), all scenarios with releases of 10 cfs or higher resulting in approximately the same flow.

To directly compare the impacts of these scenarios on only the peak flow in Alewife Brook, the reduction in peak flow can be plotted against the release rate for each scenario (Figure 3-5). This figure clearly shows that the greatest gains in terms of peak flow reductions occurred as the release rate increased from 0 to 10 cfs. Release rates greater than 10 cfs, however, yielded diminishing returns with the three highest release rates (30–50 cfs) resulting in the same reduction of 12.6 cfs.

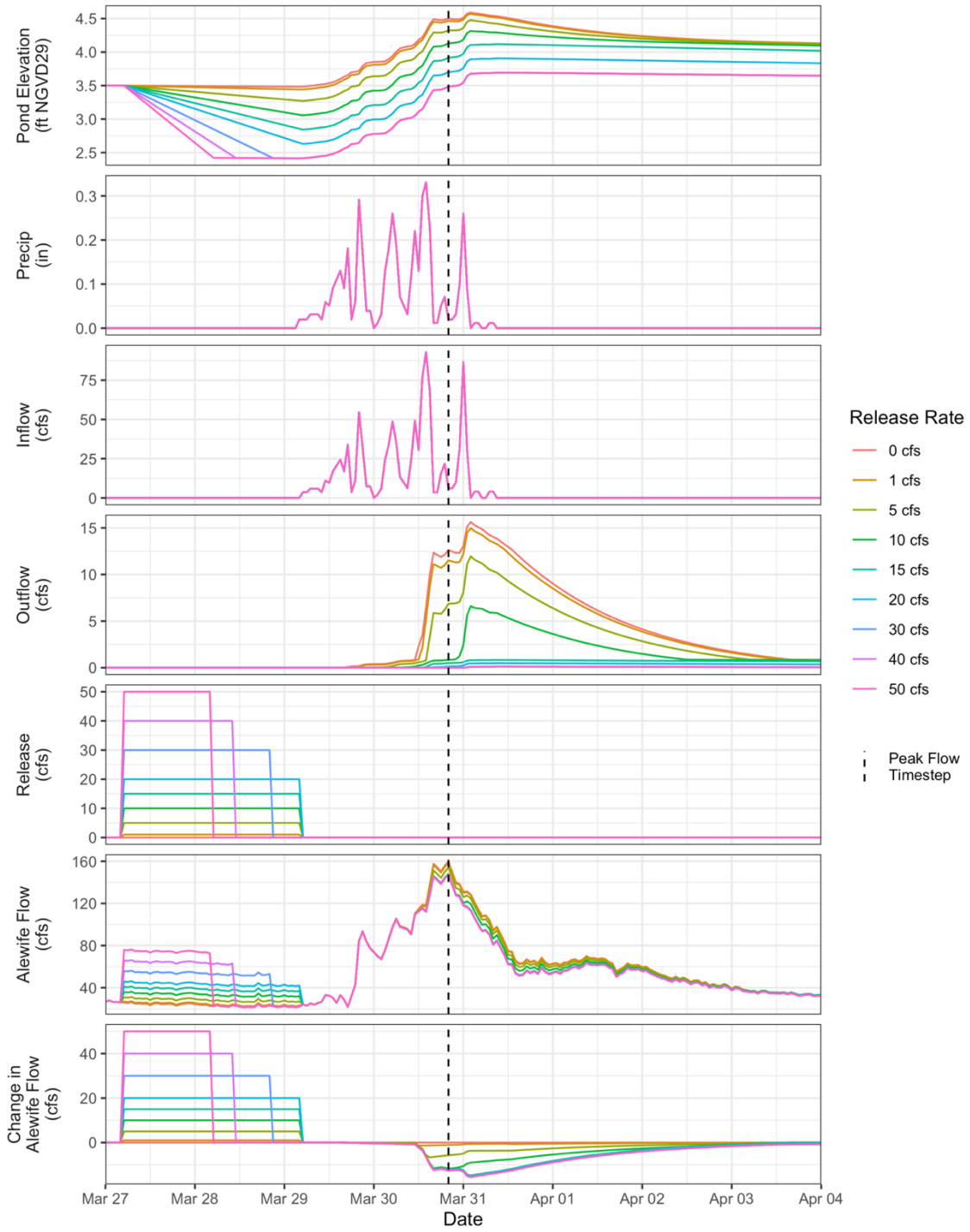

Figure 3-4: Simulated timeseries for release scenarios of example event, March 27–April 4, 2010.

Note: Vertical dashed line indicates the timestep at which Alewife Brook reached its historical peak flow.

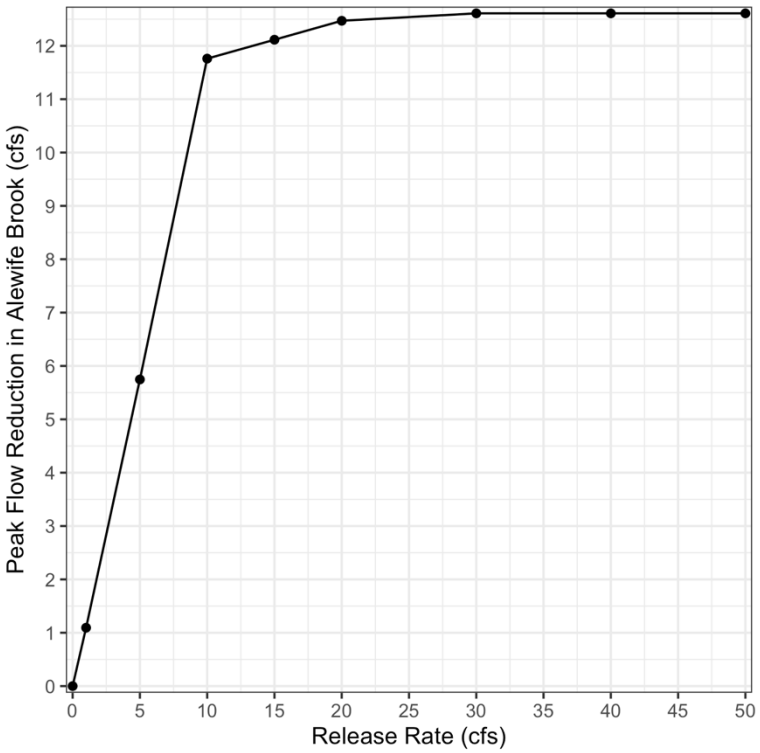

Figure 3-5: Peak flow reduction for varying release rates during example event, March 27–April 4, 2010.

3.3 SCENARIO RESULTS

The stormwater capture scenarios were simulated over the full period of record (WY 2006–WY 2018) with release rates ranging from 1 to 50 cfs. The default values were used for the other three operational parameters (forecast period, minimum event depth, and target elevation; see Table 3-1). The scenarios were primarily evaluated by comparing the peak flow reductions in Alewife Brook during the largest storm events over this period. Only storms with historical peak flows > 100 cfs, of which there were sixteen, were included in this evaluation in order to focus on events that pose a significant risk of flooding in communities along Alewife Brook[7]. Detailed figures of the model output showing hourly timeseries of the simulated pond elevation, inflows, outflows, and impacts to flows in Alewife Brook during each of these sixteen storm events are provided in Appendix B.

In addition to the peak flow reductions in Alewife Brook, the scenarios were also compared based on changes to the pond elevations resulting from stormwater capture operations to determine if any given scenario had a large impact on the long-term water level regime of the pond. Lastly, the average number of hours per year that releases occurred was also calculated in order to compare the relative frequency of releases among the scenarios.

Together, these three comparisons (peak flow reductions, changes to pond elevation, and the release frequency) provide a basis for understanding the relative trade-offs involved with varying not only the release rate, but also the other three operational parameters, as will be presented in Section 3.4.

[7] A specific flow threshold above which flooding occurs along Alewife Brook could not be determined from available information. The 100 cfs threshold used for this analysis was chosen to select for a sufficient number of large events for a meaningful comparison, but not so many that the comparison becomes overly complex.

3.3.1 PEAK FLOW REDUCTIONS

For each of the sixteen largest events with Alewife Brook peak flows > 100 cfs, a curve was generated showing the change in peak flow reduction as a function of the release rate (Figure 3-6a; each line corresponds to one of the sixteen events). In general, the results show peak flow reductions increasing as the release rate is also increased for most of the events. However, for four of the sixteen events, none of the release rates yielded flow reductions greater than 1 cfs (horizontal lines near the x-axis in Figure 3-6a). Two of these events had total precipitation less than the minimum event depth (1 inch) and were therefore did not trigger a release for stormwater capture. The high peak flows that occurred during these storms could have been due to rainfall that occurred within the Alewife Brook basin, but which was not measured at the Logan Airport weather station. The other two events did not yield high flow reductions because the historical pond level was already low enough to capture most of the runoff from these storms. In these cases, Spy Pond contributed very little flow to Alewife Brook even without the stormwater capture operations.

Among the other twelve storm events, the peak flow reduction curves all exhibit a similar pattern with large increases as the release rate is initially increased from 0 to 1 cfs, then 1 to 5 cfs, etc.; but at some point, each curve reaches a maximum value (i.e., the curve levels off) indicating that further increases in the release rate did not achieve any additional reduction for that storm. The individual curves differ widely in terms of both the maximum reduction that could be achieved, as well as the release rate at which that maximum is reached (i.e., the "levelling-off" point). For example, one storm resulted in reductions increasing steadily over all release rates up to 50 cfs at which point the reduction achieved an overall maximum of 44 cfs. Other storms reached maximum reductions of only 7 or 8 cfs with release rates around 5 or 10 cfs. In addition to comparing the change in reductions for each storm (i.e., comparing the individual lines in Figure 3-6a), the range of reductions that could be achieved at any one release rate can be compared. For example, at the 20 cfs release rate, reductions ranged from only 0.09 cfs up to a maximum of 30 cfs.

To better understand the overall patterns in terms of how the average and range of reductions change over varying release rates, a series of summary statistics were calculated based on the peak flow reductions of all sixteen large events at each release rate (Figure 3-6b; Table 3-2). The resulting curves better reflect how the distribution of peak flow reductions varies as a function of the release rate. The lower quantiles (e.g., minimum, 10^{th} and 25^{th} percentile) generally show little change due to the four storms that did not result in any significant reductions at any release rate. The median and higher quartiles (75^{th} percentile, 90^{th} percentile, and maximum), however, had larger changes as the release rate is increased. For example, at a 10 cfs release rate, the median reduction was 8.9 cfs (Figure 3-6b), which is the median reduction calculated from all sixteen events at a 10 cfs release rate as shown in Figure 3-6a. This means that for half of the largest storm events, a peak flow reduction of 8.9 cfs or less was achieved using a release rate of 10 cfs. Conversely, for the other half of the largest storm events, the flow reduction was greater than 8.9 cfs with a maximum of 17 cfs based on a 10 cfs release rate.

The median reduction curve (black line; Figure 3-6b) levels off at a release rate of 20 cfs with a maximum value of 16 cfs. Therefore, further increases in the release rate above 20 cfs did not yield any additional reductions on average. The 75^{th} and 90^{th} percentile curves (yellow and orange lines; Figure 3-6b), however, reached maximum values of 22 and 31 cfs for release rates of 30 and 40 cfs, respectively. Finally, the maximum reduction (red line; Figure 3-6b), shows that additional release capacity continues to generate greater reductions all the way up to an overall maximum of 44 cfs at a release rate of 50 cfs.

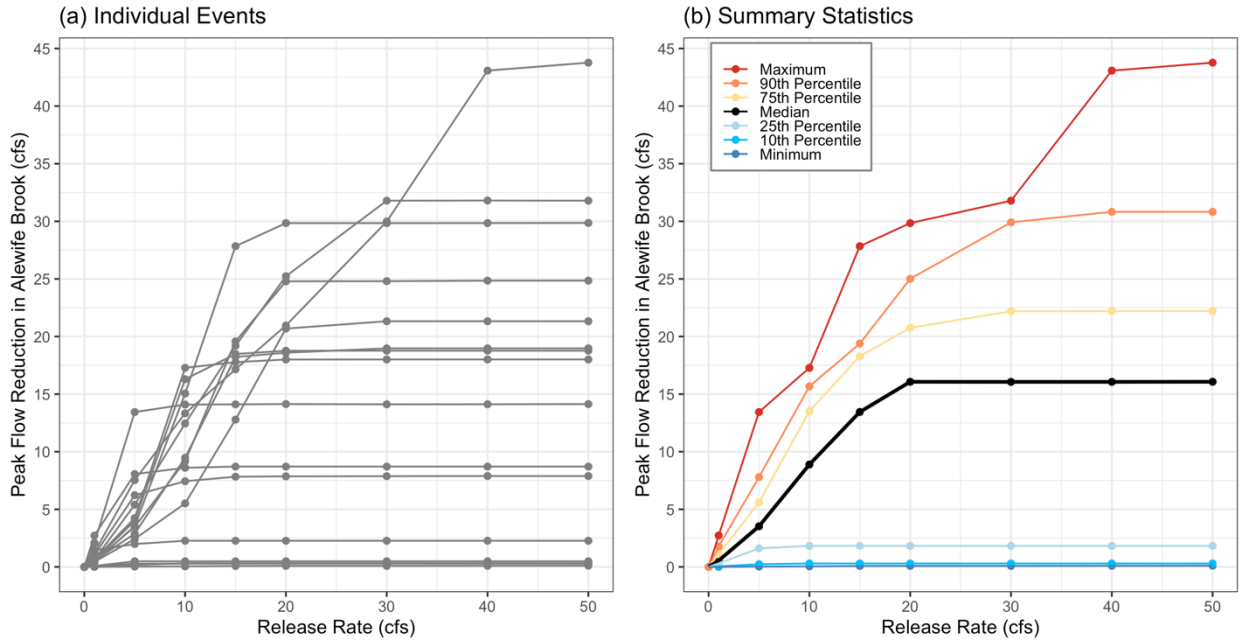

Figure 3-6: Peak flow reductions (cfs) in Alewife Brook over varying release rates of events with historical peak flows > 100 cfs.
Note: Each line in (a) shows the reductions at each release rate for one event. Lines in (b) summarize the reduction over all events with historical peak flows > 100 cfs at each release rate.

Table 3-2: Summary statistics of peak flow reductions (cfs) over varying release rates for events with historical peak flows > 100 cfs.

Release Rate	Min.	10th Quantile	25th Quantile	Median	Mean	75th Quantile	90th Quantile	Max.
0 cfs	0	0	0	0	0	0	0	0
1 cfs	0	0.06	0.3	0.5	0.8	1.1	1.8	2.7
5 cfs	0.03	0.2	1.6	3.5	4.0	5.6	7.8	13
10 cfs	0.05	0.3	1.8	8.9	8.3	14	16	17
15 cfs	0.08	0.3	1.8	13	12	18	19	28
20 cfs	0.09	0.3	1.8	16	13	21	25	30
30 cfs	0.09	0.3	1.8	16	14	22	30	32
40 cfs	0.1	0.3	1.8	16	15	22	31	43
50 cfs	0.1	0.3	1.8	16	15	22	31	44

In addition to comparing the peak flow reduction using absolute flow units (cfs), the *relative* peak reductions (as a % of the peak flow) were also compared by dividing the reduction (in cfs) by the corresponding historical peak flow (in cfs) (Figure 3-7; Table 3-3). The relative peak flow reductions exhibit similar patterns as the reductions in cfs (Figure 3-6), with the median curve reaching its highest value of about 9% at 20 cfs and the overall maximum relative reduction reaching 30% at a release rate of 50 cfs.

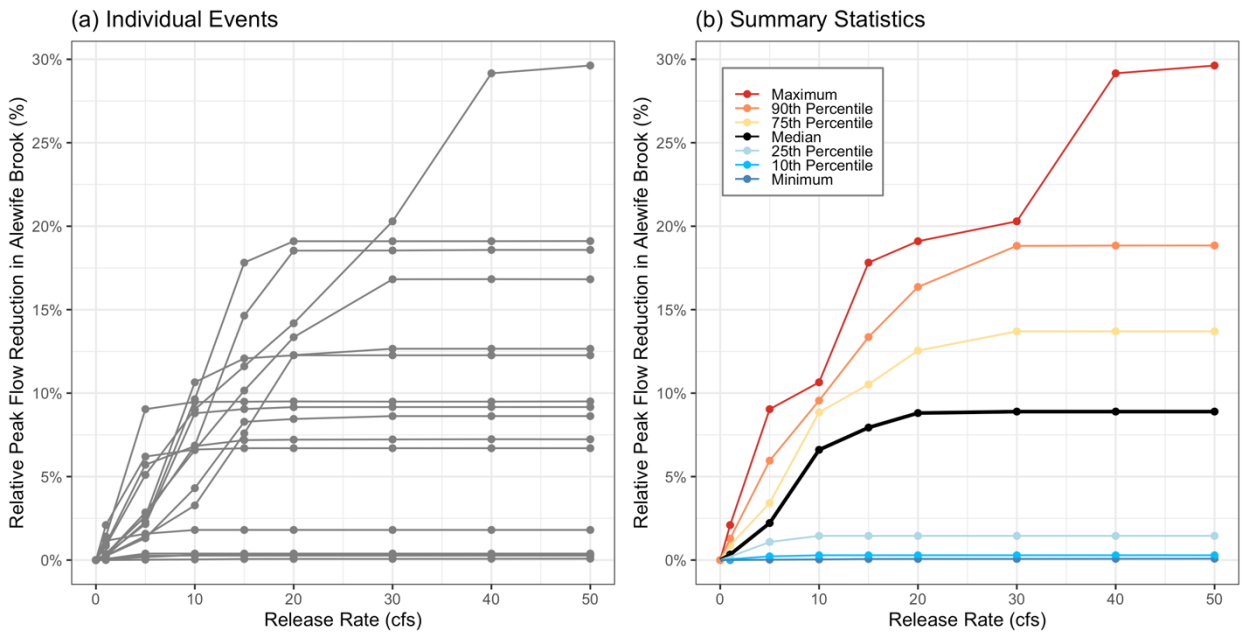

Figure 3-7: Relative peak flow reductions (%) in Alewife Brook over varying release rates of events with historical peak flows > 100 cfs.
Note: Each line in (a) corresponds to the relative reduction at each release rate for one event. Lines in (b) summarize the relative reduction over all events with historical peak flows > 100 cfs at each release rate.

Table 3-3: Summary statistics of relative peak flow reductions (%) over varying release rates for events with historical peak flows > 100 cfs.

Release Rate	Min.	10th Quantile	25th Quantile	Median	Mean	75th Quantile	90th Quantile	Max.
0 cfs	0%	0%	0%	0%	0%	0%	0%	0%
1 cfs	0%	0.05%	0.2%	0.3%	0.5%	0.9%	1.3%	2.1%
5 cfs	0.02%	0.2%	1.1%	2.2%	2.7%	3.4%	6.0%	9.0%
10 cfs	0.04%	0.3%	1.5%	6.6%	5.3%	8.9%	9.6%	11%
15 cfs	0.07%	0.3%	1.5%	7.9%	7.3%	11%	13%	18%
20 cfs	0.07%	0.3%	1.5%	8.8%	8.3%	13%	16%	19%
30 cfs	0.07%	0.3%	1.5%	8.9%	9.0%	14%	19%	20%
40 cfs	0.08%	0.3%	1.5%	8.9%	9.5%	14%	19%	29%
50 cfs	0.08%	0.3%	1.5%	8.9%	9.6%	14%	19%	30%

In summary, both the absolute and relative peak flow reductions show that the median reduction reached its highest value of 16 cfs (9% relative to peak flow) at a release rate of 20 cfs. Decreasing the release rate from 20 cfs caused approximately proportional decreases in the median peak flow reduction. For example, the 10 cfs release rate had a median reduction of 8.9 cfs, which was about half the median reduction (16 cfs) for a release of 20 cfs. Increasing the release rate above 20 cfs provided greater reductions in the higher quartiles (75th, 90th, and maximum), but did not cause any increase in the median reduction.

3.3.2 Changes to Pond Surface Elevation

In addition to comparing the peak flow reductions among the varying release rate scenarios, the impact on the long-term distribution of pond water levels was also evaluated. The cumulative frequency distribution of simulated elevations (Figure 3-8a) show a gradual shift in the distribution from higher to lower elevations as the release rate is increased. Summary statistics of the simulated elevations were also calculated for each release rate (Figure 3-8b),

similar to those for the peak flow reductions. Note that both panels in Figure 3-8 were generated using all of the hourly simulation timesteps, not just those during the largest storm events as used for the peak flow reductions. The median elevation fell by 0.38 ft (4.6 inches) from an initial value of 3.96 ft NGVD29 in the case of no release to 3.58 ft at a release of 20 cfs. Above 20 cfs, the median elevation continued to fall by a relatively small amount to a final value of 3.55 ft NGVD29 at 50 cfs. The maximum elevation, however, continuously fell from 5.90 ft NGVD29 with no release to 4.78 ft NGVD29 at 50 cfs (a total drop of 1.12 ft). The overall minimum elevation also fell continuously from 2.74 to 1.44 ft NGVD29. Therefore, drawdowns using the highest release rate (50 cfs) caused the overall minimum pond elevation to fall by as much as 1.3 ft (15.6 inches). These results indicate that the stormwater capture operations had a significant impact on the long-term pond elevations, effectively lowering the average pond level by 0.38 ft or more with release rates of 20 cfs, and lowering the overall maximum and minimum levels by 1.1 and 1.3 ft, respectively, with a maximum release of 50 cfs.

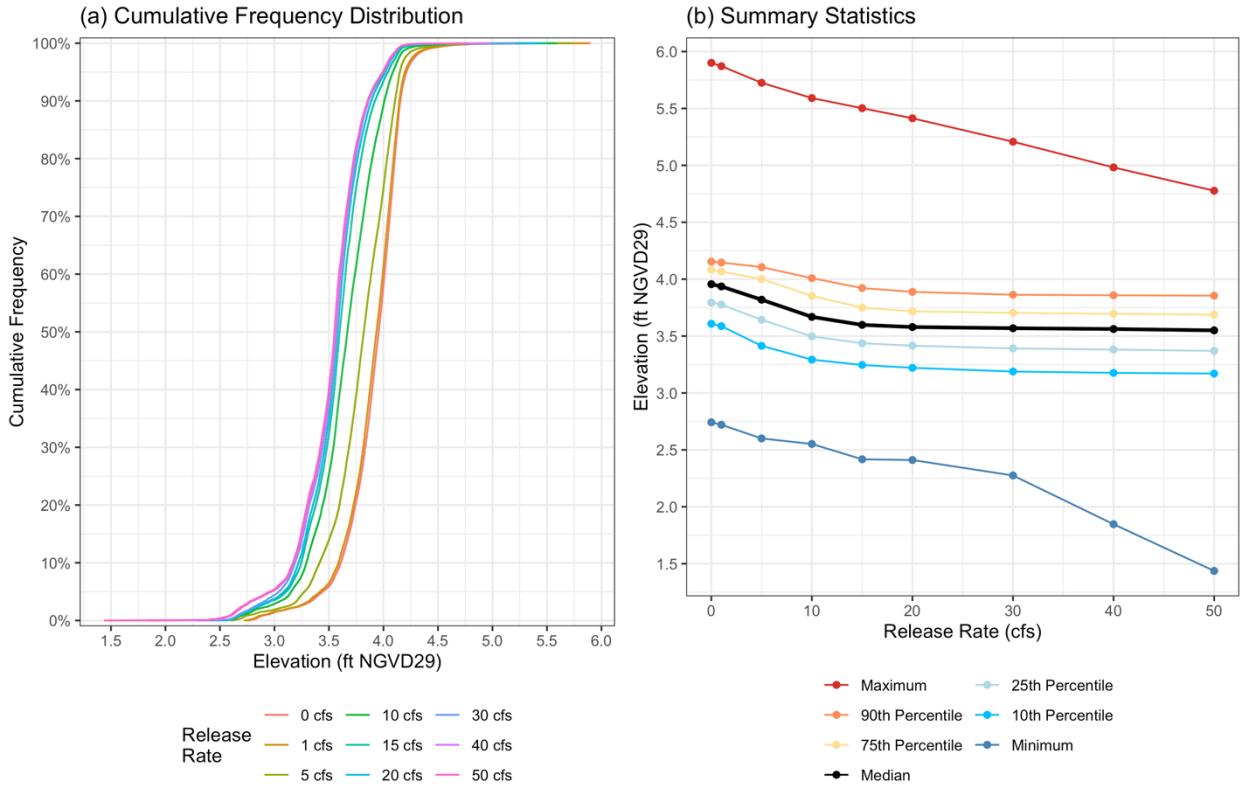

Figure 3-8: Cumulative frequency distributions and summary statistic of simulated elevations for each release scenario.
Note: Both panels are generated using simulated elevations from all timesteps, not only during the largest events.

Table 3-4: Summary statistics of simulated pond surface elevations based on all timesteps.

Release Rate	Min.	10th Quantile	25th Quantile	Median	Mean	75th Quantile	90th Quantile	Max.
0 cfs	2.74	3.61	3.79	3.96	3.91	4.08	4.15	5.90
1 cfs	2.72	3.59	3.78	3.94	3.89	4.07	4.15	5.87
5 cfs	2.60	3.41	3.64	3.82	3.79	4.00	4.11	5.73
10 cfs	2.55	3.29	3.50	3.67	3.65	3.85	4.01	5.59
15 cfs	2.42	3.25	3.44	3.60	3.58	3.75	3.92	5.50
20 cfs	2.41	3.22	3.42	3.58	3.56	3.72	3.89	5.41
30 cfs	2.28	3.19	3.39	3.57	3.54	3.70	3.86	5.21
40 cfs	1.85	3.18	3.38	3.56	3.53	3.70	3.86	4.98
50 cfs	1.44	3.17	3.37	3.55	3.52	3.69	3.86	4.78

3.3.3 Frequency of Releases

Finally, the average number of hours per year for which a release occurred was calculated to compare the frequency of releases among the scenarios (Figure 3-9). The lowest release rate of 1 cfs resulted in the greatest frequency of 633 hours (26.4 days) per year. The release frequency was about half of this maximum (331 hours or 13.8 days per year) at 20 cfs. And the lowest frequency was 139 hours (5.8 days) per year at the highest release rate of 50 cfs. Therefore, as expected, lower release rates require longer and more frequent releases in order to sufficiently draw down the pond and capture the stormwater runoff for any given event.

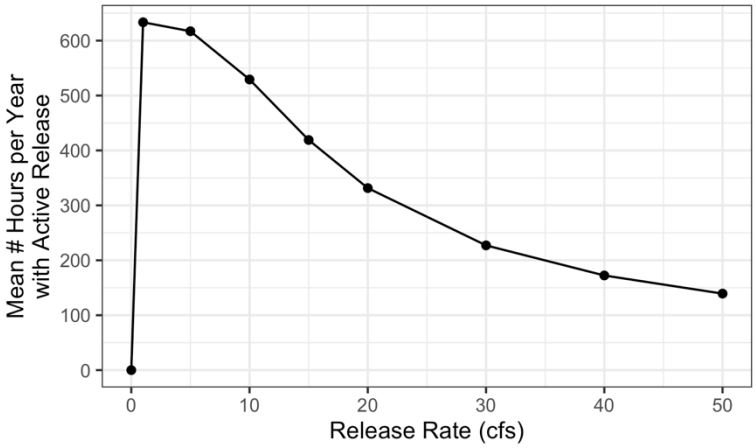

Figure 3-9: Mean release frequency in hours per year for varying release rates.

3.4 Sensitivity Analyses

The scenario results presented in Section 3.3 focused solely on evaluating the peak flow reductions that can be achieved by varying only one of the four operational parameters, namely the supplemental release rate. For those results, the other three parameters were fixed at their default values (Table 3-1). In this section, a series of sensitivity analyses are presented to show the effect of varying each of those other three parameters (forecast period, minimum event depth, and target elevation). These analyses focused on varying only one of these three parameters at a time, leaving the other two parameters at their default values.

3.4.1 FORECAST PERIOD

The forecast period represents how far into the future a reliable forecast can be made of the total precipitation depth for an upcoming storm event. In effect, this parameter governs the maximum amount of time that releases can occur prior to any given storm. The primary scenarios used a default value of 48 hours meaning that releases could begin as soon as 2 days before the start of the next event. Therefore, to evaluate the impact of using shorter or longer forecast windows, the scenarios were re-run for additional forecast periods of 24 and 72 hours.

As the forecast period is increased, peak flow reductions also increased for any given release rate since there is more time to release water in advance of each storm, and thus the ability to capture greater runoff volumes (Figure 3-10). Consequently, the release rate needed to achieve the highest median peak flow reduction (i.e., the levelling-off point) decreases as the forecast period is increased. For a forecast period of 24 hours, a release rate of 40 cfs is needed to achieve the highest median peak flow reduction of 16 cfs. If the forecast period is twice as long (48 hours), then that same peak flow reduction can be achieved using half of that release rate, or 20 cfs. And for the longest forecast period of 72 hours, only 15 cfs is needed to achieve the highest median reduction. In effect, the reduction curves are shifted horizontally because by having more time available for the release (longer forecast period) a lower release rate can generate the same total volume of additional storage capacity as a higher release rate when there is less time available (shorter forecast period).

In terms of the pond elevations, there is a similar dynamic occurring with greater impacts on the median elevation as the forecast period is increased (i.e., the curves shift horizontally from right to left). The minimum and maximum pond elevations in particular showed larger responses with longer forecast periods. The longer forecast periods also caused increases in the release frequency at the lower release rates, but do not cause a large change among the higher release rates.

In summary, the effect of changing the forecast period is inversely proportional to that of changing the release rate. Because the goal of each draw down is to release a certain volume of water prior to a storm event, that volume can be achieved with either high release rates over a shorter period of time or smaller release rates over a longer period of time. The forecast period thus primarily affects the minimum release rate needed to achieve a given level of peak flow reductions. It does not, however, affect how high the maximum (or median) peak flow reductions become; it only affects at what release rate those reductions can be achieved.

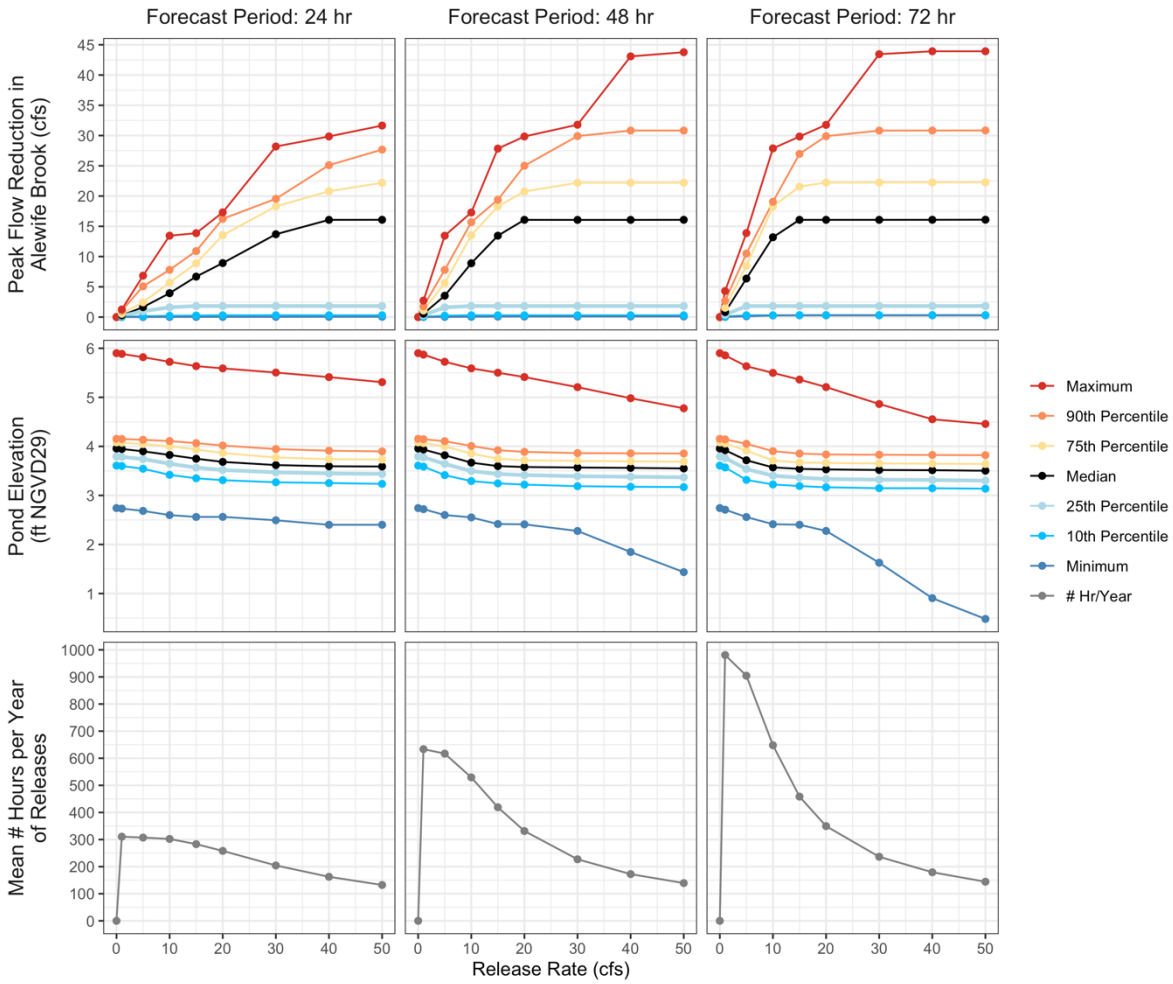

Figure 3-10: Sensitivity analysis results for varying forecast period (24-72 hours).

Note: minimum event depth and target elevation set to default values (1 inch and 3.5 ft NGVD29, respectively).

3.4.2 Minimum Event Depth

The minimum event depth governs how large a given event must be (in terms of the total precipitation depth) in order for a release to occur. The default value used in the primary scenarios was 1 inch meaning all events with precipitation of 1 inch or more could trigger a release. By increasing the minimum event depth, releases would be less frequent since the smaller storms would no longer be targeted for stormwater capture. A sensitivity analysis was thus performed to evaluate the impacts of varying the minimum event depth from 1 (default) up to 3 inches.

Increasing the event depth primarily caused significant decreases in the median peak flow reduction curve, and, to a lesser degree, decreases in the 75th, 90th and maximum reduction curves (Figure 3-11). The highest median values decreased from 16 cfs for a minimum depth of 1 inch to 13.4 cfs at 2 inches, and then down to only 1.1 cfs at 3 inches. Therefore, targeting only events with precipitation > 3 inches would yield almost no peak reduction for half of the events. However, the 75th, 90th, and maximum reduction curves show less of a decrease than the median indicating that substantial peak flow reductions could still be achieved in some storms.

Increasing the minimum event depth also reduced the impact of releases on the median, 75th and 90th percentiles of the pond elevation; however, the minimum and maximum pond elevations were relatively unchanged. By increasing the minimum event depth, release operations were less frequent since fewer storms were targeted for

release. This in turn reduced the impacts on the long-term average pond elevation. But as a consequence of this, the operations successfully captured runoff and reduced peak flows for a fewer number of the largest events, and thus the median peak flow reductions decreased.

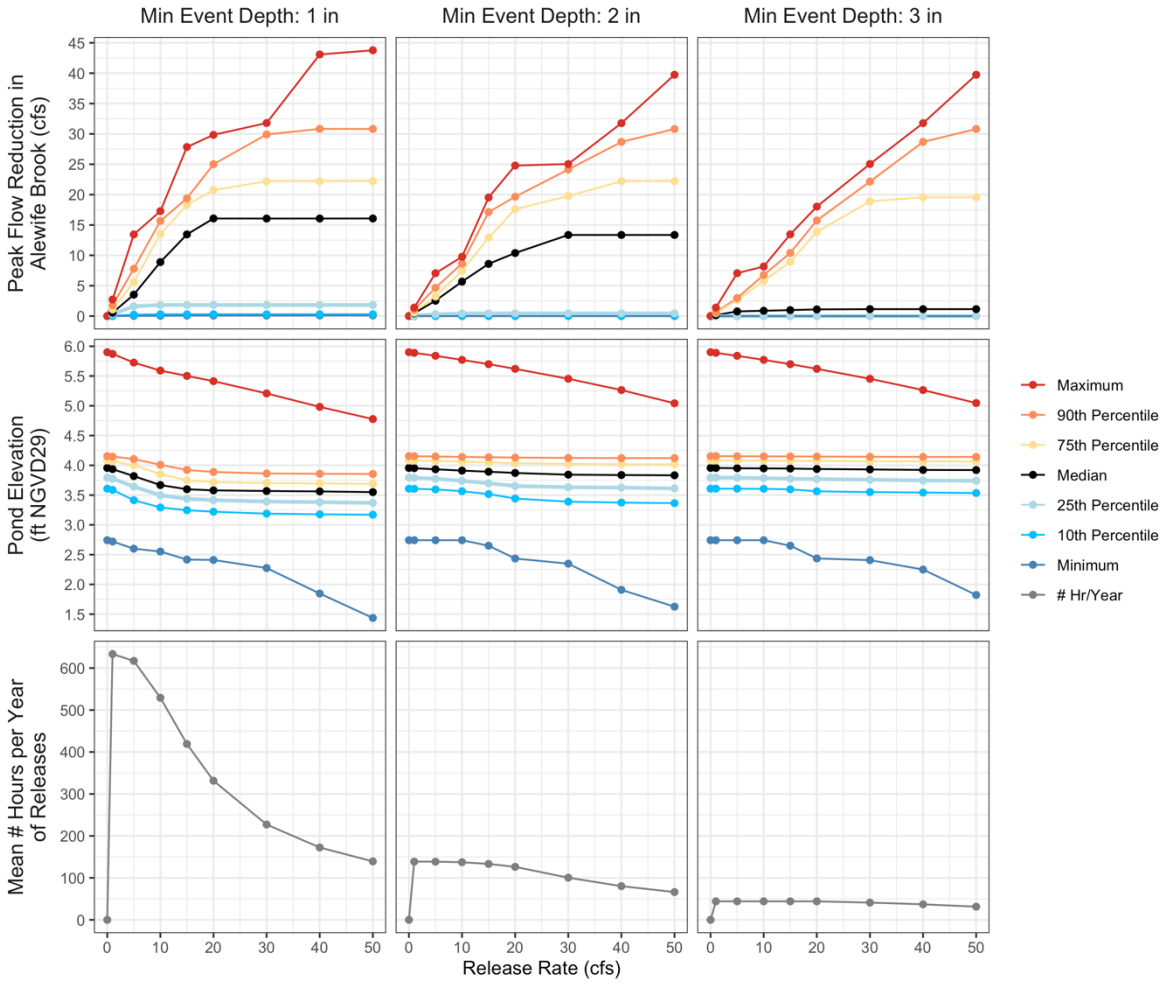

Figure 3-11: Sensitivity analysis results for varying the minimum event depth (1-3 inches).
Note: forecast period and target elevation set to default values (48 hours and 3.5 ft NGVD29, respectively).

3.4.3 Target Pond Elevation

The target pond elevation determines how much extra storage capacity is needed in order to capture runoff from each storm without causing outflows during times of peak flow. Because there is some error associated with estimating the volume of runoff that will occur for any given forecasted event depth (Figure 3-2), lower target elevations provide a greater margin of safety by ensuring that the full volume of runoff would be captured without allowing the pond to reach a relatively high elevation in case the forecasted depth is under-estimated. Sensitivity analyses were performed by varying the target elevation from 3.5 inches (default) up to 4 inches.

Increasing the target elevation caused a small decrease in the median peak flow reduction curve, and larger decreases in the 75th, 90th, and maximum reduction curves (Figure 3-12). At the lowest target elevation of 3.5 ft, the highest median reduction was 16.1 cfs at a release of 20 cfs. The highest median then decreased slightly to 15.7 cfs at a target elevation of 3.75 ft, and then to about 13 cfs at 4 ft. The maximum reduction curve, however, showed much larger decreases, especially among release rates from 15 to 40 cfs. Therefore, increasing the target elevation

had relatively little impact on the average (median) reduction, but caused significant reductions in the maximum reductions.

Increasing the target elevation also caused smaller changes to the pond elevations due to reductions in the release frequencies. The lowest target elevation of 3.5 ft NGVD29 resulted in median pond elevations falling from 3.96 ft NGVD29 with no releases to 3.58 ft NGVD29 at a 20 cfs release rate. The highest target elevation of 4 ft, however, resulted in a drop to only 3.88 ft NGVD29 at 20 cfs.

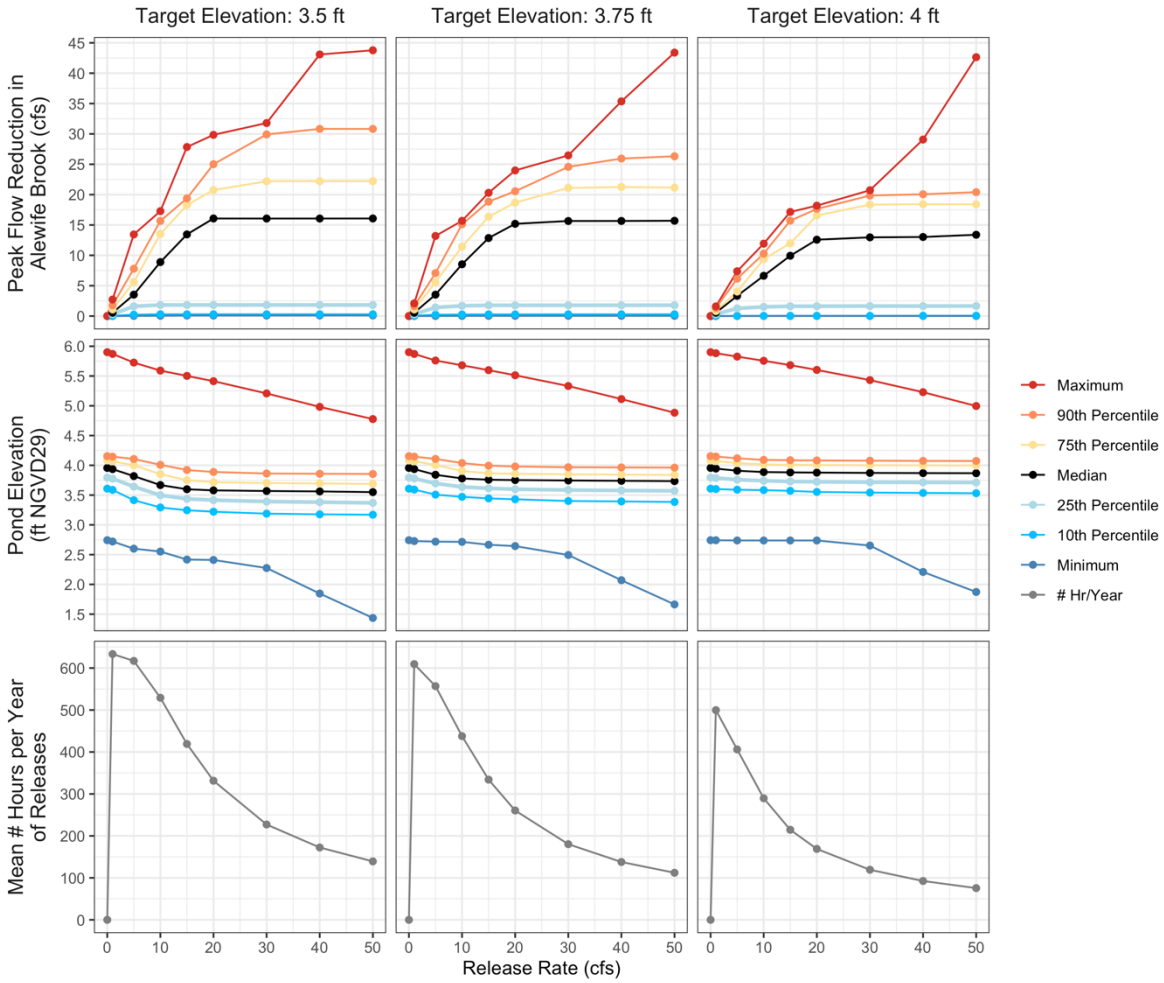

Figure 3-12: Sensitivity analysis results for varying the target pond elevation (3.5-4 ft NGVD29).
Note: forecast period and minimum event depth set to default values (48 hours and 1 inch, respectively).

4 Discussion

In this study, a water budget model was used to evaluate the potential impacts of operating Spy Pond as a stormwater capture system with the goal of reducing peak flows downstream in Alewife Brook. The model was developed using a number of publicly available datasets including historical weather data, streamflow records for Alewife Brook, and various GIS layers, as well as continuous measurements of water levels on Spy Pond collected by MyRWA from July 2017 to July 2018. Inflows to the pond were estimated using a watershed runoff model that was based on algorithms from the P8 Urban Catchment Model (Walker, 1990). Because no observation data were available for calibrating the runoff model, default parameters were used and assumed to generate reasonable

estimates for the hourly rates of rainfall- and snowmelt-driven runoff. Historical pond outflow rates were estimated using observed fluctuations in pond volume, which were calculated from MyRWA's continuous water level measurements. The estimated outflow rates were then used to develop an empirical relationship between the pond surface elevation and outflow for performing long-term simulations. Together, the estimated inflows and elevation-outflow relationship along with historical precipitation records and estimated monthly evaporation rates were used to perform an hourly simulation of the pond water budget over a 13-year period of record from Oct 1, 2005 to Sep 30, 2018 (WY 2006 – WY 2018).

The historical simulation results were validated against the measured water levels from July 2017 to July 2018 and found to provide a sufficiently accurate representation of water level fluctuations during this period. The average error (RSME) of the observed and simulated water levels was 0.16 ft (1.9 in) (Table 2-3; Section 2.2.3.1). Although there were some periods when the observed and simulated water levels differed by greater amounts, many of these differences were caused by inaccuracies in the inflows to the pond, which in turn caused the simulated pond level to rise more (or less) in response to any given storm. As is common with timeseries-based models in general, large errors in any one timestep can propagate for an extended period of time. These errors could be caused by both inaccuracies associated with the runoff model, which was not calibrated due to the lack of flow data for tributaries and stormwater drainage systems discharging to Spy Pond, as well as errors associated with the historical precipitation dataset, which was based on measurements at Logan Airport located 7.5 miles away from Spy Pond. Despite these errors, the simulated and observed water levels showed similar behavior in terms of how quickly the pond drained following each event, and also showed that the model did not exhibit any systemic bias in terms of over- or under-predicting pond water levels over this 12-month period.

The historical simulation results were then used to estimate the frequency and magnitude of shoreline flooding in Spy Pond using a high-resolution land elevation dataset (Section 2.2.3.2). The results showed that only one significant flooding event occurred during the simulation period in May 2006, during which the maximum pond elevation reached 5.9 ft NGVD29 resulting in an estimated 1.6 acres of inundated area (Figure 2-27). In addition to this event, three other events resulted in the pond elevation exceeding the minimum flood elevation of 5 ft NGVD29, but these events only caused a relatively minimal amount of flood inundation. Therefore, because historical flooding was relatively infrequent, it was not evaluated as part of the scenario analyses.

The historical results were also compared to hourly streamflow in Alewife Brook to determine how much flow Spy Pond discharges contribute to downstream flows, and in particular to the peak flows occurring during large storm events (Section 2.2.3.3). This comparison assumed that outflows from Spy Pond are not attenuated in the reaches between the pond outfall and the Alewife Brook streamflow gage, and that these outflows would reach the gage location with a travel time of 1 hour or less. Among the largest storm events for which the peak flow in Alewife Brook exceeded 100 cfs, the median outflows from Spy Pond were 16 cfs, or 9% of the peak flow in Alewife Brook (Figure 2-31, Figure 2-33). The maximum outflow during these events was 44 cfs, or 30% of the peak flow. These results provided an upper limit as to the maximum potential benefits of operating Spy Pond as a stormwater capture system. If outflows from Spy Pond could be eliminated during times of peak flows, then the average (median) expected flow reduction would be 16 cfs (9% of the peak flow), although the maximum flow reduction in any one storm could be as high as 44 cfs (30% of the peak flow).

A set of operational rules and assumptions were then defined and used to evaluate the impact of releasing water from Spy Pond in advance of upcoming storms in order to capture stormwater runoff and reduce pond outflows during times of peak flow in Alewife Brook (Section 3.1). A series of scenarios were simulated for the full 13-year period of record (WY 2006 – WY 2018) with release rates varying from 1 to 50 cfs. Three other operational parameters were fixed at default values (forecast period = 48 hours, minimum event depth = 1 inch, target elevation

= 3.5 ft NGVD29) in order to focus the analysis on the impact of varying only the release rate. The results were summarized by calculating the summary statistics (minimum, median, maximum and various intermediary quantiles) of the peak flow reductions at each release rate based on the sixteen largest events with peak flows > 100 cfs in Alewife Brook. Relative peak flow reductions were also compared by dividing each flow reduction by the corresponding peak flow. These reduction curves showed that the highest median peak flow reduction was 16 cfs (or 9% of peak flow) for a release rate of 20 cfs (Figure 3-6, Figure 3-7). Higher release rates did not yield any increase in the median peak flow reduction. However, the upper quartiles and maximum peak flow reductions did show further increases with greater release rates. The overall maximum peak flow reduction was 44 cfs (30% relative to the peak flow) at 50 cfs. Both the median and overall maximum peak flow reductions were approximately equal to the same median and maximum outflow rates that occurred during the historical simulation without releases. Therefore, these results indicate that outflows could be effectively eliminated during times of peak flow if the supplemental release has sufficient capacity (i.e., 20 cfs to eliminate outflows in half of the storms, 50 cfs to eliminate the outflow of all storms).

The scenario results were also used to compare the impacts of release operations on the long-term average and range of pond elevations (Section 3.3.2). The long-term median pond elevation decreased as release rates were increased, with the largest change occurring from an initial 3.96 ft NGVD29 with no releases to 3.58 ft NGVD29 at 20 cfs, which is a difference of 0.38 ft (4.5 inches) (Figure 3-8). For release rates greater than 20 cfs, further drops in the median elevation were relatively minor. The maximum pond elevation, however, fell continuously from 5.90 ft NGVD29 with no releases to 4.78 ft NGVD29 at the maximum 50 cfs release. The overall minimum elevation also fell by as much as 1.3 ft from 2.74 to 1.44 ft NGVD29 at the maximum 50 cfs release. Therefore, the higher release rates would not only reduce the risk of shoreline flooding by lowering the overall maximum pond level but could also have significant impacts on shoreline vegetation by reducing the minimum pond level by a significant amount.

Finally, sensitivity analyses were performed using alternative values for the forecast period, minimum event depth, and target pond elevation, all of which set to fixed default values for the primary set of scenarios (Section 3.4). The forecast period, which governs how early releases can begin prior to an upcoming event, did not change how high the potential peak flow reductions could reach, but rather changed the minimum release rate needed to achieve maximum reductions. Because the goal of these operations was to capture a specific runoff volume for any given event, the storage capacity needed to capture that volume could be achieved using either a small release rate over a long period of time, or a high release rate over a shorter period of time. Therefore, changing the forecast period (and thus the time available for each release) only affected how large the release needed to be to reach any given level of reductions.

Increasing the minimum event depth from 1 to 3 inches caused a large reduction in the median peak flow reductions, but caused less of a change in the upper quantiles and maximum reductions. By only targeting the largest storms (>= 3 inches of precipitation), the releases were less frequent, and as a result the median pond elevation was not as greatly affected as when a greater number of storms were included (>= 1 inch of precipitation). As a result, pond elevations were generally higher at the start of any given event, which in turn required greater release volumes in order to create sufficient storage capacity to fully capture all of the runoff during the event.

Varying the target elevation from 3.5 to 4 ft NGVD29 had relatively little impact on the highest median reduction, which fell from 16 to 13 cfs, but did have somewhat larger impacts on the higher quantiles and maximum reductions. Because the predicted total runoff volume of any given event is somewhat uncertain based on its forecasted total depth of precipitation, lower target elevations provide a greater margin of safety by ensuring that if the runoff volume is greater than what is predicted, then there is still sufficient capacity available to capture that extra runoff and prevent significant outflows.

4.1 SOURCES OF UNCERTAINTY

The models in this study incorporate some significant sources of uncertainties given the limited amount of observation data. Specifically, the continuous water level measurements collected by MyRWA from July 2017 to July 2018 was the only timeseries dataset available for developing these models. Due to the lack of observed flow data for both the pond inflows and outflows, the watershed runoff and water budget models could not be directly calibrated. Nevertheless, a validation of the water budget model was performed by comparing the simulated and observed water levels during the monitoring period (July 2017 to July 2018), and showed that the model generated reasonably accurate predictions of hourly water surface elevations for the conditions that occurred during this period.

The greatest source of uncertainty in this study is related to the estimation of outflow rates from the pond, which were calculated by difference from the water budget equation using the continuous measurements of pond water levels (Section 2.2.2). Using these estimated outflow rates, an empirical relationship was developed for calculating the outflow rate as a function of the pond surface elevation. This empirical relationship was then used for the long-term simulation to determine the outflow rate at each timestep based on the simulated water surface elevation. However, the empirical relationship was based on a limited range of observed outflow rates and elevations. Specifically, during the July 2017 – July 2018 monitoring period, the pond reached a maximum water level of 4.3 ft NVD29, corresponding to an estimated outflow rate of 6.1 cfs. For both the historical and scenario simulations, this empirical model was extrapolated beyond the range of the observed data assuming the linear relationship persisted between outflow and elevation. At the maximum simulated elevation (5.90 ft NGVD29), the estimated outflow rate based on this extrapolation was 58.8 cfs. However, in reality this relationship is likely non-linear as the outflow structure and concrete pipe to which it discharges will ultimately reach some limit due to their hydraulic capacities. Furthermore, this approach did not account for the possibility that the outflow structure may have been subject to blockages or other changes during the monitoring period that could have altered the rate of discharge at any given pond elevation. A detailed hydraulic analysis of the outflow structure could provide additional estimates of the potential discharge rates at the higher range of pond surface elevations for which no data is currently available. Additionally, continued monitoring of the pond water levels could provide more data to further refine this empirical relationship by capturing observations over a greater range of pond elevations.

Uncertainty in the inflow rates from watershed runoff could also have an impact on the results by causing errors in the estimated runoff volumes. If the runoff model systematically under- or over-estimated inflow volumes to the pond, this in turn would affect the water budget calculations. Flow measurements of one or more tributaries or drainage outfalls to the pond are needed to calibrate and validate the watershed runoff model. Furthermore, this study used meteorological data collected 7.5 miles away at Logan Airport, which may not always accurately represent the timing and depth of precipitation falling on the Spy Pond watershed. Therefore, local meteorological measurements collected from within the watershed may improve the accuracy of the runoff model predictions.

Lastly, the impacts of Spy Pond outflows on peak flows in Alewife Brook assumed no attenuation of flow between the pond outfall and the USGS streamflow gage. However, it is likely that these flows are in fact attenuated to some degree, especially within Little Pond to which Spy Pond discharges and due to the newly constructed stormwater wetland along Little River. If outflows from the pond are attenuated, then the contributions of Spy Pond to peak flows in Alewife Brook would be less than those estimated in this study. Therefore, these results should be interpreted as the maximum potential flow reductions in light of the assumption that flows are not attenuated between Spy Pond and the Alewife Brook streamflow gage.

4.2 Recommendations for Future Work

The following recommendations are provided for guiding future efforts to build on or refine the results of this study:

1. Continue monitoring water levels in Spy Pond in order to capture a larger range of elevation and outflow conditions with which the empirical elevation-outflow relationship could be refined, especially for outflows occurring at higher elevations greater than 4.3 ft NGVD29, which is currently the highest observed elevation in this dataset.
2. Perform a hydraulic analysis of the pond outfall structure and concrete pipe connecting this structure to Little Pond in order to constrain the relationship between elevation and outflow, especially at higher elevations.
3. Collect flow measurements at tributaries and/or stormwater discharge outlets during multiple storm events of varying magnitudes to calibrate the watershed runoff model.
4. Compile local observations of historical flooding to validate the frequency and extent of shoreline flooding as estimated by the water budget model simulations.
5. Perform a hydraulic analysis of the reaches between Spy Pond and the Alewife Brook streamflow gage to estimate the amount of flow attenuation and the travel time for peak flows. In this study, the impacts of outflows on Alewife Brook assumed no attenuation and that the travel time of outflows between these two points was less than one hour (the simulation timestep). To more accurately evaluate the contributions of Spy Pond outflows to downstream peak flows, flow attenuation and travel time should be accounted for.
6. Perform sensitivity analyses related to the level of uncertainty associated with forecasting the timing and total precipitation depth of upcoming storm events. The scenario analyses assumed perfect forecast knowledge by using the historical dataset to generate the forecasted precipitation at each timestep. Further sensitivity analyses could be performed by introducing error into the forecasted precipitation, which would likely result in diminished performance of the system. Therefore, the results presented in this study reflect the maximum potential benefits, which in reality could be less due to forecast uncertainty.
7. Evaluate the ecological impacts of altering the long-term average and distribution of pond elevations, which could change due to stormwater capture operations. The scenario analysis showed that in some cases operating Spy Pond to capture stormwater resulted in significant impacts on the long-term median water level. For example, a 50 cfs release could cause as much as a 4.5 inch drop in the median elevation, and as much as 1.3 ft in the overall minimum elevation. Changes to the pond water level regime could have ecological impacts, especially on native shoreline vegetation and other species that may require certain water levels to survive.
8. Evaluate the water quality impacts due to stormwater capture operations. In addition to the ecological impacts, release operations could also change the water quality dynamics in the pond. By capturing inflow volumes prior to and preventing outflows during storm events, these operations may increase the hydraulic residence time of the pond, which in turn could cause additional settling of particulate phosphorus. Therefore, these operations may change the net fluxes of phosphorus within the pond and thus potentially cause greater eutrophication.
9. Evaluate the hydraulic impacts of releasing water (especially at potentially high flow rates such as 50 cfs) from Spy Pond to downstream reaches (e.g., Little Pond, stormwater wetland along Little River, and downstream reaches along Alewife Brook). The operations simulated in these scenarios not only reduced peak flows, but also increased dry weather flows as water was released in advance of upcoming storms. The impacts of these dry weather releases may further constrain the range of release rates that are feasible.
10. Perform a cost-benefit analysis by estimating the costs (construction, operations, and maintenance) associated with each scenario, and comparing these costs to the benefits associated with peak flow

reductions. This study did not consider any cost factors, and thus focused on identifying the maximum benefits solely from a hydrologic perspective.

5 CONCLUSIONS

In summary, the overall findings and conclusions of this study are as follows:

1. For storms with historical peak flows exceeding 100 cfs, operating Spy Pond as a stormwater capture basin could potentially reduce peak flows in Alewife Brook by up to 16 cfs (9% of the peak flow) on average and by as much as 30 cfs (19%) in any one storm with a release rate of 20 cfs. With the highest release rate of 50 cfs, the maximum reduction among all storms increased to 44 cfs (30%).
2. The greatest benefits in terms of the average (median) peak flow reductions were gained as the supplemental release rate was increased from 1 to 20 cfs. Although release rates above 20 cfs generated greater peak flow reductions in some storms, they did not yield any additional increases with respect to the median peak flow reduction among storms with historical peak flows exceeding 100 cfs.
3. As a consequence of drawing down the pond, the long-term minimum, median, and maximum pond elevations decreased to varying degrees based on the release rate. As release rates increased from 0 to 20 cfs, the median pond level fell by 0.38 ft (4.5 inches). Further increases in the release rate did not cause much additional decrease in the median pond level. The minimum and maximum pond levels, however, continued to fall by as much as 1.1 and 1.3 ft, respectively, at the highest release of 50 cfs.
4. Based on the historical simulations without any release operations, shoreline flooding around Spy Pond was relatively infrequent with only one storm (May 2006) causing a significant amount of flooding over the 13-year simulation period. Therefore, there appears to be relatively little potential to reduce shoreline flooding through stormwater capture operations since flooding is infrequent to begin with. However, additional observational data is needed to validate the model predictions with respect to the historical frequency and extent of shoreline flooding.
5. Sensitivity analyses of the operational parameters (forecast period, minimum event depth, and target elevation) demonstrated various tradeoffs between the peak flow reductions, impacts on long-term average water levels, and frequency of releases associated with each release rate. Understanding these trade-offs is important for comparing stormwater capture operations at various release rates in terms of not only the average and maximum potential peak flow reductions that can be achieved, but also the resulting impacts on the pond itself.
6. Due to the limited observation data and numerous assumptions made in this study, these results should be interpreted as estimates of the maximum potential benefits under ideal conditions. Further work is needed to study the effects of additional constraints and uncertainties (e.g., forecast uncertainty, hydraulic constraints, cost, attenuation of outflows through Little Pond and Little River, etc.) on these results.

6 REFERENCES

Chesebrough, E.W., and C Duerring (1982). Spy Pond: A Diagnostic Study, 1980-1981. Massachusetts Department of Environmental Quality Engineering, Divison of Water Pollution Control, Westborough Massachusetts. December 1982.

City of Cambridge (2015). Climate Change Vulnerability Assessment, Part 1. City of Cambridge, Massachusetts. November 2015.

City of Cambridge (2017). Climate Change Vulnerability Assessment, Part 2. City of Cambridge, Massachusetts. February 2017.

Environmental Design & Planning, Inc (EDP) (1982). Feasibility Study of Lake Restoration in Spy Pond, Arlington. Prepared for Division of Water Pollution Control, State of Massachusetts and the Town of Arlington by Environmental Design and Planning, Inc. Allston (Boston). September, 1982.

Fennessey, N.M., and R.M. Vogel (1996). Regional Models of Potential Evaporation and Reference Evapotranspiration for the Northeast USA. Journal of Hydrology, Vol. 184, pp. 337-354.

Haith, D.A. and L.L. Schoemaker (1987). Generalized Watershed Loading Functions for Stream Flow Nutrients. Water Resources Bulletin, American Water Resources Association, Vol. 23, No. 3, pp. 471-478.

Lefkowitz, J.R., Sarmanian, A.K., and M. Quigley. Continuous monitoring and adaptive control-the internet of things transforms stormwater management. Journal of the New England Water Environment Association, Vol. 50, No. 1, pp. 44-51.

MassGIS (2011). Crop Evapotranspiration and Potential Evaporation Grids (Last Updated 6/2/2011). Accessed January 31, 2019 from https://docs.digital.mass.gov/dataset/massgis-data-crop-evapotranspiration-and-potential-evaporation-grids

MassGIS (2017). Impervious Surface 2005 (Last Updated 5/30/2013). Accessed January 31, 2019 from https://docs.digital.mass.gov/dataset/massgis-data-impervious-surface-2005

MassGIS (2017). LiDAR Terrain Data (Last Updated 10/13/2017). Accessed January 31, 2019 from https://docs.digital.mass.gov/dataset/massgis-data-lidar-terrain-data

National Oceanic and Atmospheric Administration National Centers for Environmental Information (NOAA NCEI) (2001). Integrated Surface Dataset (ISD) - Lite. NOAA National Centers for Environmental Information. Accessed September 2, 2019 from https://www1.ncdc.noaa.gov/pub/data/noaa/isd-lite/

NOAA (2019). VERTCON Orthometric Height Conversion Utility. Accessed January 31, 2019 from https://www.ngs.noaa.gov/cgi-bin/VERTCON/vert_con.prl

Pilgrim, D.H., and I. Cordery (1993). Flood runoff. Chapter 9 in Handbook of Hydrology, Maidment, D.R., editor. New York, McGraw-Hill, p. 9.1–9.42.

QGIS Development Team (2019). QGIS Geographic Information System. Open Source Geospatial Foundation Project. http://qgis.osgeo.org

R Core Team (2019). R: A language and environment for statistical computing. R Foundation for Statistical Computing, Vienna, Austria. https://www.R-project.org/

Shanahan, P., J. Spink, and A. Morales (1997). Review of Recommendations for the Restoration of Spy Pond, Arlington, Massachusetts. Prepared for Town of Arlington, Arlington, MA. December 1997.

Sutherland, R.C. (2000). Methods for Estimating Effective Impervious Cover. Article 32 in The Practice of Watershed Protection. Center for Watershed Protection, Ellicott City, MD.

Tri-Community Working Group (2005). Progress Report, Tri-Community Working Group. August 2005. 35 pp. + appendices.

U.S. Department of Agriculture, Soil Conservation Service (USDA SCS) (1964). National Engineering Handbook. Section 4: Hydrology. 1964.

U.S. Geological Survey (USGS) (2019). National Water Information System data available on the World Wide Web (USGS Water Data for the Nation). Accessed January 31, 2019 at http://waterdata.usgs.gov/nwis/

Walker, W.W. (1990). P8 Urban Catchment Model - Program Documentation. DOS Version 1.1. Prepared for IEP, Inc. & Narragansett Bay Project. 73 pp. October 1990. http://wwwalker.net/p8

Wetzel, R.G. (2001). Limnology Lake and River Ecosystems, Third Edition. Academic Press. San Diego, CA. 1006 pp.

Appendix A

Watershed Runoff Model Parameters

Table A-1: Default parameter values used in the watershed runoff model.

Note: see P8 documentation for more information about how these parameters are used in the watershed runoff algorithms (http://wwwalker.net/p8/v35/webhelp/p8HelpWebMain.html)

Parameter	Value	Description
Mit	10	Interevent Period (hr)
Mhr	4	Timesteps per hour
Tsnow	32	Temperature threshold below which precipitation is treated as snowfall (degrees F)
Tmelt	32	Temperature threshold above which melting occurs (degrees F)
Smcoef	0.06	Snowmelt coefficient (in per degrees F-day)
ETcal	1	ET calibration factor
Cover	0.5, 0.5, 0.5, 0.5, 0.75, 1, 1, 1, 1, 1, 0.75, 0.5	Fraction of vegetation cover by month (Jan-Dec)
Dhours	9.5, 10.6, 11.9, 13.4, 14.6, 15.2, 14.9, 13.9, 12.5, 11.1, 9.8, 9.1	Number of daylight hours per day by month (Jan-Dec)
Absmelt	1	Curve number adjustment factor for frozen soils
Tamc3	32	Temperature at which ground is frozen (degrees F)
Igs	5, 10	First and last month in growing season
Pcut1	0.5, 1.4	Precipitation cutoff 1 for non-growing and growing seasons
Pcut2	1.1, 2.1	Precipitation cutoff 2 for non-growing and growing seasons
Iamcopt	1	Antecedent moisture condition option
RcBreakpoint	0.8	Runoff coefficient breakpoint
CN (Pervious)	49	Curve number for pervious surfaces
Depres	0.02	Depression storage (in)
Rcoef (Impervious)	1	Runoff coefficient for impervious surfaces

Appendix B

Model Scenario Output of Storm Events with a Historical Peak Flows > 100 cfs in Alewife Brook